Hydraulics of Closed Conduit Spillways

Part XII:

The Two-Way Drop Inlet with a Flat Bottom

ARS-NC-14
September 1974

NORTH CENTRAL REGION

DOC EX AGRICULTURAL RESEARCH SERVICE • U.S. DEPARTMENT OF AGRICULTURE

Agricultural Research Service
UNITED STATES DEPARTMENT OF AGRICULTURE
in cooperation with
Minnesota Agricultural Experiment Station
and
St. Anthony Falls Hydraulic Laboratory
of the
University of Minnesota

Preface

This publication, the 12th part of a group of publications dealing with the hydraulics of closed conduit spillways, reports tests on the two-way drop inlet. The previous 11 parts were published as technical papers under the major title "Hydraulics of Closed Conduit Spillways" by the St. Anthony Falls Hydraulic Laboratory (SAFHL), University of Minnesota, Minneapolis, Minn. The earlier publications are:

Part I. Theory and Its Application, by F. W. Blaisdell. SAFHL Tech. Paper No. 12, Ser. B, 22 pp., illus., Jan. 1952 (rev. Feb. 1958). Gives theory, symbols, and bibliography.

Parts II through VII. Results of Tests on Several Forms of the Spillway, by F. W. Blaisdell. SAFHL Tech. Paper No. 18, Ser. B, 50 pp., illus., March 1958. Parts II through VI describe the hydraulic performance and present discharge coefficients for five forms of the closed conduit spillway; Part VII discusses vortices and their effect on the spillway capacity.

Part VIII. Miscellaneous Laboratory Tests; Part IX. Field Tests, by F. W. Blaisdell. SAFHL Tech. Paper No. 19, Ser. B, 54 pp., illus., March 1958. Reports tests on models of specific field structures and on field structures themselves.

Part X. The Hood Inlet, by F. W. Blaisdell and C. A. Donnelly. SAFHL Tech. Paper No. 20, Ser. B, 41 pp., illus., April 1958. Reports the development of the hood inlet.

Part XI. Tests Using Air, by F. W. Blaisdell and G. G. Hebaus. SAFHL Tech. Paper No. 44, Ser. B, 53 pp., illus., Jan. 1966. Discusses the use of air for tests of closed conduit spillways.

Summary

This report presents the results of experiments on a rectangular drop inlet having a width equal to the barrel diameter, a flat bottom, and a flat, horizontal antivortex plate supported above the drop inlet crest by extensions of the drop inlet endwalls. This structure is called a two-way drop inlet because the water enters over only the two sides of the rectangular drop inlet. The experiments were conducted as a generalized study; that is, all dimensions are expressed in terms of the pipe diameter and the results are applicable to any size structure that is geometrically similar to the structure tested.

Two separate apparatus were used to expedite the test program. In one, the test fluid was water; in the other, it was air. Inlet capacity, pipe priming, and vortex phenomena were studied using water. Entrance loss and pressure coefficients for various inlet proportions were studied using air, since full pipe flow tests can be conducted more advantageously with air than with water.

Contents

Hydraulics of Closed Conduit Spillways [1]

Part XII: The Two-Way Drop Inlet with a Flat Bottom

By Charles A. Donnelly, George G. Hebaus, and Fred W. Blaisdell [2]

Introduction

The two-way drop inlet is used as an entrance to closed conduit spillways. The drop inlet, shown in figure XII–1, is rectangular. Water enters the inlet over the two sides that are parallel to the pipe axis, hence the name "two-way drop inlet." The endwalls are extended upward and outward to support a flat, horizontal antivortex plate over the drop inlet crest. Trash racks can be conveniently mounted on the extended endwalls and outer edges of the antivortex plate.

The two-way drop inlet is used by the Soil Conservation Service (SCS) as a closed conduit spillway entrance for upstream flood prevention, watershed protection, and water conservation reservoirs. The self-regulating siphonic action of the antivortex plate provides a relatively constant reservoir level over a considerable range of discharge—a characteristic that is particularly desirable to preserve reservoir storage volume to reduce the flood peak or, if the reservoir is used for recreation, to reduce the reservoir surface variation for the more frequent floods. The antivortex plate is also a desirable safety feature because it discourages injudicious access to the drop inlet. On the other hand, if economics dictates that a two-stage inlet be used, low-stage orifices can be incorporated into the drop inlet walls. The two-way covered drop inlet concept originated with M. M. Culp, now chief, Design Branch, Engineering Division, SCS, when he was head of the Engineering Standards Unit in 1951. The study reported here refines and expands the design concept.

[1] Research by the St. Anthony Falls Hydraulic Laboratory Conservation Structures Investigations Unit, Agr. Res. Serv., U.S. Dept. of Agr., in cooperation with the Minn. Agr. Exp. Sta. and the St. Anthony Falls Hydraulic Lab., Univ. of Minn., Minneapolis.

Drop Inlet Description

The two-way drop inlet is illustrated in figure XII–1. The drop inlet models were made of transparent plastic. For the water tests, the barrel inside diameter D was 2.25 inches. D was 3 inches for the air tests.

The drop inlet width W was equal to the barrel diameter for all tests.

The drop inlet height Z_i was 5D for all air tests. Heights of 5D, 4D, 3D, and 2D were used in the water tests to determine the minimum height at which the pipe would prime satisfactorily.

Drop inlet lengths B of 1D, 1.5D, 2D, 3D, 5D, and 10D were tested using both water and air. Most of the drop inlets were built 10D long. Shorter inlets were formed by inserting a false wall into the drop inlet at the proper location to give the desired length.

The bottom of the inlet was flat and horizontal.

Crest thicknesses t_c of 0.111D and 0.444D were used in the water tests, and thicknesses of 0.104D, 0.157D, 0.242D, 0.331D, 0.500D, and 0.658D in the air tests. In all tests the outside edge of the crest was square. The inside of the crest had a radius r of one-half the crest thickness as shown in figure XII–1.

The antivortex plate overhang L_o is measured outward from the outside of the drop inlet as shown in figure XII–1. The length of the antivortex plate is the same as the drop inlet length B. The antivortex characteristics of the plate were determined in the water tests for plate overhangs of 0.4D, 0.6D, 0.8D, 1.0D, 1.5D, 2D, 3D, and 4D. The effect of plate overhang on the loss coefficient was evaluated in the air tests for L_o values of 0.295D, 0.506D, 0.753D, 1.00D, 1.41D, 1.5D, 2D, 3D, and 4D.

The antivortex plate height Z_p is the distance from the drop inlet crest to the bottom of the antivortex plate. A recommended range of values of Z_p over which good inlet performance prevails was determined in the water tests using plate heights ranging from 0.1D to 1.4D. Nominal plate heights of 0.1D, 0.2D, 0.4D, 0.6D, and 0.8D were used in the air experiments.

The sine definition—the vertical drop divided by the slope length—of barrel slope S was used. All water tests were conducted at a slope of 20 percent. Slopes of 0, 2.5, 5, 10, 20, 30, and 40 percent were used in the air tests.

For the water tests, the barrel entrance was square edged. For the air tests, both a square-edged and a grooved entrance were used. Two types of square-edged entrances were used. The square-edged barrel inlet shown in figure XII–1(a) and labeled "a" in table XII–1 had its invert at the level of the drop inlet bottom and its crown in the plane of the downstream endwall. The square-edged barrel inlet shown in figure XII–1(b) and labeled "b" in table XII–1 had its invert at the level of the drop inlet bottom but its crown was offset D/8 in the plane of the inlet face from the downstream endwall. The details of the grooved entrance labeled "c" in table XII–1 are shown in figure XII–1(c). The dimensions closely correspond to the American Society for Testing Materials Specifications C 75-41 and C 76-41 for reinforced concrete pipe.

Test Apparatus, Test Procedure, and Analytical Methods

The apparatus, test procedure, and analytical methods used with the water experiments were essentially the same as those described in Part X[3] of this series of technical papers. The air apparatus and testing procedures have been described in Part XI[3].

Test Data

The test data are summarized in table XII–1. Included are the series number, the prefixes W- denoting tests with water, and A- denoting tests with air; the geometry of the two-way drop inlets tested; pertinent notes on the performance of the drop inlet; the observed average energy loss coefficients for the drop inlet crest K_c, the barrel entrance K_i, and the complete entrance K_e for each series for which they were determined; energy loss coefficients computed using the equations and rules developed from the tests; the percentage deviation of the computed coefficients from the experimentally determined average coefficients; and the ratios of the local pressure head

[3]See references listed in Preface for complete citation.

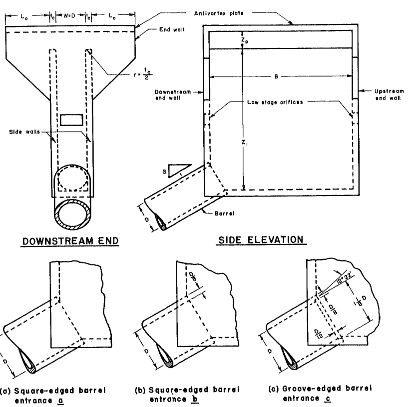

FIGURE XII-1.—The two-way drop inlet.

deviations from the hydraulic grade line h_n to the velocity head in the conduit h_{vp} at the crown and invert of the conduit D/2 from the drop inlet.

Some of the Notes in table XII-1 require explanation.

Many of the water tests were made primarily to determine the spillway performance. The presence or absence of vortices was used as a measure of the performance of the antivortex wall. The Notes, "p, No vortices," "s, Small vortices," "t, Weak vortices," or "r, Surface vortices" indicate that the vortices had no measurable effect on the spillway performance. The presence of "q, Vortices" or "u, Strong vortices" adversely affected the spillway performance and indicated that some feature of the drop inlet was not satisfactory.

The Note, "y, Orifice flow at crest," indicates that the opening between the antivortex plate and the crest acted as an orifice to control the flow, and that the height of the antivortex plate above the crest was so low that the spillway performance was not satisfactory.

A surface tension depressant was added to the water for series W-311 through W-314 to determine the effect of surface tension on the spillway performance. The Note in table XII-1 is "o, Surface tension test."

The Note, "v, Inlet vibrates," indicates that

Text continues on page 22.

TABLE XII-1.—*Summary of tests*

Water tests (W-): D = 0.1875 ft.; W = D; ℓ/D = 110.21
Air tests (A-): D = 0.249 ft.; W = D; ℓ/D = 137.

Series	B/D	Z_1/D	t_c/D	Z_p/D	L_s/D	S	Barrel entrance	Notes[1]	K_c Observed	K_c Computed	K_c Error	K_i Observed	K_i Computed	K_i Error	K_e Observed	K_e Computed	K_e Error	h_r/h_{vp} @ D/2 Crown	h_r/h_{vp} @ D/2 Invert
											Percent			*Percent*			*Percent*		
W-254..	2	5	0.111	0.746	1.808	0.20	a[2]	p	1.12	0.96	−14.2	0.45	0.51	+13.3	0.62	0.66	+ 6.4	—	—
W-255..	2	5	.111	.597	1.808	.20	a	p	1.53	1.19	−22.2	.45	.51	+13.3	.67	.69	+ 3.0	—	—
W-256..	2	5	.111	.448	1.808	.20	a	p X	2.43	—	—	.40	—	—	.75	—	—	—	—
W-257..	2	5	.111	.298	1.808	.20	a	p X	5.43	—	—	.35	—	—	1.14	—	—	—	—
W-258..	2	5	.111	.149	1.808	.20	a	y X	—	—	—	—	—	—	4.10	—	—	—	—
W-259..	2	5	.111	.746	.849	.20	a	p	1.14	.96	−15.8	.42	.51	+21.4	.59	.66	+11.9	—	—
W-260..	2	5	.111	.597	.849	.20	a	p	1.45	1.19	−17.9	.43	.51	+18.6	.64	.69	+ 7.8	—	—
W-261..	2	5	.111	.448	.849	.20	a	s X	2.27	—	—	.41	—	—	.73	—	—	—	—
W-262..	2	5	.111	.298	.849	.20	a	u X	4.48	—	—	.42	—	—	1.10	—	—	—	—
W-263..	2	5	.111	.149	.849	.20	a	u X	—	—	—	—	—	—	4.15	—	—	—	—
W-264..	2	5	.111	.746	.369	.20	a	r X	1.26	—	—	.41	—	—	.60	—	—	—	—
W-265..	2	5	.111	.597	.369	.20	a	r X	1.60	—	—	.42	—	—	.67	—	—	—	—
W-266..	2	5	.111	.448	.369	.20	a	u X	2.23	—	—	.40	—	—	.75	—	—	—	—
W-267..	2	5	.111	.298	.369	.20	a	u X	—	—	—	—	—	—	—	—	—	—	—
W-268..	2	5	.111	.149	.369	.20	a	u X	—	—	—	—	—	—	—	—	—	—	—
W-269..	2	5	.111	.746	.609	.20	a	p	1.26	.96	−23.8	.42	.51	+21.4	.62	.66	+ 6.4	—	—
W-270..	2	5	.111	.597	.609	.20	a	p	1.53	1.19	−22.2	.43	.51	+18.6	.66	.69	+ 4.5	—	—
W-271..	2	5	.111	.448	.609	.20	a	u X	—	—	—	—	—	—	—	—	—	—	—
W-272..	2	5	.111	.746	.249	.20	a	r X	1.36	—	—	.40	—	—	.61	—	—	—	—
W-273..	2	5	.111	.597	.249	.20	a	u X	—	—	—	—	—	—	.70	—	—	—	—
W-274..	2	5	.111	.746	.129	.20	a	u X	—	—	—	—	—	—	—	—	—	—	—
W-275..	2	5	.111	.746	1.48	.20	a	p	.50	.96	+92.0	.52	.51	− 1.9	.60	.66	+10.0	—	—
W-276..	2	5	.111	.597	1.48	.20	a	p	.62	1.19	+91.9	.51	.51	.0	.61	.69	+13.1	—	—
W-277..	2	5	.111	.448	1.48	.20	a	r	1.34	1.83	+36.6	.53	.51	− 3.8	.74	.79	+ 6.8	—	—
W-278..	2	5	.111	.298	1.48	.20	a	r X	—	—	—	—	—	—	1.11	—	—	—	—
W-279..	2	5	.111	.149	1.48	.20	a	r X	—	—	—	—	—	—	3.68	—	—	—	—
W-280..	2	5	.111	.746	.516	.20	a	r X	.57	—	—	.52	—	—	.60	—	—	—	—
W-281..	2	5	.111	.597	.516	.20	a	r X	.74	—	—	.52	—	—	.64	—	—	—	—
W-282..	2	5	.111	.448	.516	.20	a	u X	—	—	—	—	—	—	.75	—	—	—	—
W-283..	2	5	.111	.746	.276	.20	a	u X	—	—	—	—	—	—	.64	—	—	—	—
W-284..	2	5	.111	.597	.276	.20	a	u X	—	—	—	—	—	—	.67	—	—	—	—
W-285..	10	5	.444	.149	1.48	.20	a	p X	13.93	—	—	.47	—	—	.56	—	—	—	—
W-286..	10	5	.444	.298	1.48	.20	a	p	7.21	bb[3]	—	.42	bb[3]	—	.46	.41	−10.9	—	—
W-287..	10	5	.444	.448	1.48	.20	a	p	1.37	bb	—	.49	bb	—	.48	.40	−16.7	—	—
W-288..	10	5	.444	.597	1.48	.20	a	p cc	.90	bb	—	.43	bb	—	.44	.39	−11.4	—	—
W-289..	10	5	.444	.746	1.48	.20	a	p cc	1.10	bb	—	.46	bb	—	.47	.39	−17.0	—	—

W-290..	10	5	.444	.746	.516	.20	a	p cc	3.66	bb	—	.42	bb	—	.45	.39	−13.3	—	—
W-291..	10	5	.444	.597	.516	.20	a	p cc	3.93	bb	—	.42	bb	—	.44	.39	−11.4	—	—
W-292..	10	5	.444	.448	.516	.20	a	p	4.32	bb	—	.42	bb	—	.45	.40	−11.1	—	—
W-293..	10	5	.444	.298	.516	.20	a	p	5.74	bb	—	.42	bb	—	.46	.41	−10.9	—	—
W-294..	10	5	.444	.149	.516	.20	a	y X	—	bb	—	—	bb	—	—	—	—	—	—
W-295..	10	5	.444	.746	.276	.20	a	p cc	25.55	bb	—	.28	bb	—	.44	.39	−11.4	—	—
W-296..	10	5	.444	.597	.276	.20	a	r cc	3.51	bb	—	.44	bb	—	.46	.39	−15.2	—	—
W-297..	10	5	.444	.448	.276	.20	a	r	4.32	bb	—	.42	bb	—	.46	.40	−13.0	—	—
W-298..	10	5	.444	.298	.276	.20	a	r	6.49	bb	—	.42	bb	—	.46	.41	−10.9	—	—
W-299..	10	5	.444	.149	.276	.20	a	y X	—	—	—	—	—	—	—	—	—	—	—
W-300..	10	5	.444	.746	.072	.20	a	r X	4.02	bb	—	.42	bb	—	.44	—	—	—	—
W-301..	10	5	.444	.597	.072	.20	a	r X	4.13	bb	—	.42	bb	—	.44	—	—	—	—
W-302..	10	5	.444	.448	.072	.20	a	r X	4.55	bb	—	.41	bb	—	.46	—	—	—	—
W-303..	10	5	.444	.298	.072	.20	a	r X	6.53	bb	—	.42	bb	—	.46	—	—	—	—
W-304..	10	5	.444	d[4]	—	.20	a	s X	—	—	—	—	—	—	—	—	—	−0.93	−0.34
W-305..	2	5	.111	d	—	.20	a	u X	—	—	—	—	—	—	—	—	—	− .95	− .04
W-306..	2	5	.111	.746	4.0	.20	a	p	.97	.96	+ 1.0	.52	.51	− 1.9	.66	.66	.0	− .87	− .05
W-307..	2	5	.111	.597	4.0	.20	a	p	1.23	1.19	− 3.2	.54	.51	− 5.5	.71	.69	+ 2.8	− .85	− .05
W-308..	2	5	.111	.448	4.0	.20	a	p X	1.84	—	—	.52	—	—	.78	—	—	− .80	− .02
W-309..	2	5	.111	.298	4.0	.20	a	p X	5.23	—	—	.39	—	—	1.19	—	—	− .43	+ .23
W-310..	2	5	.111	.149	4.0	.20	a	y X	—	—	—	—	—	—	—	—	—	—	—
W-311..	2	5	.111	.298	4.0	.20	a	o X	—	—	—	—	—	—	—	—	—	—	—
W-312..	2	5	.111	.448	4.0	.20	a	o X	—	—	—	—	—	—	—	—	—	—	—
W-313..	2	5	.111	.597	4.0	.20	a	o	—	—	—	—	—	—	—	—	—	—	—
W-314..	2	5	.111	.448	4.0	.20	a	o X	—	—	—	—	—	—	—	—	—	—	—
W-315..	2	5	.111	.746	3.0	.20	a	p	1.04	.96	− 7.7	.53	.51	− 3.8	.70	.66	− 5.7	− .97	− .03
W-316..	2	5	.111	.597	3.0	.20	a	p	1.23	1.19	− 3.2	.51	.51	.0	.70	.69	− 1.4	− .94	− .02
W-317..	2	5	.111	.448	3.0	.20	a	p X	1.96	—	—	.51	—	—	.81	—	—	− .85	+ .03
W-318..	2	5	.111	.298	3.0	.20	a	p X	—	—	—	—	—	—	1.19	—	—	− .41	+ .25
W-319..	2	5	.111	.149	3.0	.20	a	y X	—	—	—	—	—	—	—	—	—	—	—
W-320..	2	5	.111	1.40	3.0	.20	a	p	1.15	—	—	.44	—	—	.62	—	—	− .86	.00
W-321..	2	5	.111	1.20	3.0	.20	a	p	1.24	—	—	.47	—	—	.66	—	—	− .88	− .16
W-322..	2	5	.111	1.04	3.0	.20	a	p	1.24	—	—	.45	—	—	.64	—	—	− .86	.00
W-323..	2	5	.111	1.40	2.0	.20	a	p	.97	—	—	.45	—	—	.60	—	—	− .86	− .01
W-324..	2	5	.111	1.20	2.0	.20	a	p	1.14	—	—	.45	—	—	.60	—	—	− .89	− .01
W-325..	2	5	.111	1.04	2.0	.20	a	p X	1.30	—	—	.42	—	—	.62	—	—	− .88	.00
W-326..	2	5	.111	1.04	1.5	.20	a	r X	1.18	—	—	.42	—	—	.62	—	—	− .87	− .01
W-327..	2	5	.111	1.2	1.5	.20	a	p X	1.14	—	—	.45	—	—	.62	—	—	− .92	− .02
W-328..	2	5	.111	1.4	1.5	.20	a	p X	1.06	—	—	.43	—	—	.59	—	—	− .90	− .03
W-329..	2	5	.111	1.4	1.0	.20	a	p X	1.09	—	—	.44	—	—	.60	—	—	− .95	− .09
W-330..	2	5	.111	1.2	1.0	.20	a	p X	1.13	—	—	.43	—	—	.61	—	—	− .93	− .05
W-331..	2	5	.111	1.04	1.0	.20	a	p X	1.19	—	—	.42	—	—	.60	—	—	− .86	− .05

[1] See footnotes at end of table, p. 21.

TABLE XII-1.—*Summary of tests* (Continued)

Series	S/D	Z_1/D	t_c/D	Z_2/D	L/D	S	Barrel entrance	Notes[1]	K_c Observed	K_c Computed	K_c Error	K_t Observed	K_t Computed	K_t Error	K_s Observed	K_s Computed	K_s Error	h_c/h_v @ D/2 Crown	h_c/h_v @ D/2 Invert
											Percent			Percent			Percent		
W-332..	2	5	0.111	1.40	0.8	0.20	a	p X	0.98	—	—	0.45	—	—	0.59	—	—	−0.93	−0.08
W-333..	2	5	.111	1.20	.8	.20	a	p X	1.07	—	—	.42	—	—	.58	—	—	− .96	− .08
W-334..	2	5	.111	1.04	.8	.20	a	p X	1.15	—	—	.45	—	—	.61	—	—	− .93	− .06
W-335..	2	5	.111	1.40	.6	.20	a	q X	1.10	—	—	.43	—	—	.60	—	—	− .94	− .08
W-336..	2	5	.111	1.2	.6	.20	a	p X	1.07	—	—	.44	—	—	.61	—	—	− .96	− .07
W-337..	2	5	.111	1.04	.6	.20	a	u X	1.17	—	—	.43	—	—	.62	—	—	− .88	− .06
W-338..	2	5	.111	1.04	.4	.20	a	u X	1.19	—	—	.43	—	—	.61	—	—	− .89	− .07
W-339..	2	5	.111	1.20	.4	.20	a	u X	1.17	—	—	.43	—	—	.62	—	—	− .94	− .08
W-340..	2	5	.111	1.40	.4	.20	a	u X	—	—	—	—	—	—	.59	—	—	− .93	− .08
W-341..	5	5	.444	.8	4.0	.20	a	p cc	1.75	bb	—	.45	bb	—	.50	0.41	−18.0	− .94	− .37
W-342..	5	5	.444	.7	4.0	.20	a	p	.70	bb	—	.46	bb	—	.49	.42	−14.3	− .93	− .37
W-343..	5	5	.444	.6	4.0	.20	a	p	1.09	bb	—	.48	bb	—	.50	.42	−16.0	− .88	− .35
W-344..	5	5	.444	.5	4.0	.20	a	p	.94	bb	—	.48	bb	—	.49	.43	−12.2	− .87	− .33
W-345..	5	5	.444	.4	4.0	.20	a	p	1.00	bb	—	.47	bb	—	.49	.45	− 8.2	− .83	− .34
W-346..	5	5	.444	.3	4.0	.20	a	p	1.95	bb	—	.46	bb	—	.51	.50	− 2.0	− .74	− .29
W-347..	5	5	.444	.2	4.0	.20	a	p X	8.94	bb	—	.42	bb	—	.64	—	—	− .59	− .20
W-348..	5	5	.444	.1	4.0	.20	a	y X	—	—	—	—	—	—	—	—	—	—	—
W-349..	5	5	.444	.8	3.0	.20	a	p cc	5.51	bb	—	.37	bb	—	.50	.41	−18.0	− .95	− .39
W-350..	5	5	.444	.7	3.0	.20	a	p	.40	bb	—	.47	bb	—	.48	.42	−12.5	− .94	− .37
W-351..	5	5	.444	.6	3.0	.20	a	p	1.11	bb	—	.48	bb	—	.52	.42	−19.2	− .90	− .34
W-352..	5	5	.444	.5	3.0	.20	a	p	.95	bb	—	.48	bb	—	.51	.43	−15.6	− .90	− .33
W-353..	5	5	.444	.4	3.0	.20	a	p	1.81	bb	—	.44	bb	—	.49	.45	− 8.2	− .88	− .35
W-354..	5	5	.444	.3	3.0	.20	a	p	2.19	bb	—	.48	bb	—	.52	.50	− 3.8	− .72	− .31
W-355..	5	5	.444	.2	3.0	.20	a	p X	9.31	bb	—	.46	bb	—	.69	—	—	− .50	− .19
W-356..	5	5	.444	.1	3.0	.20	a	v X	—	—	—	—	—	—	—	—	—	—	—
W-357..	5	5	.444	.8	2.0	.20	a	p cc	3.00	bb	—	.44	bb	—	.49	.41	−16.3	− .93	− .37
W-358..	5	5	.444	.7	2.0	.20	a	p	.41	bb	—	.49	bb	—	.50	.42	−16.0	− .93	− .37
W-359..	5	5	.444	.6	2.0	.20	a	p	.44	bb	—	.48	bb	—	.49	.42	−14.3	− .91	− .36
W-360..	5	5	.444	.5	2.0	.20	a	p	.58	bb	—	.48	bb	—	.50	.43	−14.0	− .92	− .35
W-361..	5	5	.444	.4	2.0	.20	a	p	2.20	bb	—	.42	bb	—	.48	.45	− 6.2	− .88	− .35
W-362..	5	5	.444	.3	2.0	.20	a	p	2.34	bb	—	.47	bb	—	.52	.50	− 3.8	− .84	− .34
W-363..	5	5	.444	.2	2.0	.20	a	p X	8.94	bb	—	.47	bb	—	.68	—	—	− .61	− .20
W-364..	5	5	.444	.1	2.0	.20	a	y X	—	—	—	—	—	—	—	—	—	—	—
W-365..	5	5	.444	.8	1.5	.20	a	p cc	3.65	bb	—	.44	bb	—	.48	.41	−14.6	− .92	− .37
W-366..	5	5	.444	.7	1.5	.20	a	p	3.15	bb	—	.48	bb	—	.49	.42	−14.3	− .92	− .37
W-367..	5	5	.444	.6	1.5	.20	a	p	8.70	bb	—	.45	bb	—	.48	.42	−12.5	− .89	− .35
W-368..	5	5	.444	.5	1.5	.20	a	p	3.26	bb	—	.42	bb	—	.48	.43	−10.4	− .91	− .36
W-369..	5	5	.444	.4	1.5	.20	a	p	1.15	bb	—	.48	bb	—	.50	.45	−10.0	− .90	− .36
W-370..	5	5	.444	.3	1.5	.20	a	r	2.32	bb	—	.49	bb	—	.54	.50	− 7.4	− .86	− .34

W-371..	5	5	.444	.2	1.5	.20	a	r X	10.07	bb	—	.45	bb	—	.69	—	—	−.60	−.20
W-372..	5	5	.444	.1	1.5	.20	a	y X	—	—	—	—	—	—	—	—	—	—	—
W-373..	5	5	.444	.8	1.0	.20	a	r cc	3.23	bb	—	.41	bb	—	.48	.41	−14.6	−.91	−.37
W-374..	5	5	.444	.7	1.0	.20	a	r	.50	bb	—	.46	bb	—	.48	.42	−12.5	−.92	−.36
W-375..	5	5	.444	.6	1.0	.20	a	p	.51	bb	—	.49	bb	—	.50	.42	−16.0	−.92	−.37
W-376..	5	5	.444	.5	1.0	.20	a	r	.59	bb	—	.48	bb	—	.50	.43	−14.0	−.94	−.37
W-377..	5	5	.444	.4	1.0	.20	a	r	.96	bb	—	.46	bb	—	.48	.45	− 6.2	−.88	−.36
W-378..	5	5	.444	.3	1.0	.20	a	r	2.68	bb	—	.48	bb	—	.55	.50	− 9.1	−.88	−.35
W-379..	5	5	.444	.2	1.0	.20	a	r X	8.26	bb	—	.44	bb	—	.64	—	—	−.64	−.21
W-380..	5	5	.444	.1	1.0	.20	a	v X	—	—	—	—	—	—	—	—	—	—	—
W-381..	5	5	.444	.8	.8	.20	a	p cc	.26	bb	—	.48	bb	—	.50	.41	−18.0	−.91	−.36
W-382..	5	5	.444	.7	.8	.20	a	r	.98	bb	—	.46	bb	—	.50	.42	−16.0	−.92	−.37
W-383..	5	5	.444	.6	.8	.20	a	r	1.22	bb	—	.47	bb	—	.50	.42	−16.0	−.93	−.37
W-384..	5	5	.444	.5	.8	.20	a	r	.71	bb	—	.49	bb	—	.51	.43	−15.7	−.92	−.37
W-385..	5	5	.444	.4	.8	.20	a	r	1.33	bb	—	.47	bb	—	.50	.45	−10.0	−.89	−.36
W-386..	5	5	.444	.3	.8	.20	a	r	2.67	bb	—	.46	bb	—	.52	.50	− 3.8	−.84	−.34
W-387..	5	5	.444	.2	.8	.20	a	v X	—	—	—	—	—	—	—	—	—	—	—
W-388..	5	5	.444	.8	.6	.20	a	r X	1.30	—	—	.48	—	—	.50	—	—	−.92	−.36
W-389..	5	5	.444	.7	.6	.20	a	r X	.42	—	—	.46	—	—	.46	—	—	−.90	−.36
W-390..	5	5	.444	.6	.6	.20	a	r	3.72	bb	—	.48	bb	—	.50	.42	−16.0	−.90	−.37
W-391..	5	5	.444	.5	.6	.20	a	r	1.71	bb	—	.47	bb	—	.47	.43	− 8.5	−.91	−.37
W-392..	5	5	.444	.4	.6	.20	a	r	1.22	bb	—	.50	bb	—	.51	.45	−11.8	−.90	−.35
W-393..	5	5	.444	.3	.6	.20	a	r	2.46	bb	—	.46	bb	—	.51	.50	− 2.0	−.83	−.34
W-394..	5	5	.444	.2	.6	.20	a	v X	—	—	—	—	—	—	.53	—	—	—	—
W-395..	5	5	.444	.8	.4	.20	a	r cc	.31	bb	—	.49	bb	—	.50	.41	−18.0	−.90	−.35
W-396..	5	5	.444	.7	.4	.20	a	r	.24	bb	—	.47	bb	—	.47	.42	−10.6	−.88	−.35
W-397..	5	5	.444	.6	.4	.20	a	r	2.41	bb	—	.46	bb	—	.51	.42	−17.6	−.93	−.35
W-398..	5	5	.444	.5	.4	.20	a	r	.72	bb	—	.49	bb	—	.51	.43	−15.7	−.94	−.36
W-399..	5	5	.444	.4	.4	.20	a	r	1.05	bb	—	.48	bb	—	.53	.45	−15.1	−.93	−.34
W-400..	5	5	.444	.3	.4	.20	a	v X	—	—	—	—	—	—	—	—	—	—	—
W-401..	5	5	.444	d	—	.20	a	t X	—	—	—	—	—	—	—	—	—	—	—
W-402..	3	5	.444	e[5]	—	.20	a	u X	—	—	—	—	—	—	—	—	—	—	—
W-403..	3	5	.444	d	—	.20	a	u X	—	—	—	—	—	—	—	—	—	—	—
W-404..	—	—	—	—	—	—	—	No test	—	—	—	—	—	—	—	—	—	—	—
W-405..	3	5	.444	.8	4.0	.20	a	p	4.31	bb	—	.45	bb	—	.48	.46	− 4.2	−.93	−.32
W-406..	3	5	.444	.7	4.0	.20	a	p	—	bb	—	—	bb	—	.50	.47	− 6.0	−.93	−.33
W-407..	3	5	.444	.6	4.0	.20	a	p	—	bb	—	—	bb	—	.48	.48	.0	−.90	−.30
W-408..	3	5	.444	.5	4.0	.20	a	p	.40	bb	—	.46	bb	—	.52	.51	− 1.9	−.85	−.30
W-409..	3	5	.444	.4	4.0	.20	a	p	1.41	bb	—	.49	bb	—	.59	.56	− 5.1	−.78	−.27
W-410..	3	5	.444	.3	4.0	.20	a	p X	2.91	—	—	.45	—	—	.65	—	—	−.74	−.23
W-411..	3	5	.444	.2	4.0	.20	a	y X	—	—	—	—	—	—	—	—	—	—	—
W-412..	3	5	.444	.8	3.0	.20	a	p	—	bb	—	—	bb	—	.53	.46	−13.2	−.91	−.32
W-413..	3	5	.444	.7	3.0	.20	a	p	.67	bb	—	.51	bb	—	.55	.47	−14.5	−.93	−.32
W-414..	3	5	.444	.6	3.0	.20	a	p	.65	bb	—	.50	bb	—	.55	.48	−12.7	−.93	−.32

[1]See footnotes at end of table, p. 21.

TABLE XII-1.—*Summary of tests* (Continued)

Series	B/D	Z_1/D	t_b/D	Z_2/D	L_b/D	S	Barrel entrance	Notes[1]	K_c Observed	K_c Computed	K_c Error	K_t Observed	K_t Computed	K_t Error	K_e Observed	K_e Computed	K_e Error	h_u/h_{vp} @ D/2 Crown	h_u/h_{vp} @ D/2 Invert
											Percent			Percent			Percent		
W-415	3	5	0.444	0.5	3.0	0.20	a	p	0.91	bb	—	0.50	bb	—	0.57	0.51	−10.5	−0.93	−0.33
W-416	3	5	.444	.4	3.0	.20	a	p	1.40	bb	—	.49	bb	—	.58	.56	− 3.4	− .87	− .30
W-417	3	5	.444	.3	3.0	.20	a	p X	2.86	—	—	.47	—	—	.67	—	—	− .78	− .26
W-418	3	5	.444	.2	3.0	.20	a	y X	—	—	—	—	—	—	—	—	—	—	—
W-419	3	5	.444	d	—	.20	a	u X	—	—	—	—	—	—	—	—	—	—	—
W-420	3	5	.444	.8	2.0	.20	a	p	.67	bb	—	.50	bb	—	.55	.46	−16.4	− .90	− .33
W-421	3	5	.444	.7	2.0	.20	a	p	.72	bb	—	.51	bb	—	.56	.47	−16.1	− .92	− .31
W-422	3	5	.444	.6	2.0	.20	a	p	.73	bb	—	.50	bb	—	.55	.48	−12.7	− .91	− .31
W-423	3	5	.444	.5	2.0	.20	a	p	.98	bb	—	.51	bb	—	.57	.51	−10.5	—	− .34
W-424	3	5	.444	.4	2.0	.20	a	p	1.66	bb	—	.47	bb	—	.58	.56	− 3.4	− .86	− .32
W-425	3	5	.444	.3	2.0	.20	a	p X	2.94	—	—	.40	—	—	.60	—	—	− .79	− .29
W-426	3	5	.444	.2	2.0	.20	a	y X	—	—	—	—	—	—	—	—	—	—	—
W-427	3	5	.444	.8	1.5	.20	a	p	.70	bb	—	.47	bb	—	.52	.46	−11.5	− .92	− .32
W-428	3	5	.444	.7	1.5	.20	a	p	.77	bb	—	.49	bb	—	.54	.47	−13.0	− .93	− .32
W-429	3	5	.444	.6	1.5	.20	a	p	.76	bb	—	.48	bb	—	.52	.48	− 7.7	− .96	− .33
W-430	3	5	.444	.5	1.5	.20	a	p	1.02	bb	—	.46	bb	—	.54	.51	− 5.6	− .90	− .33
W-431	3	5	.444	.4	1.5	.20	a	p	1.68	bb	—	.45	bb	—	.56	.56	.0	− .85	− .32
W-432	3	5	.444	.3	1.5	.20	a	p X	3.17	—	—	.47	—	—	.67	—	—	− .80	− .29
W-433	3	5	.444	.2	1.5	.20	a	y X	—	—	—	—	—	—	—	—	—	—	—
W-434	3	5	.444	.8	1.0	.20	a	r	.55	bb	—	.49	bb	—	.53	.46	−13.2	− .91	− .31
W-435	3	5	.444	.7	1.0	.20	a	r	.62	bb	—	.48	bb	—	.52	.47	− 9.6	− .90	− .31
W-436	3	5	.444	.6	1.0	.20	a	r	.34	bb	—	.50	bb	—	.52	.48	− 7.7	− .93	− .32
W-437	3	5	.444	.5	1.0	.20	a	r	.72	bb	—	.50	bb	—	.55	.50	− 9.1	− .90	− .31
W-438	3	5	.444	.4	1.0	.20	a	r	1.23	bb	—	.49	bb	—	.58	.56	− 3.4	− .81	− .32
W-439	3	5	.444	.3	1.0	.20	a	r X	2.96	—	—	.51	—	—	.71	—	—	− .78	− .27
W-440	3	5	.444	.2	1.0	.20	a	y X	—	—	—	—	—	—	—	—	—	—	—
W-441	3	5	.444	.8	.8	.20	a	r	.47	bb	—	.45	bb	—	.48	.46	− 4.2	− .88	− .29
W-442	3	5	.444	.7	.8	.20	a	r	.39	bb	—	.50	bb	—	.52	.47	− 9.6	− .89	− .30
W-443	3	5	.444	.6	.8	.20	a	r	.43	bb	—	.49	bb	—	.52	.48	− 7.7	− .91	− .31
W-444	3	5	.444	.5	.8	.20	a	r	.61	bb	—	.50	bb	—	.54	.50	− 7.4	− .90	− .32
W-445	3	5	.444	.4	.8	.20	a	r	1.28	bb	—	.50	bb	—	.59	.56	− 5.1	− .84	− .31
W-446	3	5	.444	.3	.8	.20	a	r X	2.79	—	—	.50	—	—	.69	—	—	− .76	− .26
W-447	3	5	.444	.2	.8	.20	a	y X	—	—	—	—	—	—	—	—	—	—	—
W-448	3	5	.444	.8	.6	.20	a	p	.39	.52	+33.3	.50	.43	−14.0	.53	.46	−13.2	− .87	− .30
W-449	3	5	.444	.7	.6	.20	a	r	.39	.62	+59.0	.50	.43	−14.0	.53	.47	−11.3	− .87	− .29
W-450	3	5	.444	.6	.6	.20	a	r	.78	.79	+ 1.3	.50	.43	−14.0	.56	.48	−14.3	− .89	− .31
W-451	3	5	.444	.5	.6	.20	a	r	.66	1.12	+69.7	.50	.43	−14.0	.55	.51	− 7.3	− .88	− .31
W-452	3	5	.444	.4	.6	.20	a	r	1.10	1.88	+70.9	.50	.43	−14.0	.58	.56	− 3.4	− .84	− .30
W-453	3	5	.444	.3	.6	.20	a	u X	2.62	—	—	.51	—	—	.69	—	—	− .77	− .27
W-454	3	5	.444	.8	.4	.20	a	r X	.27	—	—	.47	—	—	.52	—	—	− .82	− .30

W-455..	3	5	.444	.7	.4	.20	a	r X	.46	—	—	.49	—	—	.55	—	—	− .85	− .29
W-456..	3	5	.444	.6	.4	.20	a	r X	.55	—	—	.52	—	—	.59	—	—	− .86	− .30
W-457..	3	5	.444	.5	.4	.20	a	r X	.85	—	—	.48	—	—	.56	—	—	− .85	− .30
W-458..	3	5	.444	.4	.4	.20	a	u X	—	—	—	—	—	—	—	—	—	—	—
W-459..	3	5	.444	.8	.2	.20	a	u X	.49	—	—	.49	—	—	.53	—	—	− .82	− .31
W-460..	1	5	.444	.8	4.0	.20	a	p X	—	—	—	—	—	—	1.07	—	—	− .70	− .14
W-461..	1	5	.444	.7	4.0	.20	a	p X	—	—	—	—	—	—	1.09	—	—	− .67	− .12
W-462..	1	5	.444	.6	4.0	.20	a	p X	—	—	—	—	—	—	1.14	—	—	− .75	− .15
W-463..	1	5	.444	.5	4.0	.20	a	p X	—	—	—	—	—	—	1.26	—	—	− .75	− .15
W-464..	1	5	.444	.4	4.0	.20	a	v X	—	—	—	—	—	—	—	—	—	—	—
W-465..	1.5	5	.444	.8	4.0	.20	a	p	.44	.26	−40.9	.55	.62	+12.7	.74	.69	− 6.8	− .96	− .23
W-466..	1.5	5	.444	.7	4.0	.20	a	p X	.46	—	—	.52	—	—	.73	—	—	− .96	− .22
W-467..	1.5	5	.444	.6	4.0	.20	a	p X	.60	—	—	.48	—	—	.76	—	—	− .91	− .20
W-468..	1.5	5	.444	.5	4.0	.20	a	p X	.80	—	—	.59	—	—	.81	—	—	− .88	− .19
W-469..	1.5	5	.444	.4	4.0	.20	a	p X	1.52	—	—	.58	—	—	1.00	—	—	− .87	− .25
W-470..	1.5	5	.444	.3	4.0	.20	a	v X	—	—	—	—	—	—	—	—	—	—	—
W-471..	1.5	5	.444	.8	3.0	.20	a	p	.40	.26	−35.0	.61	.62	+ 1.6	.72	.69	− 4.2	− .98	− .25
W-472..	1.5	5	.444	.7	3.0	.20	a	p X	.50	—	—	.62	—	—	.75	—	—	− .99	− .24
W-473..	1.5	5	.444	.6	3.0	.20	a	p X	1.22	—	—	.54	—	—	.88	—	—	− .70	− .20
W-474..	1.5	5	.444	.5	3.0	.20	a	p X	.86	—	—	.62	—	—	.85	—	—	− .94	− .24
W-475..	1.5	5	.444	.4	3.0	.20	a	v X	—	—	—	—	—	—	—	—	—	—	—
W-476..	1.5	5	.444	.8	2.0	.20	a	r	.43	.26	−39.5	.62	.62	.0	.73	.69	− 5.5	− .97	− .25
W-477..	1.5	5	.444	.7	2.0	.20	a	r X	.46	—	—	.61	—	—	.73	—	—	− .98	− .24
W-478..	1.5	5	.444	.6	2.0	.20	a	r X	.34	—	—	.67	—	—	.76	—	—	− .95	− .24
W-479..	1.5	5	.444	.5	2.0	.20	a	r X	1.28	—	—	.58	—	—	.93	—	—	− .83	− .24
W-480..	1.5	5	.444	.4	2.0	.20	a	v X	1.43	—	—	.55	—	—	.94	—	—	− .84	− .24
W-481..	1.5	5	.444	.3	2.0	.20	a	v X	—	—	—	—	—	—	—	—	—	—	—
W-482..	1.5	5	.444	.8	1.5	.20	a	r	.43	.26	−39.5	.60	.62	+ 3.3	.73	.69	− 5.5	− .95	− .23
W-483..	1.5	5	.444	.7	1.5	.20	a	r X	.46	—	—	.60	—	—	.73	—	—	− .95	− .24
W-484..	1.5	5	.444	.6	1.5	.20	a	r X	.60	—	—	.57	—	—	.73	—	—	− .90	− .22
W-485..	1.5	5	.444	.5	1.5	.20	a	r X	.82	—	—	.57	—	—	.80	—	—	− .86	− .23
W-486..	1.5	5	.444	.4	1.5	.20	a	r X	1.54	—	—	.56	—	—	.98	—	—	− .81	− .22
W-487..	1.5	5	.444	.3	1.5	.20	a	y X	—	—	—	—	—	—	—	—	—	—	—
W-488..	1.5	5	.444	.8	1.0	.20	a	r	.44	.26	−40.9	.61	.62	+ 1.6	.73	.69	− 5.5	− .94	− .25
W-489..	1.5	5	.444	.7	1.0	.20	a	r X	.47	—	—	.61	—	—	.74	—	—	− .94	− .24
W-490..	1.5	5	.444	.6	1.0	.20	a	q X	.56	—	—	.61	—	—	.76	—	—	− .93	− .21
W-491..	1.5	5	.444	.5	1.0	.20	a	u X	.81	—	—	.60	—	—	.82	—	—	− .87	− .20
W-492..	1.5	5	.444	.4	1.0	.20	a	v X	—	—	—	—	—	—	—	—	—	—	—
W-493..	1.5	5	.444	.8	.8	.20	a	q X	.54	—	—	.61	—	—	.76	—	—	− .95	− .27
W-494..	1.5	5	.444	.7	.8	.20	a	u X	—	—	—	—	—	—	—	—	—	—	—
W-495..	3	5	.444	1.0	.8	.20	a	p X	—	—	—	—	—	—	.42	—	—	− .98	− .31
W-496..	5	4	.111	f[6]	—	.20	a	aa X	—	—	—	—	—	—	—	—	—	—	—
W-497..	3	4	.111	f	—	.20	a	aa X	—	—	—	—	—	—	—	—	—	—	—
W-498..	2	4	.111	f	—	.20	a	aa X	—	—	—	—	—	—	—	—	—	—	—
W-499..	1.5	4	.111	f	—	.20	a	aa X	—	—	—	—	—	—	—	—	—	—	—

[1] See footnotes at end of table, p. 21.

TABLE XII–1.—*Summary of tests* (Continued)

Series	B/D	Z_i/D	t_c/D	Z_p/D	L_p/D	S	Barrel entrance	Notes[1]	K_c Observed	K_c Computed	K_c Error	K_1 Observed	K_1 Computed	K_1 Error	K_v Observed	K_v Computed	K_v Error	h_c/h_{vp} @ D/2 Crown	h_c/h_{vp} @ D/2 Invert
											Percent			*Percent*			*Percent*		
W-500	1	4	0.111	f	—	.20	a	aa X	—	—	—	—	—	—	—	—	—	—	—
W-501	5	3	.111	f	—	.20	a	aa X	—	—	—	—	—	—	—	—	—	—	—
W-502	3	3	.111	f	—	.20	a	aa X	—	—	—	—	—	—	—	—	—	—	—
W-503	2	3	.111	f	—	.20	a	aa X	—	—	—	—	—	—	—	—	—	—	—
W-504	1.5	3	.111	f	—	.20	a	aa X	—	—	—	—	—	—	—	—	—	—	—
W-505	1	3	.111	f	—	.20	a	z X	—	—	—	—	—	—	—	—	—	—	—
W-506	5	2	.111	f	—	.20	a	z X	—	—	—	—	—	—	—	—	—	—	—
W-507	3	2	.111	f	—	.20	a	z X	—	—	—	—	—	—	—	—	—	—	—
W-508	2	2	.111	f	—	.20	a	aa X	—	—	—	—	—	—	—	—	—	—	—
W-509	1.5	2	.111	f	—	.20	a	aa X	—	—	—	—	—	—	—	—	—	—	—
W-510	1.0	2	.111	f	—	.20	a	z X	—	—	—	—	—	—	—	—	—	—	—
A-4	2	5	.104	0.820	1.87	0.204	a		1.00	0.92	− 8.0	0.50	0.51	+ 2.0	0.65	0.65	0.0	−1.02	−0.08
A-5	3	5	.104	.820	1.87	.204	a	cc	1.30	1.12	−13.8	.45	.43	− 4.4	.52	.51	− 1.9	−1.01	− .15
A-6	5	5	.104	.820	1.87	.204	a		2.20	1.93	−12.3	.37	.38	+ 2.7	.43	.43	− .0	−1.01	− .20
A-7	10	5	.104	.820	1.87	.204	a	cc	7.80	7.13	− 8.6	.29	.35	+20.7	.38	.39	+ 2.6	−1.01	− .25
A-8	10	5	.104	.616	1.86	.204	a	cc	8.0	7.38	− 7.8	.35	.35	.0	.39	.40	+ 2.6	−1.01	− .24
A-9	5	5	.104	.616	1.86	.204	a		2.50	2.18	−12.8	.37	.38	+ 2.7	.44	.43	− 2.3	− .99	− .20
A-10	3	5	.104	.616	1.86	.204	a		1.55	1.37	−11.6	.42	.43	+ 2.4	.52	.52	.0	− .99	− .15
A-11	2	5	.104	.616	1.86	.204	a		1.40	1.17	−16.4	.50	.51	+ 2.0	.71	.69	− 2.8	−1.00	− .07
A-12	2	5	.104	.412	1.86	.204	a	X	2.4	—	—	.49	—	—	.84	—	—	− .97	− .05
A-13	3	5	.104	.412	1.86	.204	a		2.8	2.36	−15.7	.41	.43	+ 4.9	.60	.59	− 1.7	− .96	− .12
A-14	5	5	.104	.412	1.86	.204	a		4.0	3.17	−20.8	.36	.38	+ 5.6	.46	.46	.0	− .97	− .18
A-15	10	5	.104	.412	1.86	.204	a		9.5	8.38	−11.8	.35	.35	.0	.41	.40	− 2.4	− .99	− .22
A-16	10	5	.104	.206	1.86	.204	a		23.6	18.44	−21.9	.37	.35	− 5.4	.50	.46	− 8.0	− .88	− .15
A-17	5	5	.104	.206	1.86	.204	a	i X	14.1	—	—	.37	—	—	.71	—	—	− .71	− .04
A-18	3	5	.104	.206	1.86	.204	a	i l X	11.0	—	—	.46	—	—	1.15	—	—	− .66	+ .07
A-19	2	5	.104	.206	1.86	.204	a	i X	10.2	—	—	.51	—	—	2.0	—	—	− .85	+ .11
A-20	2	5	.104	.107	1.86	.204	a	i m X	44.0	—	—	neg.	—	—	6.4	—	—	—	—
A-21	3	5	.104	.107	1.86	.204	a	i X	46.0	—	—	0 ±	—	—	3.2	—	—	− .05	+ .22
A-22	5	5	.104	.107	1.86	.204	a	i X	49.0	—	—	.25	—	—	1.45	—	—	− .49	+ .04
A-23	10	5	.104	.107	1.86	.204	a	i X	48.0	—	—	.35	—	—	.63	—	—	− .81	− .12
A-24	1.5	5	.104	.107	1.86	.204	a	i X	41.0	—	—	neg.	—	—	10.8	—	—	—	—
A-25	1.5	5	.104	.206	1.86	.204	a	i X	10.1	—	—	.60	—	—	3.3	—	—	− .75	+ .19
A-26	1.5	5	.104	.400	1.86	.204	a	X	2.30	—	—	.53	—	—	1.14	—	—	−1.00	.00
A-27	1.5	5	.104	.600	1.86	.204	a	X	1.35	—	—	.53	—	—	.89	—	—	−1.04	− .01
A-28	1.5	5	.104	.813	1.86	.204	a		1.08	.87	−19.4	.55	.62	+12.7	.83	.86	+ 3.6	−1.06	− .02
A-29	10	5	.500	.793	1.50	.000	b[7]	cc	5.5	6.56	+19.3	.44	.44	.0	.48	.48	.0	−1.22	− .37
A-30	5	5	.500	.793	1.50	.000	b		1.27	1.32	+ 3.9	.47	.47	.0	.51	.50	− 2.0	−1.20	− .34
A-31	3	5	.500	.808	1.50	.000	b		.38	.50	+31.6	.53	.52	− 1.9	.56	.55	− 1.8	−1.20	− .30

A-32....	2	5	.500	.808	1.50	.000	b		.21	.30	+42.8	.60	.60	.0	.64	.65	+ 1.6	-1.23	- .24
A-33....	1.5	5	.500	.808	1.50	.000	b		.18	.24	+33.3	.71	.71	.0	.76	.78	+ 2.6	-1.30	- .16
A-34....	1.5	5	.500	.617	1.50	.000	b	X	.28	—	—	.71	—	—	.79	—	—	-1.30	- .14
A-35....	2	5	.500	.617	1.50	.000	b		.31	.54	+74.2	.60	.60	.0	.66	.68	+ 3.0	-1.23	- .22
A-36....	3	5	.500	.610	1.50	.000	b		.50	.75	+50.0	.55	.52	- 5.5	.58	.57	- 1.7	-1.19	- .27
A-37....	5	5	.500	.610	1.50	.000	b		1.46	1.56	+ 6.9	.49	.47	- 4.1	.53	.51	- 3.8	-1.20	- .32
A-38....	10	5	.500	.604	1.50	.000	b	n cc	6.23	6.78	+ 8.8	.46	.44	- 4.3	.50	.48	- 4.0	-1.20	- .35
A-39....	10	5	.500	.400	1.50	.000	b		7.0	7.89	+12.7	.45	.44	- 2.2	.50	.49	- 2.0	-1.20	- .34
A-40....	5	5	.500	.410	1.50	.000	b	n	2.2	2.57	+16.8	.48	.47	- 2.1	.54	.53	- 1.8	-1.21	- .32
A-41....	3	5	.500	.416	1.50	.000	b		1.25	1.70	+36.2	.54	.52	- 3.7	.63	.64	+ 1.6	-1.23	- .27
A-42....	2	5	.500	.416	1.50	.000	b	X	1.16	—	—	.61	—	—	.80	—	—	-1.25	- .21
A-43....	1.5	5	.500	.424	1.50	.000	b	X	1.16	—	—	.73	—	—	1.04	—	—	-1.28	- .12
A-44....	1.5	5	.500	.224	1.50	.000	b	X	8.4	—	—	.69	—	—	2.95	—	—	-1.23	- .09
A-45....	2	5	.500	.227	1.50	.000	b	X	8.7	—	—	.60	—	—	1.90	—	—	-1.13	- .07
A-46....	3	5	.500	.220	1.50	.000	b	X	9.5	—	—	.51	—	—	1.17	—	—	-1.08	- .12
A-47....	5	5	.500	.217	1.50	.000	b	x X	11.5	—	—	.47	—	—	.75	—	—	-1.06	- .13
A-48....	10	5	.500	.200	1.50	.000	b		21.0	18.82	-10.4	.45	.44	- 2.2	.58	.56	- 3.4	-1.13	- .23
A-49....	10	5	.500	.100	1.50	.000	b	X	38.0	—	—	.46	—	—	.69	—	—	-1.14	- .23
A-50....	5	5	.500	.117	1.50	.000	b	X	30.0	—	—	.47	—	—	1.18	—	—	-1.09	- .14
A-51....	3	5	.500	.110	1.50	.000	b	X	26.3	—	—	.54	—	—	2.37	—	—	-1.20	- .07
A-52....	2	5	.500	.110	1.50	.000	b	X	26.0	—	—	.80	—	—	4.76	—	—	-1.43	+ .06
A-53....	1.5	5	.500	.100	1.50	.000	b	X	26.5	—	—	.87	—	—	8.0	—	—	-1.35	+ .20
A-54....	5	5	.500	.812	1.50	.025	b		1.33	1.31	- 1.5	.46	.46	.0	.50	.49	- 2.0	-1.19	- .33
A-55....	3	5	.500	.812	1.50	.025	b		.42	.50	+19.0	.54	.51	- 5.6	.56	.54	- 3.6	-1.18	- .29
A-56....	2	5	.500	.812	1.50	.025	b		.24	.30	+25.0	.61	.60	- 1.6	.63	.65	+ 3.2	-1.21	- .23
A-57....	1.5	5	.500	.816	1.50	.025	b		.19	.24	+26.3	.72	.70	- 2.8	.76	.77	+ 1.3	-1.28	- .15
A-58....	1	5	.500	.816	1.50	.025	b	X	.21	—	—	1.02	—	—	1.13	—	—	-1.42	+ .10
A-59....	5	5	.500	.812	1.50	.05	b	cc	1.3	1.31	+ 0.7	.44	.46	+ 4.5	.48	.49	+ 2.1	-1.18	- .34
A-60....	3	5	.500	.812	1.50	.05	b		.40	.50	+25.0	.51	.51	.0	.54	.54	.0	-1.17	- .29
A-61....	2	5	.500	.812	1.50	.05	b		.22	.30	+36.4	.58	.59	+ 1.7	.62	.64	+ 3.2	-1.21	- .24
A-62....	1.5	5	.500	.812	1.50	.05	b		.20	.24	+20.0	.70	.70	.0	.76	.77	+ 1.3	-1.28	- .16
A-63....	1	5	.500	.812	1.50	.05	b	X	.24	—	—	1.01	—	—	1.14	—	—	-1.41	+ .09
A-64....	5	5	.500	.812	1.50	.10	b	cc	1.39	1.31	- 5.7	.44	.44	.0	.50	.47	- 6.0	-1.17	- .34
A-65....	3	5	.500	.812	1.50	.10	b		.44	.50	+13.6	.52	.49	- 5.8	.55	.52	- 5.4	-1.16	- .28
A-66....	2	5	.500	.812	1.50	.10	b		.23	.30	+30.4	.58	.58	.0	.62	.63	+ 1.6	-1.18	- .22
A-67....	1.5	5	.500	.812	1.50	.10	b		.21	.24	+14.3	.69	.68	- 1.4	.75	.75	.0	-1.25	- .15
A-68....	1	5	.500	.812	1.50	.10	b	X	.24	—	—	.99	—	—	1.12	—	—	-1.41	+ .07
A-69....	1	5	.500	.812	1.50	.10	c[8]	X	.24	—	—	.77	—	—	.90	—	—	-1.06	+ .22
A-70....	1.5	5	.500	.812	1.50	.10	c		.26	.24	- 7.7	.48	.50	+ 4.2	.55	.57	+ 3.6	- .93	+ .02
A-71....	2	5	.500	.812	1.50	.10	c		.23	.30	+30.4	.40	.40	.0	.44	.45	+ 2.3	- .87	- .02
A-72....	3	5	.500	.812	1.50	.10	c		.43	.50	+16.3	.34	.31	- 8.8	.36	.34	- 5.6	- .84	- .06
A-73....	5	5	.500	.812	1.50	.10	c	cc	1.30	1.31	+ .7	.29	.26	-10.3	.32	.29	- 9.4	- .83	- .09
A-74....	5	5	.500	.812	1.50	.20	c	cc	1.28	1.31	+ 2.3	.25	.24	- 4.0	.29	.27	- 6.9	- .74	- .06

[1]See footnotes at end of table, p. 21.

TABLE XII-1.—*Summary of tests* (Continued)

				Z_o/D	L_o/D	S	Barrel entrance	Notes[1]	K_c Observed	K_c Computed	K_c Error	K_t Observed	K_t Computed	K_t Error	K_w Observed	K_w Computed	K_w Error	h_c/h_{cp} @ D/2 Crown	h_c/h_{cp} @ D/2 Invert
											Percent			Percent			Percent		
				0.812	1.50	0.20	c		0.40	0.50	+25.0	0.30	0.29	− 3.3	0.33	0.32	− 3.0	−0.77	−0.04
				.812	1.50	.20	c		.21	.30	+42.8	.35	.37	+ 5.7	.39	.42	− 7.7	− .82	− .02
				.812	1.50	.20	c		.19	.24	+26.3	.45	.48	+ 6.7	.50	.55	+10.0	− .89	+ .03
				.812	1.50	.20	c	X	.23	—	—	.72	—	—	.85	—	—	− .99	+ .21
				.812	1.50	.20	b	X	.24	—	—	.95	—	—	1.07	—	—	−1.41	+ .03
				.812	1.50	.20	b		.20	.24	+20.0	.65	.66	+ 1.5	.71	.73	+ 2.8	−1.24	− .16
			[illegible]	.812	1.50	.20	b		.23	.30	+30.4	.55	.55	.0	.59	.60	+ 1.7	−1.17	− .20
			500	.812	1.50	.20	b		.40	.50	+25.0	.48	.47	− 2.1	.51	.50	− 2.0	−1.13	− .22
			500	.816	1.50	.20	b	cc	1.27	1.30	+ 2.4	.41	.42	+ 2.4	.46	.45	− 2.2	−1.13	− .27
			.500	.812	1.50	.30	b	cc	1.31	1.31	.0	.41	.39	− 4.9	.45	.42	− 6.7	−1.09	− .29
A-[illegible]....	[illegible]	[illegible]	.500	.812	1.50	.30	b		.41	.50	+21.9	.46	.44	− 4.3	.49	.47	− 4.1	−1.09	− .25
A-86....	2	5	.500	.812	1.50	.30	b		.23	.30	+30.4	.53	.53	.0	.57	.58	+ 1.8	−1.13	− .20
A-87....	1.5	5	.500	.812	1.50	.30	b		.20	.24	+20.0	.64	.64	.0	.69	.71	+ 2.9	−1.19	− .15
A-88....	1	5	.500	.812	1.50	.30	b	X	.25	—	—	.93	—	—	1.04	—	—	−1.39	− .01
A-89....	1	5	.500	.812	1.50	.30	c	X	.25	—	—	.69	—	—	.82	—	—	−1.03	+ .14
A-90....	1.5	5	.500	.812	1.50	.30	c		.20	.24	+20.0	.44	.46	+ 4.5	.49	.53	+ 8.2	− .88	+ .03
A-91....	2	5	.500	.812	1.50	.30	c		.21	.30	+42.8	.34	.35	+ 2.9	.38	.40	+ 5.3	− .81	− .02
A-92....	3	5	.500	.812	1.50	.30	c		.42	.50	+19.0	.29	.26	−10.3	.32	.29	− 9.4	− .73	− .03
A-93....	5	5	.500	.812	1.50	.30	c	cc	1.29	1.31	+ 1.5	.22	.21	− 4.5	.27	.24	−11.1	− .70	− .05
A-94....	5	5	.500	.812	1.50	.40	c	cc	1.24	1.31	+ 5.6	.19	.19	.0	.23	.22	− 4.3	− .60	− .04
A-95....	3	5	.500	.812	1.50	.40	c		.35	.50	+42.8	.25	.24	− 4.0	.28	.27	− 3.6	− .65	− .02
A-96....	2	5	.500	.812	1.50	.40	c		.21	.30	+42.8	.31	.32	+ 3.2	.35	.37	+ 5.7	− .77	− .02
A-97....	1.5	5	.500	.812	1.50	.40	c		.19	.24	+26.3	.41	.43	+ 4.9	.46	.50	+ 8.7	− .86	+ .01
A-98....	1	5	.500	.812	1.50	.40	c	X	.23	—	—	.67	—	—	.78	—	—	−1.04	+ .11
A-99....	1	5	.500	.812	1.50	.40	b	X	.22	—	—	.88	—	—	.99	—	—	−1.42	− .10
A-100...	1.5	5	.500	.812	1.50	.40	b		.19	.24	+26.3	.60	.61	+ 1.7	.65	.68	+ 4.6	−1.17	− .17
A-101...	2	5	.500	.812	1.50	.40	b		.22	.30	+36.4	.51	.50	− 2.0	.55	.55	.0	−1.11	− .20
A-102...	3	5	.500	.812	1.50	.40	b		.37	.50	+35.1	.44	.42	− 4.5	.47	.45	− 4.3	−1.06	− .24
A-103...	5	5	.500	.812	1.50	.40	b	cc	1.20	1.31	+ 9.2	.37	.37	.0	.41	.40	− 2.4	−1.06	− .29
A-104...	5	5	.500	.812	1.50	.00	c	cc	1.28	1.31	+ 2.3	.30	.29	− 3.3	.34	.32	− 5.9	− .88	− .11
A-105...	3	5	.500	.812	1.50	.00	c		.43	.50	+16.3	.37	.34	− 8.1	.40	.37	− 7.5	− .89	− .08
A-106...	2	5	.500	.812	1.50	.00	c		.22	.30	+36.4	.44	.42	− 4.5	.48	.47	− 2.1	− .91	− .03
A-107...	1.5	5	.500	.812	1.50	.00	c		.18	.24	+33.3	.52	.53	+ 1.9	.57	.60	+ 5.3	− .96	+ .02
A-108...	1	5	.500	.812	1.50	.00	c	X	.22	—	—	.82	—	—	.95	—	—	−1.08	+ .22
A-109...	1	5	.500	.812	1.50	.025	c	X	.24	—	—	.80	—	—	.91	—	—	−1.05	+ .22
A-110...	1.5	5	.500	.812	1.50	.025	c		.18	.24	+33.3	.51	.52	+ 2.0	.56	.59	+ 5.4	− .94	+ .03
A-111...	2	5	.500	.812	1.50	.025	c		.21	.30	+42.8	.40	.42	+ 5.0	.44	.47	+ 6.8	− .89	− .03
A-112...	3	5	.500	.812	1.50	.025	c		.40	.50	+25.0	.33	.33	.0	.35	.36	+ 2.9	− .86	− .08
A-113...	5	5	.500	.812	1.50	.025	c	cc	1.30	1.31	+ .8	.27	.28	+ 3.7	.31	.31	.0	− .86	− .11
A-114...	5	5	.500	.812	1.50	.05	c	cc	1.32	1.31	− .8	.25	.28	+12.0	.29	.31	+ 6.9	− .84	− .11

A-115...	3	5	.500	.812	1.50	.05	c		.38	.50	+31.6	.32	.33	+ 3.1	.35	.36	+ 2.9	− .84	− .07
A-116...	2	5	.500	.812	1.50	.05	c		.19	.30	+57.9	.39	.41	+ 5.1	.43	.46	+ 7.0	− .87	− .03
A-117...	1.5	5	.500	.812	1.50	.05	c		.18	.24	+33.3	.49	.52	+ 6.1	.55	.59	+ 7.3	− .93	+ .01
A-118...	1	5	.500	.812	1.50	.05	c	X	.18	—	—	.79	—	—	.88	—	—	−1.05	+ .21
A-119...	5	5	.500	.811	4.00	.05	c	cc	1.29	1.31	+ 1.5	—	—	—	—	—	—	—	—
A-120...	5	5	.500	.609	4.00	.05	c		1.40	1.56	+11.4	—	—	—	—	—	—	—	—
A-121...	5	5	.500	.406	4.00	.05	c		2.06	2.62	+27.2	—	—	—	—	—	—	—	—
A-122...	5	5	.500	.206	4.00	.05	c	x X	12.65	—	—	—	—	—	—	—	—	—	—
A-123...	3	5	.500	.205	4.00	.05	c	X	12.16	—	—	—	—	—	—	—	—	—	—
A-124...	3	5	.500	.403	4.00	.05	c		1.28	1.84	+43.7	—	—	—	—	—	—	—	—
A-125...	3	5	.500	.608	4.00	.05	c		.48	.77	+60.4	—	—	—	—	—	—	—	—
A-126...	3	5	.500	.810	4.00	.05	c		.37	.50	+35.1	—	—	—	—	—	—	—	—
A-127...	2	5	.500	.812	4.00	.05	c		.18	.30	+66.7	—	—	—	—	—	—	—	—
A-128...	2	5	.500	.609	4.00	.05	c		.33	.56	+69.7	—	—	—	—	—	—	—	—
A-129...	2	5	.500	.405	4.00	.05	c	X	1.19	—	—	—	—	—	—	—	—	—	—
A-130...	2	5	.500	.206	4.00	.05	c	X	10.90	—	—	—	—	—	—	—	—	—	—
A-131...	1.5	5	.500	.205	4.00	.05	c	X	10.17	—	—	—	—	—	—	—	—	—	—
A-132...	1.5	5	.500	.407	4.00	.05	c	X	1.25	—	—	—	—	—	—	—	—	—	—
A-133...	1.5	5	.500	.607	4.00	.05	c	X	.31	—	—	—	—	—	—	—	—	—	—
A-134...	1.5	5	.500	.817	4.00	.05	c		.16	.24	+50.0	—	—	—	—	—	—	—	—
A-135...	1.5	5	.500	.817	1.00	.05	c		.21	.24	+14.3	—	—	—	—	—	—	—	—
A-136...	1.5	5	.500	.607	1.00	.05	c	X	.34	—	—	—	—	—	—	—	—	—	—
A-137...	1.5	5	.500	.407	1.00	.05	c	X	1.21	—	—	—	—	—	—	—	—	—	—
A-138...	1.5	5	.500	.205	1.00	.05	c	X	8.42	—	—	—	—	—	—	—	—	—	—
A-139...	2	5	.500	.206	1.00	.05	c	X	8.78	—	—	—	—	—	—	—	—	—	—
A-140...	2	5	.500	.405	1.00	.05	c	X	1.16	—	—	—	—	—	—	—	—	—	—
A-141...	2	5	.500	.609	1.00	.05	c		.33	.56	+69.7	—	—	—	—	—	—	—	—
A-142...	2	5	.500	.812	1.00	.05	c		.22	.30	+36.4	—	—	—	—	—	—	—	—
A-143...	3	5	.500	.810	1.00	.05	c		.42	.50	+19.0	—	—	—	—	—	—	—	—
A-144...	3	5	.500	.608	1.00	.05	c		.50	.77	+54.0	—	—	—	—	—	—	—	—
A-145..	3	5	.500	.403	1.00	.05	c		1.36	1.84	+35.3	—	—	—	—	—	—	—	—
A-146...	3	5	.500	.205	1.00	.05	c	X	9.35	—	—	—	—	—	—	—	—	—	—
A-147...	5	5	.500	.206	1.00	.05	c	x X	10.85	—	—	—	—	—	—	—	—	—	—
A-148...	5	5	.500	.406	1.00	.05	c		2.34	2.62	+12.0	—	—	—	—	—	—	—	—
A-149...	5	5	.500	.609	1.00	.05	c		1.42	1.56	+ 9.8	—	—	—	—	—	—	—	—
A-150...	5	5	.500	.811	1.00	.05	c	cc	1.31	1.30	− 1.5	—	—	—	—	—	—	—	—
A-151...	5	5	.500	.811	.50	.05	c	cc	1.41	1.30	− 7.8	—	—	—	—	—	—	—	—
A-152...	5	5	.500	.609	.50	.05	c		1.51	1.56	+ 3.3	—	—	—	—	—	—	—	—
A-153...	5	5	.500	.406	.50	.05	c		2.41	2.61	+ 8.3	—	—	—	—	—	—	—	—
A-154...	5	5	.500	.205	.50	.05	c	x X	10.39	—	—	—	—	—	—	—	—	—	—
A-155...	3	5	.500	.205	.50	.05	c	X	9.08	—	—	—	—	—	—	—	—	—	—
A-156...	3	5	.500	.403	.50	.05	c		1.45	1.84	+26.9	—	—	—	—	—	—	—	—
A-157...	3	5	.500	.608	.50	.05	c		.57	.75	+31.6	—	—	—	—	—	—	—	—

[1]See footnotes at end of table, p. 21.

TABLE XII-1.—*Summary of tests* (Continued)

Series	B/D	Z_1/D	t_c/D	Z_2/D	L_1/D	S	Barrel entrance	Notes[1]	K_c Observed	K_c Computed	K_c Error	K_t Observed	K_t Computed	K_t Error	K_e Observed	K_e Computed	K_e Error	h_c/h_{vp} @ D/2 Crown	h_c/h_{vp} @ D/2 Invert
											Percent			*Percent*			*Percent*		
A-158...	3	5	0.500	0.810	0.50	0.05	c		0.53	0.50	− 5.7	—	—	—	—	—	—	—	—
A-159...	2	5	.500	.812	.50	.05	c	X	.38	—	—	—	—	—	—	—	—	—	—
A-160...	2	5	.500	.609	.50	.05	c	X	.43	—	—	—	—	—	—	—	—	—	—
A-161...	2	5	.500	.405	.50	.05	c	X	1.29	—	—	—	—	—	—	—	—	—	—
A-162...	2	5	.500	.206	.50	.05	c	X	8.55	—	—	—	—	—	—	—	—	—	—
A-163...	1.5	5	.500	.205	.50	.05	c	X	8.50	—	—	—	—	—	—	—	—	—	—
A-164...	1.5	5	.500	.407	.50	.05	c	X	1.39	—	—	—	—	—	—	—	—	—	—
A-165...	1.5	5	.500	.607	.50	.05	c	X	.40	—	—	—	—	—	—	—	—	—	—
A-166...	1.5	5	.500	.817	.50	.05	c	X	.64	—	—	—	—	—	—	—	—	—	—
A-167...	1.5	5	.500	.817	.50	.05	c	X	.58	—	—	—	—	—	—	—	—	—	—
A-168...	2	5	.500	.812	.50	.05	c	X	.37	—	—	—	—	—	—	—	—	—	—
A-169...	2	5	.500	.186	4.00	.05	c	x X	14.04	—	—	—	—	—	—	—	—	—	—
A-170...	2	5	.500	.583	4.00	.05	c		.35	.62	+77.1	—	—	—	—	—	—	—	—
A-171...	2	5	.500	.788	4.00	.05	c		.20	.32	+60.0	—	—	—	—	—	—	—	—
A-172...	1.5	5	.500	.787	4.00	.05	c		.18	.26	+44.4	—	—	—	—	—	—	—	—
A-173...	1.5	5	.500	.587	4.00	.05	c	X	.36	—	—	—	—	—	—	—	—	—	—
A-174...	1.5	5	.500	.187	4.00	.05	c	x X	13.69	—	—	—	—	—	—	—	—	—	—
A-175...	3	5	.500	.192	4.00	.05	c	X	15.13	—	—	—	—	—	—	—	—	—	—
A-176...	5	5	.500	.189	4.00	.05	c	x X	16.25	—	—	—	—	—	—	—	—	—	—
A-177...	5	5	.500	.388	4.00	.05	c		2.36	2.83	+19.9	—	—	—	—	—	—	—	—
A-178...	1.5	5	.500	.607	.50	.05	c	X	.37	—	—	—	—	—	—	—	—	—	—
A-179...	1.5	5	.500	.205	.50	.05	c	X	8.30	—	—	—	—	—	—	—	—	—	—
A-180...	2	5	.500	.206	.50	.05	c	X	8.31	—	—	—	—	—	—	—	—	—	—
A-181...	3	5	.500	.205	.50	.05	c	X	8.79	—	—	—	—	—	—	—	—	—	—
A-182...	5	5	.500	.206	.50	.05	c	X	9.99	—	—	—	—	—	—	—	—	—	—
A-183...	5	5	.500	.786	3.00	.05	c	cc	1.25	1.33	+ 6.4	—	—	—	—	—	—	—	—
A-184...	5	5	.500	.584	3.00	.05	c		1.41	1.62	+14.9	—	—	—	—	—	—	—	—
A-185...	5	5	.500	.388	3.00	.05	c		2.35	2.83	+20.4	—	—	—	—	—	—	—	—
A-186...	5	5	.500	.189	3.00	.05	c	x X	15.45	—	—	—	—	—	—	—	—	—	—
A-187...	3	5	.500	.192	3.00	.05	c	X	14.17	—	—	—	—	—	—	—	—	—	—
A-188...	3	5	.500	.388	3.00	.05	c		1.53	2.02	+32.0	—	—	—	—	—	—	—	—
A-189...	3	5	.500	.583	3.00	.05	c		.51	.82	+60.8	—	—	—	—	—	—	—	—
A-190...	3	5	.500	.785	3.00	.05	c		.38	.52	+36.8	—	—	—	—	—	—	—	—
A-191...	2	5	.500	.787	3.00	.05	c		.17	.32	+88.2	—	—	—	—	—	—	—	—
A-192...	2	5	.500	.581	3.00	.05	c		.34	.62	+82.3	—	—	—	—	—	—	—	—
A-193...	2	5	.500	.386	3.00	.05	c	X	1.51	—	—	—	—	—	—	—	—	—	—
A-194...	2	5	.500	.188	3.00	.05	c	X	13.26	—	—	—	—	—	—	—	—	—	—
A-195...	1.5	5	.500	.187	3.00	.05	c	X	12.32	—	—	—	—	—	—	—	—	—	—
A-196...	1.5	5	.500	.387	3.00	.05	c	X	1.63	—	—	—	—	—	—	—	—	—	—

A-197...	1.5	5	.500	.587	3.00	.05	c	X	.32	—	—	—	—	—	—	—	—	—	—
A-198...	1.5	5	.500	.787	3.00	.05	c		.15	.26	+73.3	—	—	—	—	—	—	—	—
A-199...	1.5	5	.500	.387	3.00	.05	c	X	1.68	—	—	—	—	—	—	—	—	—	—
A-200...	1.5	5	.500	.187	3.00	.05	c	X	11.92	—	—	—	—	—	—	—	—	—	—
A-201...	1.5	5	.500	.587	3.00	.05	c	X	.35	—	—	—	—	—	—	—	—	—	—
A-202...	1.5	5	.500	.787	3.00	.05	c		.18	.26	+44.4	—	—	—	—	—	—	—	—
A-203...	1.5	5	.500	.787	3.00	.05	c		.20	.26	+30.0	—	—	—	—	—	—	—	—
A-204...	2	5	.500	.581	3.00	.05	c		.36	.62	+72.2	—	—	—	—	—	—	—	—
A-205...	2	5	.500	.386	3.00	.05	c	X	1.65	—	—	—	—	—	—	—	—	—	—
A-206...	2	5	.500	.188	3.00	.05	c	X	13.36	—	—	—	—	—	—	—	—	—	—
A-207...	2	5	.500	.192	3.00	.05	c	X	14.94	—	—	—	—	—	—	—	—	—	—
A-208...	3	5	.500	.388	3.00	.05	c		1.59	2.02	+27.0	—	—	—	—	—	—	—	—
A-209...	3	5	.500	.583	3.00	.05	c		.54	.82	+51.8	—	—	—	—	—	—	—	—
A-210...	3	5	.500	.785	3.00	.05	c		.38	.52	+36.8	—	—	—	—	—	—	—	—
A-211...	5	5	.500	.786	3.00	.05	c	cc	1.32	1.33	+ .7	—	—	—	—	—	—	—	—
A-212...	5	5	.500	.584	3.00	.05	c		1.45	1.62	+11.7	—	—	—	—	—	—	—	—
A-213...	5	5	.500	.388	3.00	.05	c		2.37	2.83	+19.4	—	—	—	—	—	—	—	—
A-214...	5	5	.500	.189	3.00	.05	c	x X	15.77	—	—	—	—	—	—	—	—	—	—
A-215...	5	5	.500	.786	2.00	.05	c	cc	1.47	1.32	− 1.0	—	—	—	—	—	—	—	—
A-216...	5	5	.500	.584	2.00	.05	c		1.66	1.62	− 2.4	—	—	—	—	—	—	—	—
A-217...	5	5	.500	.390	2.00	.05	c		2.67	2.80	+ 4.8	—	—	—	—	—	—	—	—
A-218...	5	5	.500	.187	2.00	.05	c	x X	15.40	—	—	—	—	—	—	—	—	—	—
A-219...	3	5	.500	.188	2.00	.05	c	X	13.97	—	—	—	—	—	—	—	—	—	—
A-220...	3	5	.500	.387	2.00	.05	c		1.74	2.04	+17.2	—	—	—	—	—	—	—	—
A-221...	3	5	.500	.587	2.00	.05	c		.57	.81	+42.1	—	—	—	—	—	—	—	—
A-222...	3	5	.500	.787	2.00	.05	c		.41	.52	+26.8	—	—	—	—	—	—	—	—
A-223...	2	5	.500	.786	2.00	.05	c		.20	.32	+60.0	—	—	—	—	—	—	—	—
A-224...	2	5	.500	.583	2.00	.05	c		.36	.62	+72.2	—	—	—	—	—	—	—	—
A-225...	2	5	.500	.386	2.00	.05	c	X	1.57	—	—	—	—	—	—	—	—	—	—
A-226...	2	5	.500	.186	2.00	.05	c	X	12.80	—	—	—	—	—	—	—	—	—	—
A-227...	1.5	5	.500	.188	2.00	.05	c	X	11.74	—	—	—	—	—	—	—	—	—	—
A-228...	1.5	5	.500	.388	2.00	.05	c	X	1.45	—	—	—	—	—	—	—	—	—	—
A-229...	1.5	5	.500	.586	2.00	.05	c	X	.31	—	—	—	—	—	—	—	—	—	—
A-230...	1.5	5	.500	.788	2.00	.05	c		.18	.26	+44.4	—	—	—	—	—	—	—	—
A-231...	5	5	.500	.788	2.00	.05	c	cc	1.31	1.32	+ .8	—	—	—	—	—	—	—	—
A-232...	5	5	.500	.585	2.00	.05	c		1.52	1.62	+ 6.6	—	—	—	—	—	—	—	—
A-233...	5	5	.500	.388	2.00	.05	c		2.46	2.83	+15.0	—	—	—	—	—	—	—	—
A-234...	5	5	.500	.189	2.00	.05	c	x X	15.72	—	—	—	—	—	—	—	—	—	—
A-235...	5	5	.500	.786	1.41	.05	c	cc	1.35	1.32	− 2.2	—	—	—	—	—	—	—	—
A-236...	5	5	.500	.585	1.41	.05	c		1.49	1.62	+ 8.7	—	—	—	—	—	—	—	—
A-237...	5	5	.500	.389	1.41	.05	c		2.55	2.82	+10.6	—	—	—	—	—	—	—	—
A-238...	5	5	.500	.189	1.41	.05	c	x X	14.73	—	—	—	—	—	—	—	—	—	—
A-239...	3	5	.500	.189	1.41	.05	c	X	13.02	—	—	—	—	—	—	—	—	—	—

[1] See footnotes at end of table, p. 21.

TABLE XII-1.—*Summary of tests* (Continued)

Series	B/D	Z_1/D	t_c/D	Z_p/D	L_p/D	$\dot{S}$	Barrel entrance	Notes[1]	K_c Observed	K_c Computed	K_c Error	K_r Observed	K_r Computed	K_r Error	K_s Observed	K_s Computed	K_s Error	h_a/h_p @ D/2 Crown	h_a/h_p @ D/2 Invert
											Percent			Percent			Percent		
A-240...	3	5	0.500	0.392	1.41	.05	c		1.62	1.97	+21.6	—	—	—	—	—	—	—	—
A-241...	3	5	.500	.588	1.41	.05	c		.55	.80	+45.4	—	—	—	—	—	—	—	—
A-242...	3	5	.500	.791	1.41	.05	c		.40	.51	+27.5	—	—	—	—	—	—	—	—
A-243...	2	5	.500	.786	1.41	.05	c		.22	.32	+45.4	—	—	—	—	—	—	—	—
A-244...	2	5	.500	.586	1.41	.05	c		.34	.61	+79.4	—	—	—	—	—	—	—	—
A-245...	2	5	.500	.388	1.41	.05	c	X	1.44	—	—	—	—	—	—	—	—	—	—
A-246...	2	5	.500	.187	1.41	.05	c	X	12.18	—	—	—	—	—	—	—	—	—	—
A-247...	1.5	5	.500	.189	1.41	.05	c	X	10.89	—	—	—	—	—	—	—	—	—	—
A-248...	1.5	5	.500	.390	1.41	.05	c	X	1.37	—	—	—	—	—	—	—	—	—	—
A-249...	1.5	5	.500	.588	1.41	.05	c	X	.30	—	—	—	—	—	—	—	—	—	—
A-250...	1.5	5	.500	.788	1.41	.05	c		.19	.26	+36.8	—	—	—	—	—	—	—	—
A-251...	1.5	5	.500	.789	1.00	.05	c		.22	.26	+18.2	—	—	—	—	—	—	—	—
A-252...	1.5	5	.500	.587	1.00	.05	c	X	.36	—	—	—	—	—	—	—	—	—	—
A-253...	1.5	5	.500	.391	1.00	.05	c	X	1.39	—	—	—	—	—	—	—	—	—	—
A-254...	1.5	5	.500	.188	1.00	.05	c	X	10.73	—	—	—	—	—	—	—	—	—	—
A-255...	2	5	.500	.188	1.00	.05	c	X	11.35	—	—	—	—	—	—	—	—	—	—
A-256...	2	5	.500	.389	1.00	.05	c	X	1.40	—	—	—	—	—	—	—	—	—	—
A-257...	2	5	.500	.586	1.00	.05	c		.37	.61	+64.9	—	—	—	—	—	—	—	—
A-258...	2	5	.500	.788	1.00	.05	c		.26	.32	+23.1	—	—	—	—	—	—	—	—
A-259...	3	5	.500	.787	1.00	.05	c		.45	.52	+15.6	—	—	—	—	—	—	—	—
A-260...	3	5	.500	.587	1.00	.05	c		.52	.81	+55.8	—	—	—	—	—	—	—	—
A-261...	3	5	.500	.392	1.00	.05	c		1.59	1.97	+23.9	—	—	—	—	—	—	—	—
A-262...	3	5	.500	.187	1.00	.05	c	X	12.39	—	—	—	—	—	—	—	—	—	—
A-263...	5	5	.500	.191	1.00	.05	c	X	13.99	—	—	—	—	—	—	—	—	—	—
A-264...	5	5	.500	.392	1.00	.05	c		2.57	2.78	+ 8.2	—	—	—	—	—	—	—	—
A-265...	5	5	.500	.586	1.00	.05	c		1.52	1.62	+ 6.6	—	—	—	—	—	—	—	—
A-266...	5	5	.500	.788	1.00	.05	c	cc	1.41	1.32	− 6.4	—	—	—	—	—	—	—	—
A-267...	5	5	.500	.788	1.00	.05	c	cc	1.42	1.32	− 7.0	—	—	—	—	—	—	—	—
A-268...	3	5	.500	.786	1.00	.05	c		.45	.52	+15.6	—	—	—	—	—	—	—	—
A-269...	2	5	.500	.786	1.00	.05	c		.24	.32	+33.3	—	—	—	—	—	—	—	—
A-270...	1.5	5	.500	.189	.75	.05	c	X	10.26	—	—	—	—	—	—	—	—	—	—
A-271...	1.5	5	.500	.389	.75	.05	c	X	1.37	—	—	—	—	—	—	—	—	—	—
A-272...	1.5	5	.500	.586	.75	.05	c	X	.40	—	—	—	—	—	—	—	—	—	—
A-273...	1.5	5	.500	.790	.75	.05	c	X	.23	.26	+13.0	—	—	—	—	—	—	—	—
A-274...	2	5	.500	.787	.75	.05	c		.27	.32	+18.5	—	—	—	—	—	—	—	—
A-275...	2	5	.500	.584	.75	.05	c		.37	.62	+67.6	—	—	—	—	—	—	—	—
A-276...	2	5	.500	.389	.75	.05	c	X	1.37	—	—	—	—	—	—	—	—	—	—
A-277...	2	5	.500	.186	.75	.05	c	X	10.67	—	—	—	—	—	—	—	—	—	—
A-278...	3	5	.500	.191	.75	.05	c	X	11.05	—	—	—	—	—	—	—	—	—	—
A-279...	3	5	.500	.394	.75	.05	c		1.49	1.95	+30.9	—	—	—	—	—	—	—	—

A-280...	3	5	.500	.586	.75	.05	c		.55		.81	+47.3		—	—	—	—	—	—	—	—
A-281...	3	5	.500	.787	.75	.05	c		.48		.52	+ 8.3		—	—	—	—	—	—	—	—
A-282...	5	5	.500	.787	.75	.05	c	cc	1.35		1.32	− 2.2		—	—	—	—	—	—	—	—
A-283...	5	5	.500	.584	.75	.05	c		1.53		1.62	+ 5.9		—	—	—	—	—	—	—	—
A-284...	5	5	.500	.390	.75	.05	c		2.57		2.80	+ 8.9		—	—	—	—	—	—	—	—
A-285...	5	5	.500	.189	.75	.05	c	x X	12.73		—	—		—	—	—	—	—	—	—	—
A-286...	5	5	.500	.789	.51	.05	c	cc	1.41		1.32	− 6.4		—	—	—	—	—	—	—	—
A-287...	5	5	.500	.583	.51	.05	c		1.53		1.62	+ 5.8		—	—	—	—	—	—	—	—
A-288...	5	5	.500	.392	.51	.05	c		2.48		2.78	+12.1		—	—	—	—	—	—	—	—
A-289...	5	5	.500	.191	.51	.05	c	x X	11.71		—	—		—	—	—	—	—	—	—	—
A-290...	3	5	.500	.190	.51	.05	c	X	10.77		—	—		—	—	—	—	—	—	—	—
A-291...	3	5	.500	.391	.51	.05	c		1.51		1.98	+31.1		—	—	—	—	—	—	—	—
A-292...	3	5	.500	.585	.51	.05	c		.66		.81	+22.7		—	—	—	—	—	—	—	—
A-293...	3	5	.500	.787	.51	.05	c		.55		.52	− 5.5		—	—	—	—	—	—	—	—
A-294...	2	5	.500	.787	.51	.05	c	X	.39		—	—		—	—	—	—	—	—	—	—
A-295...	2	5	.500	.583	.51	.05	c	X	.49		—	—		—	—	—	—	—	—	—	—
A-296...	2	5	.500	.388	.51	.05	c	X	1.44		—	—		—	—	—	—	—	—	—	—
A-297...	2	5	.500	.186	.51	.05	c	X	10.51		—	—		—	—	—	—	—	—	—	—
A-298...	1.5	5	.500	.189	.51	.05	c	X	10.09		—	—		—	—	—	—	—	—	—	—
A-299...	1.5	5	.500	.387	.51	.05	c	X	1.61		—	—		—	—	—	—	—	—	—	—
A-300...	1.5	5	.500	.586	.51	.05	c	X	.42		—	—		—	—	—	—	—	—	—	—
A-301...	1.5	5	.500	.789	.51	.05	c	X	.56		—	—		—	—	—	—	—	—	—	—
A-302...	1.5	5	.500	.789	.51	.05	c	j X	.41	.63	—	—		—	—	—	—	—	—	—	—
A-303...	1.5	5	.500	.692	.51	.05	c	j X	.33	.38	—	—		—	—	—	—	—	—	—	—
A-304...	1.5	5	.500	.585	.51	.05	c	j X	.42	.49	—	—		—	—	—	—	—	—	—	—
A-305...	2	5	.500	.583	.51	.05	c	j X	.45	.50	—	—		—	—	—	—	—	—	—	—
A-306...	2	5	.500	.690	.51	.05	c	j X	.37	.47	—	—		—	—	—	—	—	—	—	—
A-307...	2	5	.500	.786	.51	.05	c	j X	.42	.47	—	—		—	—	—	—	—	—	—	—
A-308...	3	5	.500	.786	.51	.05	c	j	.54	.60	.52	− 3.7	−13.3	—	—	—	—	—	—	—	—
A-309...	3	5	.500	.690	.51	.05	c	j	.56	.60	.62	+10.7	+ 3.3	—	—	—	—	—	—	—	—
A-310...	3	5	.500	.582	.51	.05	c	j	.64	.68	.82	+28.1	+20.6	—	—	—	—	—	—	—	—
A-311...	1.5	5	.500	.806	.51	.05	c	g X	.25		—	—		—	—	—	—	—	—	—	—
A-312...	1.5	5	.500	.618	.51	.05	c	g X	.46		—	—		—	—	—	—	—	—	—	—
A-313...	2	5	.500	.614	.51	.05	c	g X	.43		—	—		—	—	—	—	—	—	—	—
A-314...	2	5	.500	.808	.51	.05	c	g X	.29		—	—		—	—	—	—	—	—	—	—
A-315...	3	5	.500	.811	.51	.05	c	g	.50		.50	.0		—	—	—	—	—	—	—	—
A-316...	3	5	.500	.611	.51	.05	c	g	.62		.75	+21.0		—	—	—	—	—	—	—	—
A-317...	3	5	.500	.612	.75	.05	c	g	.54		.75	+38.9		—	—	—	—	—	—	—	—
A-318...	3	5	.500	.808	.75	.05	c	g	.45		.50	+11.1		—	—	—	—	—	—	—	—
A-319...	3	5	.500	.809	1.00	.05	c	g	.44		.50	+13.6		—	—	—	—	—	—	—	—
A-320...	3	5	.500	.613	1.00	.05	c	g	.52		.75	+42.3		—	—	—	—	—	—	—	—
A-321...	2	5	.500	.613	1.00	.05	c	g	.31		.55	+77.4		—	—	—	—	—	—	—	—
A-322...	2	5	.500	.809	1.00	.05	c	g	.24		.30	+25.0		—	—	—	—	—	—	—	—
A-323...	2	5	.500	.809	.75	.05	c	g	.27		.30	+11.1		—	—	—	—	—	—	—	—
A-324...	2	5	.500	.613	.75	.05	c	g	.35		.55	+57.1		—	—	—	—	—	—	—	—

[1]See footnotes at end of table, p. 21.

See footnotes at end of table, p. 21.

TABLE XII–1.—*Summary of tests* (Continued)

Series	B/D	Z_i/D	t_s/D	Z_p/D	L_s/D	S	Barrel entrance	Notes[1]	K_e Observed	K_e Computed	K_e Error	K_s Observed	K_s Computed	K_s Error	K_u Observed	K_u Computed	K_u Error	h_n/h_{vp} @ D/2 Crown	h_n/h_{vp} @ D/2 Invert
											Percent			*Percent*			*Percent*		
A-325...	1.5	5	0.500	0.613	0.75	0.05	c	g X	0.33	—	—	—	—	—	—	—	—	—	—
A-326...	1.5	5	.500	.808	.75	.05	c	g X	.26	—	—	—	—	—	—	—	—	—	—
A-327...	1.5	5	.500	.807	1.00	.05	c	g	.19	.024	+26.3	—	—	—	—	—	—	—	—
A-328...	1.5	5	.500	.612	1.00	.05	c	g X	.28	—	—	—	—	—	—	—	—	—	—
A-329...	1.5	5	.500	.809	.29	.05	c	g X	.31	—	—	—	—	—	—	—	—	—	—
A-330...	1.5	5	.500	.616	.29	.05	c	g X	.46	—	—	—	—	—	—	—	—	—	—
A-331...	1.5	5	.500	.417	.29	.05	c	g j X	1.71 1.60	—	—	—	—	—	—	—	—	—	—
A-332...	1.5	5	.500	.212	.29	.05	c	g j X	8.25 8.08	—	—	—	—	—	—	—	—	—	—
A-333...	2	5	.500	.213	.29	.05	c	g j X	8.33 8.08	—	—	—	—	—	—	—	—	—	—
A-334...	2	5	.500	.413	.29	.05	c	g X	1.52	—	—	—	—	—	—	—	—	—	—
A-335...	2	5	.500	.615	.29	.05	c	g X	.50	—	—	—	—	—	—	—	—	—	—
A-336...	2	5	.500	.808	.29	.05	c	g X	.34	—	—	—	—	—	—	—	—	—	—
A-337...	3	5	.500	.810	.29	.05	c	g X	.56	—	—	—	—	—	—	—	—	—	—
A-338...	3	5	.500	.613	.29	.05	c	g X	.71	—	—	—	—	—	—	—	—	—	—
A-339...	3	5	.500	.413	.29	.05	c	g X	1.50	—	—	—	—	—	—	—	—	—	—
A-340...	3	5	.500	.209	.29	.05	c	g X	8.39	—	—	—	—	—	—	—	—	—	—
A-341...	5	5	.500	.209	.29	.05	c	g x X	9.25	—	—	—	—	—	—	—	—	—	—
A-342...	5	5	.500	.415	.29	.05	c	g X	2.34	—	—	—	—	—	—	—	—	—	—
A-343...	5	5	.500	.616	.29	.05	c	g X	1.68	—	—	—	—	—	—	—	—	—	—
A-344...	5	5	.500	.809	.29	.05	c	g X	1.47	—	—	—	—	—	—	—	—	—	—
A-345...	1.5	5	.500	.786	.29	.05	c	j X	.80 .66	—	—	—	—	—	—	—	—	—	—
A-346...	1.5	5	.500	.583	.29	.05	c	j X	.93 .82	—	—	—	—	—	—	—	—	—	—
A-347...	1.5	5	.500	.386	.29	.05	c	j X	1.85 1.75	—	—	—	—	—	—	—	—	—	—
A-348...	1.5	5	.500	.186	.29	.05	c	j X	11.21 11.08	—	—	—	—	—	—	—	—	—	—
A-349...	2	5	.500	.186	.29	.05	c	X	10.99	—	—	—	—	—	—	—	—	—	—
A-350...	2	5	.500	.385	.29	.05	c	X	1.66	—	—	—	—	—	—	—	—	—	—
A-351...	2	5	.500	.582	.29	.05	c	X	.85	—	—	—	—	—	—	—	—	—	—
A-352...	2	5	.500	.786	.29	.05	c	X	.61	—	—	—	—	—	—	—	—	—	—
A-353...	3	5	.500	.787	.29	.05	c	X	.70	—	—	—	—	—	—	—	—	—	—
A-354...	3	5	.500	.582	.29	.05	c	X	.91	—	—	—	—	—	—	—	—	—	—
A-355...	3	5	.500	.387	.29	.05	c	X	1.78	—	—	—	—	—	—	—	—	—	—
A-356...	3	5	.500	.186	.29	.05	c	X	10.69	—	—	—	—	—	—	—	—	—	—
A-357...	5	5	.500	.189	.29	.05	c	x X	12.18	—	—	—	—	—	—	—	—	—	—
A-358...	5	5	.500	.388	.29	.05	c	X	2.66	—	—	—	—	—	—	—	—	—	—
A-359...	5	5	.500	.584	.29	.05	c	X	1.89	—	—	—	—	—	—	—	—	—	—
A-360...	5	5	.500	.788	.29	.05	c	X	1.65	—	—	—	—	—	—	—	—	—	—
A-361...	3	5	.500	.690	.29	.05	c	X	.78	—	—	—	—	—	—	—	—	—	—
A-362...	2	5	.500	.690	.29	.05	c	X	.71	—	—	—	—	—	—	—	—	—	—
A-363...	1.5	5	.500	.692	.29	.05	c	j X	1.25 1.05	—	—	—	—	—	—	—	—	—	—
A-364...	1.5	5	.500	.691	.29	.05	c	j X	1.15 1.04	—	—	—	—	—	—	—	—	—	—

A-365...	1.5	5	.500	.786	.29	.05	c	j X	.88 .76	—	—	—	—	—	—	—	—	—	—
A-366...	5	5	.157	.206	4.00	.204	a	X	14.55	—	—	.35	—	—	.69	—	—	– .77	– .05
A-367...	3	5	.157	.222	4.00	.204	a	h X	11.02	—	—	.33	—	—	1.05	—	—	– .50	+ .11
A-368...	2	5	.157	.222	4.00	.204	a	X	10.44	—	—	.42	—	—	1.96	—	—	– .34	+ .28
A-369...	1.5	5	.157	.223	4.00	.204	a	x X	10.09	—	—	.51	—	—	3.16	—	—	– .20	+ .44
A-370...	1.5	5	.157	.417	4.00	.204	a	X	2.36	—	—	.57	—	—	1.19	—	—	– .87	+ .15
A-371...	2	5	.157	.414	4.00	.204	a	X	2.55	—	—	.48	—	—	.85	—	—	– .87	+ .06
A-372...	3	5	.157	.412	4.00	.204	a	h	2.67	2.21	–17.6	.44	.43	– 2.3	.61	.58	– 4.9	– .91	– .06
A-373...	5	5	.157	.398	4.00	.204	a		3.78	3.17	–16.1	.41	.38	– 7.3	.50	.46	– 8.0	– .96	– .15
A-374...	5	5	.157	.604	4.00	.204	a		2.21	2.04	– 7.7	.40	.38	– 5.0	.45	.43	– 4.4	–1.02	– .22
A-375...	3	5	.157	.614	4.00	.204	a		1.24	1.21	– 1.6	.45	.43	– 4.4	.52	.51	– 1.9	–1.02	– .15
A-376...	2	5	.157	.613	4.00	.204	a		1.08	1.02	– 5.6	.51	.51	.0	.67	.67	.0	–1.02	– .08
A-377...	1.5	5	.157	.614	4.00	.204	a	X	1.08	—	—	.61	—	—	.88	—	—	–1.06	+ .02
A-378...	1.5	5	.157	.813	4.00	.204	a		.75	.71	– 5.3	.61	.62	+ 1.6	.79	.81	+ 2.5	–1.10	– .01
A-379...	2	5	.157	.813	4.00	.204	a		.77	.77	.0	.52	.51	– 1.9	.63	.63	.0	–1.06	– .09
A-380...	3	5	.157	.812	4.00	.204	a		.95	.97	+ 2.1	.46	.43	– 6.5	.52	.50	– 3.8	–1.02	– ..16
A-381...	5	5	.157	.803	4.00	.204	a	cc	1.89	1.78	– 5.8	.39	.38	– 2.6	.44	.42	– 4.5	–1.04	– .24
A-382...	5	5	.242	.207	3.92	.204	a	X	12.89	—	—	.35	—	—	.65	—	—	– .83	– .10
A-383...	3	5	.242	.221	3.92	.204	a	X	10.78	—	—	.32	—	—	1.03	—	—	– .46	+ .12
A-384...	2	5	.242	.221	3.92	.204	a	w X	9.84	—	—	.45	—	—	1.91	—	—	– .49	+ .19
A-385...	1.5	5	.242	.222	3.92	.204	a	w X	9.62	—	—	.49	—	—	3.03	—	—	– .46	+ .31
A-386...	1.5	5	.242	.414	3.92	.204	a	X	1.96	—	—	.58	—	—	1.09	—	—	–1.01	+ .02
A-387...	2	5	.242	.414	3.92	.204	a	X	1.98	—	—	.50	—	—	.79	—	—	– .96	– .02
A-388...	3	5	.242	.410	3.92	.204	a		2.15	2.03	– 5.6	.43	.43	.0	.57	.57	.0	– .99	– .13
A-389...	5	5	.242	.398	3.92	.204	a		3.23	2.97	– 8.0	.38	.38	.0	.46	.45	– 2.2	–1.02	– .22
A-390...	5	5	.242	.602	3.92	.204	a		1.90	1.84	– 3.2	.39	.38	– 2.6	.43	.43	.0	–1.04	– .25
A-391...	3	5	.242	.608	3.92	.204	a		.92	1.02	+10.9	.44	.43	– 2.3	.50	.50	.0	–1.03	– .18
A-392...	2	5	.242	.611	3.92	.204	a		.77	.82	+ 6.5	.51	.51	.0	.63	.64	+ 1.6	–1.06	– .10
A-393...	1.5	5	.242	.613	3.92	.204	a	X	.77	—	—	.58	—	—	.78	—	—	–1.12	– .05
A-394...	1.5	5	.242	.813	3.92	.204	a		.39	.51	+30.8	.61	.62	+ 1.6	.71	.76	+ 7.0	–1.14	– .05
A-395...	2	5	.242	.811	3.92	.204	a		.41	.57	+39.0	.52	.51	– 1.9	.58	.60	+ 3.4	–1.07	– .13
A-396...	3	5	.242	.808	3.92	.204	a		.54	.77	+42.6	.45	.43	– 4.4	.49	.48	– 2.0	–1.04	– .20
A-397...	5	5	.242	.801	3.92	.204	a	cc	1.51	1.58	+ 4.6	.39	.38	– 2.6	.43	.42	– 2.3	–1.04	– .26
A-398...	5	5	.331	.204	3.83	.204	a	X	14.74	—	—	.32	—	—	.68	—	—	– .77	– .06
A-399...	3	5	.331	.220	3.83	.204	a	X	9.59	—	—	.37	—	—	1.01	—	—	– .85	– .10
A-400...	2	5	.331	.213	3.83	.204	a	X	10.57	—	—	.38	—	—	2.07	—	—	–0.37	+ .22
A-401...	1.5	5	.331	.213	3.83	.204	a	w X	10.93	—	—	.46	—	—	3.38	—	—	– .38	+ .31
A-402...	1.5	5	.331	.404	3.83	.204	a	X	1.66	—	—	.56	—	—	1.00	—	—	–1.07	– .05
A-403...	2	5	.331	.404	3.83	.204	a	X	1.66	—	—	.49	—	—	.74	—	—	– .99	– .06
A-404...	3	5	.331	.403	3.83	.204	a		1.84	1.95	+ 6.0	.42	.43	+ 2.4	.54	.56	+ 3.7	–1.00	– .15
A-405...	5	5	.331	.393	3.83	.204	a		2.92	2.88	– 1.4	.36	.38	+ 5.6	.43	.45	+ 4.6	–1.01	– .22
A-406...	5	5	.331	.596	3.83	.204	a		1.49	1.71	+14.8	.37	.38	+ 2.7	.41	.42	+ 2.4	–1.03	– .25
A-407...	3	5	.331	.606	3.83	.204	a		.64	.88	+37.5	.44	.43	– 2.3	.48	.49	+ 2.1	–1.02	– .18
A-408...	2	5	.331	.608	3.83	.204	a		.47	.67	+42.6	.50	.51	+ 2.0	.57	.61	+ 7.0	–1.05	– .12

[1]See footnotes at end of table, p. 21.

Table XII-1.—*Summary of tests* (Continued)

Series	B/D	Z_1/D	t_o/D	Z_o/D	L_o/D	S	Barrel entrance	Notes[1]	K_c Observed	K_c Computed	K_c Error	K_t Observed	K_t Computed	K_t Error	K_e Observed	K_e Computed	K_e Error	h_c/h_{vp} @ D/2 Crown	h_c/h_{vp} @ D/2 Invert
											Percent			Percent			Percent		
A-409...	1.5	5	0.331	0.604	3.83	0.204	a	X	0.45	—	—	0.58	—	—	0.70	—	—	−1.12	−0.08
A-410...	1.5	5	.331	.804	3.83	.204	a		.21	0.36	+71.4	.59	0.62	+ 5.1	.65	0.72	+10.8	−1.12	− .07
A-411...	2	5	.331	.806	3.83	.204	a		.23	.42	+82.6	.50	.51	+ 2.0	.53	.57	+ 7.5	−1.06	− .15
A-412...	3	5	.331	.804	3.83	.204	a		.44	.62	+40.9	.43	.43	.0	.45	.47	+ 4.4	−1.03	− .21
A-413...	5	5	.331	.800	3.83	.204	a	cc	1.28	1.43	+11.7	.37	.38	+ 2.7	.41	.42	+ 2.4	−1.03	− .25
A-414...	5	5	.658	.203	3.51	.204	a	x X	13.65	—	—	.36	—	—	.68	—	—	− .81	− .08
A-415...	3	5	.658	.211	3.51	.204	a	X	11.19	—	—	.39	—	—	1.14	—	—	− .82	− .05
A-416...	2	5	.658	.211	3.51	.204	a	w X	10.01	—	—	.45	—	—	1.95	—	—	− .89	− .02
A-417...	1.5	5	.658	.212	3.51	.204	a	w X	9.36	—	—	.54	—	—	3.03	—	—	− .70	+ .11
A-418...	1.5	5	.658	.405	3.51	.204	a	X	1.51	—	—	.56	—	—	.97	—	—	−1.06	− .09
A-419...	2	5	.658	.405	3.51	.204	a	X	1.23	—	—	.47	—	—	.66	—	—	−1.06	− .16
A-420...	3	5	.658	.405	3.51	.204	a		1.24	1.82	+46.8	.41	.43	+ 4.9	.49	.56	+14.3	−1.03	− .20
A-421...	5	5	.658	.392	3.51	.204	a		2.35	2.78	+18.3	.36	.38	+ 5.6	.51	.45	+ 9.8	−1.04	− .25
A-422...	5	5	.658	.597	3.51	.204	a		1.41	1.59	+12.8	.37	.38	+ 2.7	.40	.42	+ 5.0	−1.04	− .20
A-423...	3	5	.658	.605	3.51	.204	a		.53	.76	+43.4	.42	.43	+ 2.4	.46	.49	+ 6.5	−1.03	− .20
A-424...	2	5	.658	.606	3.51	.204	a		.36	.55	+55.6	.48	.51	+ 6.2	.54	.61	+13.0	−1.07	− .17
A-425...	1.5	5	.658	.605	3.51	.204	a	X	.36	—	—	.56	—	—	.66	—	—	−1.13	− .12
A-426...	1.5	5	.658	.803	3.51	.204	a		.18	.25	+38.9	.57	.62	+ 8.8	.62	.62	.0	−1.12	− .11
A-427...	2	5	.658	.804	3.51	.204	a		.22	.30	+36.4	.48	.51	+ 6.2	.51	.57	+11.8	−1.07	− .16
A-428...	3	5	.658	.804	3.51	.204	a		.38	.50	+31.6	.42	.43	+ 2.4	.44	.47	+ 6.8	−1.03	− .22
A-429...	5	5	.658	.796	3.51	.204	a	cc	1.30	1.32	+ 1.5	.36	.38	+ 5.6	.39	.41	+ 5.1	−1.03	− .27
A-577...	5	5	.500	.800	1.50	.00	a	cc	1.34	1.31	− 2.2	.45	.47	+ 4.4	.48	.50	+ 4.2	−1.18	− .33
A-578...	3	5	.500	.800	1.50	.00	a		.40	.51	+27.5	.50	.52	+ 4.0	.52	.55	+ 5.8	−1.16	− .28
A-579...	2	5	.500	.800	1.50	.00	a		.20	.31	+55.0	.59	.60	+ 1.7	.61	.65	+ 6.6	−1.20	− .23
A-580...	1.5	5	.500	.800	1.50	.00	a		.17	.25	+47.1	.70	.71	+ 1.4	.74	.78	+ 5.4	−1.27	− .15
A-581...	5	5	.500	.800	1.50	.025	a	cc	1.31	1.31	.0	.43	.46	+ 7.0	.46	.49	+ 6.5	−1.15	− .32
A-582...	3	5	.500	.800	1.50	.025	a		.42	.51	+21.4	.48	.51	+ 6.2	.50	.54	+ 8.0	−1.15	− .28
A-583...	2	5	.500	.800	1.50	.025	a		.20	.31	+55.0	.56	.59	+ 5.4	.59	.64	+ 8.5	−1.18	− .22
A-584...	1.5	5	.500	.800	1.50	.025	a		.17	.25	+47.1	.67	.70	+ 4.5	.72	.77	+ 6.9	−1.25	− .15
A-585...	1.5	5	.500	.800	1.50	.05	a		.17	.25	+47.1	.67	.69	+ 3.0	.71	.76	+ 7.0	−1.25	− .15
A-586...	2	5	.500	.800	1.50	.05	a		.21	.31	+47.6	.57	.58	+ 1.8	.59	.63	+ 6.8	−1.18	− .22
A-587...	3	5	.500	.800	1.50	.05	a		.42	.51	+21.4	.48	.50	+ 4.2	.50	.53	+ 6.0	−1.14	− .28
A-588...	5	5	.500	.800	1.50	.05	a	cc	1.32	1.31	− .8	.42	.44	+ 4.8	.45	.47	+ 4.4	−1.15	− .32
A-589...	5	5	.500	.800	1.50	.10	a	cc	1.32	1.31	− .8	.40	.42	+ 5.0	.42	.45	+ 7.1	−1.12	− .31
A-590...	3	5	.500	.800	1.50	.10	a		.41	.51	+24.4	.44	.47	+ 6.8	.46	.50	+ 8.7	−1.12	− .26
A-591...	2	5	.500	.800	1.50	.10	a		.20	.31	+55.0	.54	.56	+ 3.7	.57	.61	+ 7.0	−1.15	− .20
A-592...	1.5	5	.500	.800	1.50	.10	a		.18	.25	+38.9	.65	.66	+ 1.5	.69	.73	+ 5.8	−1.21	− .13
A-593...	1.5	5	.500	.800	1.50	.20	a		.17	.25	+47.1	.60	.62	+ 3.3	.64	.69	+ 7.8	−1.18	− .14
A-594...	2	5	.500	.800	1.50	.20	a		.21	.31	+47.6	.50	.51	+ 2.0	.54	.56	+ 3.7	−1.12	− .20

A-595...	3	5	.500	.800	1.50	.20	a		.40	.51	+27.5	.43	.43	.0	.45	.46	+ 2.2	−1.09	− .25
A-596...	5	5	.500	.800	1.50	.20	a	cc	1.32	1.31	− .8	.38	.38	.0	.41	.41	.0	−1.09	− .29
A-597...	5	5	.500	.800	1.50	.30	a	cc	1.32	1.31	− .8	.33	.33	.0	.36	.36	.0	−1.01	− .25
A-598...	3	5	.500	.800	1.50	.30	a		.40	.51	+27.5	.38	.38	.0	.40	.41	+ 2.5	−1.00	− .20
A-599...	2	5	.500	.800	1.50	.30	a		.20	.31	+55.0	.46	.47	+ 2.2	.49	.52	+ 6.1	−1.05	− .16
A-600...	1.5	5	.500	.800	1.50	.30	a		.18	.25	+38.9	.55	.57	+ 3.6	.59	.64	+ 8.5	−1.10	− .10
A-601...	1.5	5	.500	.800	1.50	.40	a		.18	.25	+38.9	.50	.53	+ 6.0	.54	.60	+11.1	−1.05	− .10
A-602...	2	5	.500	.800	1.50	.40	a		.20	.31	+55.0	.42	.42	.0	.45	.47	+ 4.4	− .99	− .15
A-603...	3	5	.500	.800	1.50	.40	a		.39	.51	+30.8	.38	.34	−10.5	.40	.37	− 7.5	− .96	− .18
A-604...	5	5	.500	.800	1.50	.40	a	cc	1.32	1.31	− .8	.33	.29	−12.1	.36	.32	−11.1	− .96	− .23
A-605...	5	5	.500	.800	1.50	.40	a	cc	1.32	1.31	− .8	.31	.29	− 6.4	.36	.32	−11.1	− .95	− .22
A-606...	3	5	.500	.800	1.50	.40	a		.39	.51	+30.8	.36	.34	− 5.6	.40	.37	− 7.5	− .95	− .18

[1] Notes.

a. Barrel entrance of figure XII–1(a).
b. Barrel entrance of figure XII–1(b).
c. Barrel entrance of figure XII–1(c).
d. No antivortex plate or endwalls.
e. No antivortex plate but with endwalls.
f. No antivortex plate, endwalls 0.8D high.
g. Endwalls extend 1.5D from crest.
h. One side of the crest is lower than the other.
i. Riser sidewalls and antivortex walls bowed because of low pressure in the drop inlet.
j. Left K_e value has no vortex, right K_e value has a vortex present.
k. K_e data is erratic.
l. K_f data is poor.
m. Poor hydraulic grade line in the barrel.
n. Condensation during some runs may have caused a change of state.
o. Surface tension test.
p. No vortices.
q. Vortices.
r. Surface vortices.
s. Small vortices.
t. Weak vortices.
u. Strong vortices.
v. Inlet vibrates.
w. Noisy inlet.
x. Noisy, vibrating inlet.
y. Orifice flow at crest.
z. Orifice flow at barrel entrance.
aa. Barrel primed.
bb. K_e and K_f not calculated because the piezometer location makes invalid a comparison with the observed values.
cc. Z_p/D exceeds the recommended value, but in the absence of harmful vortices the data are used in the analyses.
X. Drop inlet dimensions do not meet the recommended criteria.

[2] See item "a" in Notes, (above).
[3] See item "bb" in Notes.
[4] See item "d" in Notes.
[5] See item "e" in Notes.
[6] See item "f" in Notes.
[7] See item "b" in Notes.
[8] See item "c" in Notes.

some feature of the inlet caused the flowing water to produce severe vibrations. This was considered unsatisfactory performance.

Series W-496 through W-510 were made with reduced drop inlet heights to determine the minimum permissible height. The Note, "z, Orifice flow at barrel entrance," indicates that the barrel entrance acted as an orifice, that the barrel did not fill, and that the performance was unsatisfactory. The Note, "ae, Barrel primed," means that the barrel filled and that the inlet performance was satisfactory.

The Note, "m, Poor hydraulic gradeline in the barrel," means that the piezometric pressures poorly defined the slope of the pressure gradeline in the barrel.

The Note, "n, Condensation during some runs may have caused a change of state," indicates that water may have condensed in the barrel. This indicates a change of state of the air which would invalidate the basic airflow equations used in the analysis. The results of these runs are, therefore, of questionable value.

The Note, "x, Noisy, vibrating inlet," indicates that poor flow conditions were affecting the performance of the spillway. The observed pressures fluctuated erratically when the inlet was noisy. Geometrically similar water models showed vortices, which suggests that vortices also were present in the air models.

The conclusions presented in this publication are based on approximately 7,900 individual tests. This figure is estimated from the 20 to 24 test runs made for each of the 256 water series and from 3 to 7 runs for each of the 456 air series listed in table XII–1.

Test Results

The proportions of the two-way drop inlet that give satisfactory hydraulic performance were first determined. Subsequent tests were made to determine the weir flow capacity, the slug and mixture flow capacity, and the full-flow energy loss and pressure coefficients used to compute the capacity of and pressures in the spillway. The performance, the capacity, and the pressures will be discussed in separate sections.

Spillway Performance

Satisfactory performance of closed conduit spillways requires that (1) the head-discharge relationship be unique and reversible, (2) the structure prime smoothly and positively, and (3) harmful vortices be prevented. In each test the moment of incipient slug flow in the barrel was recorded. Any evidence of vibration in the structure was also noted. Visual observation, judgment, and careful analysis of the data were used to determine if the performance of the drop inlet was satisfactory.

Minimum drop inlet height and length

The minimum height of the two-way drop inlet that would insure priming of the barrel was determined. Drop inlet heights tested were 2D, 3D, 4D, and 5D. Lengths were 1D, 1.5D, 2D, 3D, and 5D. The width was 1D and the barrel slope was 20 percent for all tests. Endwalls were installed to a height of 0.8D above the crest of the drop inlet. No antivortex plate, however, was installed, except for the 1D-long drop inlet, because the barrel primed before the headpool water surface elevation reached the antivortex plate elevation. The antivortex plate, therefore, could have no effect on the priming. Although the head and discharge were measured, notes taken during the tests were used in evaluating the performance of the spillway.

The performance of the 1D-long drop inlet was unsatisfactory at all heights. Air sucked into the drop inlet during slug flow caused severe vibrations of the drop inlet and antivortex plate. Strong vortices were also observed after submergence of the antivortex plate.

The performance of the 2D-high drop inlet was unsatisfactory at all lengths. For this height of drop inlet, orifice flow at the barrel entrance alternated with slug flow in the barrel. This caused the headpool to build up during orifice flow and draw down during pipe or slug flow or both. Therefore, the performance of the 2D-high drop inlet does not meet the criteria previously established.

Satisfactory performance was obtained for two-way drop inlets 3D, 4D, and 5D high having lengths of 1.5D or greater. Unique head-discharge curves were obtained and vortices were fully controlled.

The results of the tests to determine the minimum height of the two-way drop inlet show that the height must be 3D or more and that the length must be 1.5D or more to insure satisfactory performance.

Minimum antivortex plate height

The authors reasoned that the antivortex plate must be high enough above the drop inlet crest so that the weir flow discharge over the crest would be sufficiently great to cause slugs to form just inside the barrel entrance. They observed that the initial formation of these slugs indicated that the barrel would eventually prime as the discharge increased. Also, if the antivortex plate was too low, the flow into the drop inlet was governed by the orifice formed by the antivortex plate and the drop inlet crest, and this flow was insufficient to form slugs inside the barrel entrance.

The two-way drop inlet head-discharge test data and notes were examined to determine the maximum discharge at which slugs did not form and the minimum discharge at which slugs were observed. The barrel slope was 20 percent for these tests.

For two-way drop inlets 2D or more in length, the onset of slug flow was observed to be at $Q/D^{5/2} \gtrless 5.1$. For the 1.5D-long drop inlet, the onset of slug flow was at $Q/D^{5/2} \gtrless 6.7$ to 7.4. Therefore, the minimum permissible height of the antivortex plate above the two-way drop inlet crest is the weir flow head corresponding to these discharges.

The minimum permissible antivortex plate height based on the criteria presented in the preceding paragraph ($Q/D^{5/2} = 7.4$ for $B/D = 1.5$ and $Q/D^{5/2} = 5.1$ for $B/D \geqq 2$) has been computed for five lengths of the drop inlet and for two values of the weir discharge coefficient C in equation I–2[4]. The results are presented in table XII–2.

TABLE XII–2.—*Minimum antivortex plate height*

$\frac{B}{D}$	(Z_p/D) minimum	
	$C = 3.1$	$C = 4.0$
1.5	0.85	0.72
2	.55	.47
3	.42	.36
5	.30	.25
10	.19	.16

Vortex Control

Vortex control means the suppression of those vortices that are of sufficient size and intensity to reduce the spillway capacity. Surface vortices may still form, but it is not necessary to attempt to control them if they have no adverse effect on the spillway capacity. A horizontal plate supported above the crest of the two-way drop inlet is a good antivortex device. However, to be fully effective the antivortex device must be located correctly and be of proper size.

Maximum antivortex plate height

Vortex formation is strongest just after the beginning of full pipe flow. This occurs at heads and discharges just exceeding those at the intersection of the extended weir flow curve and the full pipe flow curve on the head-discharge diagram shown in figure XII–2. The headpool surface elevation at the intersection of these two curves has been selected as the maximum elevation of the antivortex plate. Any higher location would permit vortices to form under the plate and thus render it ineffective.

Minimum antivortex plate overhang

The length of overhang of the antivortex plate L_o in figure XII–1 is an important dimension with regard to the ability of the antivortex plate to control vortices. If the overhang is too short, vortices that adversely affect the spillway capacity will form. If the overhang is too great, the economy of the structure will be adversely affected. Therefore, tests were made to determine

[4]See reference to Part I in Preface for complete citation.

the minimum overhang of the antivortex plate that would adequately control vortex formation.

The minimum antivortex plate overhang was determined by installing an excessively long overhang and progressively shortening it until vortices developed that affected the spillway capacity. The Stevens type M water level recorder described in Part X[5] was used to determine the effect of vortices. Charts similar to that shown in figure X-4 were obtained for each length of overhang. If there was vortex action, the full flow stage-time curve would fluctuate with the varying vortex strength. Conversely, a smooth stage-time curve indicated the absence of harmful vortices.

The drop inlets used for the antivortex plate overhang tests were 1D wide, 5D high, and had lengths B of 1D, 1.5D, 2D, 3D, 5D, and 10D. The heights of the antivortex plate above the drop inlet crest Z_p were 0.2D, 0.3D, 0.4D, 0.5D, 0.6D, 0.7D, and 0.8D. The lengths of the overhang L_o were ordinarily 4D, 3D, 2D, 1.5D, 1D, 0.8D, 0.6D, and 0.4D. Values of L_o as low as 0.1D were used for the 10D-long drop inlet. Not all the antivortex overhangs listed were tested; the tests were terminated when the length of the overhang became so small that the antivortex plate did not control the vortex. Also, not all possible combinations of drop inlet length, antivortex plate height, and antivortex plate overhang were tested if the tests would not contribute useful information.

TABLE XII-3.—*Minimum antivortex plate overhang*

B/D	(L_o/D) minimum
1.5	1.0
2	.6
3	.5
5	.4
10	.1

The results of the tests are summarized in table XII-3. It can be seen that the longest overhang is required for the shortest drop inlet. The reason for this is that the velocities approaching the crest are greatest and the vortex is strongest, therefore the overhang needed to control the vortex is longest. The height of the antivortex plate above the drop inlet crest had no effect on the minimum overhang required.

The minimum lengths of overhang listed in table XII-3 are considerably less than the length of overhang required to support trash racks. This is because the area of the trash rack is governed by the permissible velocity through it, and this area ordinarily cannot be obtained unless the overhang length is in excess of the values given in table XII-3. Using lengths of overhang exceeding the minimum is permissible.

Spillway Capacity

The discharge through a two-way drop inlet spillway is, or can be, successively controlled by the two weirs on opposite sides of the drop inlet, by the antivortex plate, and by the spillway flowing completely full. The quantitative effect of each of these controls on the spillway capacity will be considered in turn.

Typical head-discharge curves for several antivortex plate heights are shown in figure XII-2.

Weir Flow

The flow is controlled by the drop inlet crest acting as a weir when the headpool surface elevation lies between the elevations of the drop inlet crest and the bottom of the antivortex plate or the intersection of the weir and pipe flow head-discharge curves, whichever is lower.

The tests to determine the relationship between the weir flow head and the discharge produced erratic results. All attempts to develop reliable equations to predict this relationship were nonproductive. As a result, it is felt that the designer can achieve as satisfactory predictions of the weir flow discharge using published equations as he could obtain using equations that might be developed from the data obtained during the present experiments.

[5]See reference to Part X in Preface for complete citation.

Antivortex Plate Flow

The horizontal antivortex plate supported above the drop inlet crest causes the two-way drop inlet closed conduit spillway to act like a self-regulating siphon. Consequently, as the flow increases, the headpool water surface remains at approximately the same elevation from the time the water surface first touches the underside of the antivortex plate until the spillway flows completely full.

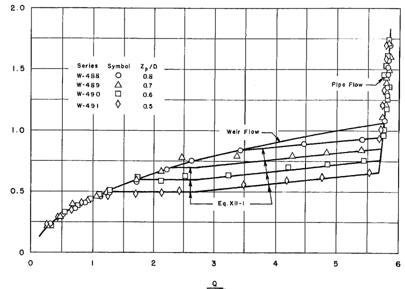

FIGURE XII-2.—Typical head-discharge curves.

The self-regulating siphonic action is a result of slugs in the barrel which cause a partial vacuum in the drop inlet during plate flow. The head causing flow through the two rectangular orifices created by the crest, the antivortex plate, and the endwalls is increased by this partial vacuum. The increased flow required by this increased head, if not supplied by an increased waterflow into the headpool, is supplied by air being sucked into the drop inlet under the antivortex plate. The amount of air entering the spillway depends on the number and frequency of the slugs in the barrel, or the vacuum created by the barrel flowing full of a mixture of water and air. As the waterflow increases after the water first touches the antivortex plate, the airflow will increase to a maximum, and then it will decrease to zero when the spillway becomes full of water alone. The headpool level increases slowly or not at all as the waterflow increases during the period of airflow.

The problem was to determine the head-discharge relationship and the factors that affect this relationship during the period of airflow. The solution assumed that the criteria for minimum and maximum antivortex plate heights specified under "Spillway Performance" have been met. The data used included 227 different combinations of drop inlet length, antivortex plate height, antivortex plate overhang, and crest thickness. All drop inlets were 5D high and from 1D to 10D long. The plate heights ranged from 0.15D to 0.8D, the plate overhang ranged from 0.13D to 4D, and the crest thicknesses were 0.11D and 0.44D.

The equation developed as a result of the analysis of the data is

$$\frac{H}{D}=\frac{Z_p}{D}-\left\langle\frac{0.2}{B/D}-0.1\log_{10}\frac{L_o}{D}\right\rangle+\left\langle 0.1-0.05\frac{L_o}{D}\right\rangle\frac{Q}{28D^{5/2}}\geqq\frac{Z_p}{D} \quad \text{(XII-1)}$$

where the quantities in pointed brackets are zero for negative values. Expressed another way,

$$\left\langle\frac{0.2}{B/D}-0.1\log_{10}\frac{L_o}{D}\right\rangle\geqq 0$$

and

$$0\leqq\left\langle 0.1-0.05\frac{L_o}{D}\right\rangle\leqq 0.1$$

that is, $0 \leqq L_o/D \leqq 2$. It can be seen that for values of L_o/D greater than 2 the last term in equation XII–1 disappears and the head does not increase as the discharge increases. As a result, the headpool level does not change during slug and mixture flow when $L_o/D \geqq 2$.

A restriction on equation XII–1 is that H/D be not less than Z_p/D. This is because plate flow cannot control the discharge unless the headpool water surface touches the underside of the antivortex plate.

Equation XII–1 is shown in figure XII–2 for several heights of the antivortex plate. The excellent agreement of equation XII–1 with the test data plotted in figure XII–2 is apparent. The agreement shown is better than was obtained in many cases, but the agreement was considered satisfactory for all the data obtained.

Surface tension effect

The effect of surface tension on the plate flow head-discharge relationship (equation XII–1) was determined. This was done because the surface tension effect in the laboratory drop inlet is greater, relatively, than it is in field size inlets. During two-phase flow, which exists during plate flow when both water and air enter the spillway, surface tension would have a maximum effect on the spillway capacity. This range of flows was covered during the tests to determine the effect of surface tension. Full pipe flow, during which surface tension has a minimum effect on the spillway capacity, could not be tested because the foaming that occurred when the surface tension was low reduced the capacity of the test apparatus.

Four sets of duplicate tests were made to determine the effect of surface tension. One set of tests used water having a measured surface tension σ of 71 dynes per centimeter. Aerosol added to the water for the other set of tests reduced the surface tension to 26 dynes per centimeter. This reduction of the surface tension to 37 percent of that of water alone should provide a good indication of the effect of surface tension on the performance and capacity of the two-way drop inlet.

Typical results of the tests are shown in figure XII–3 where it can be seen that identical results, within the limits of precision of the experiments, were obtained even for the large change in surface tension. Equally good comparisons were obtained for the other tests.

Pipe Flow

Pipe flow denotes the condition that the spillway is flowing completely full of water. There is no flow of air. The head-discharge relationship for pipe flow is given by equation I–5[6].

Tests were made to determine the entrance loss coefficient K_e in equation I–5. Both to expedite the tests and to facilitate the use of the test results by the designer, the entrance loss coefficient was separated into a crest loss coefficient K_c and a barrel entrance loss coefficient K_t. The crest loss coefficient includes the energy losses between the headpool and the midheight of the drop inlet. The barrel entrance loss coefficient includes the energy losses between the midheight of the drop inlet and the barrel entrance plus those energy losses in the barrel caused by the barrel entrance. This facilitates the design of a two-way drop inlet by making it possible to choose the crest geometry and the barrel entrance geometry independently. The method of analysis permits the loss coefficient for each to be determined separately and then combined to obtain the total entrance loss coefficient for the complete drop inlet.

The effects of the several parts of the two-way drop inlet on each of the energy loss coefficients will be discussed separately.

Crest loss coefficient[7]

The crest energy loss coefficient K_c describes the energy loss that occurs between the headpool surface and the midheight of the drop inlet. A single piezometer was used to measure this loss. For the air apparatus, the piezometer was located on the drop inlet sidewall at the midheight of the drop inlet and 1D upstream from the downstream endwall. The piezometer was similarly located for the water tests only for the 2D-long drop inlet. Thus, the air tests were the primary source of information for determining the crest loss coefficient. The only water data used were those obtained from the 1.5D- and 2D-long drop inlets.

The crest loss coefficient is defined as

$$K_c = \frac{h_c}{V_r^2/2g} \qquad \text{(XII–2)}$$

[6]See reference to Part I in Preface for complete citation.

[7]For a theoretical derivation of the crest loss and a comparison with experimental data see Hebaus, George G., Crest losses for two-way drop inlet. Amer. Soc. Civil Engin. Proc., J. Hydraul. Div., vol. 95, (HY3): 919-940, May 1969.

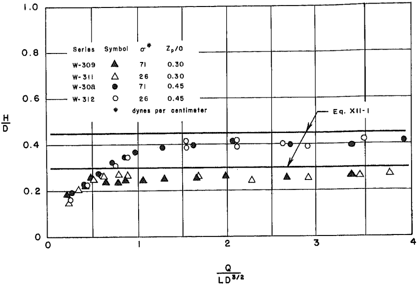

FIGURE XII-3.—The effect of surface tension on the head-discharge curve.

where h_c is the loss in head between the headpool surface and the midheight of the drop inlet in feet, $V_r = Q/A_r$ is the average velocity in the drop inlet or riser in feet per second, Q is the rate of flow in cubic feet per second, A_r is the area of the drop inlet or riser in square feet, and g is the acceleration of gravity in feet per second per second.

Because the crest loss coefficient K_c varied with the drop inlet length, the antivortex plate height, and the crest thickness, the effect of each will be discussed. The apparent lack of effect of the antivortex plate overhang will be shown. As expected, the type of barrel entrance and the slope of the barrel had no effect on the crest loss coefficients. Also, there was no definite indication that viscosity as measured by the Reynolds' number had an effect on the crest loss coefficient. The section will conclude with a description of the method used to develop an equation for the crest loss coefficient.

Effect of drop inlet length.—The effect of the relative length of the drop inlet B/D on the crest loss coefficient K_c is shown by the typical curve presented in figure XII-4. The coefficient increases rapidly as the relative drop inlet length in

lowing equation is obtained for the crest head loss.

$$\frac{h_c}{Q^2/2\,g\,D^4} = \frac{K_c}{(B/D)^2} \qquad \text{(XII-3)}$$

The dimensionless crest head loss data for the crest loss coefficients presented in figure XII-4 are also plotted there. The data and curves that represent the data show that the actual crest head loss for any given discharge and barrel diameter decreases with an increase in the relative length of the drop inlet even though the crest loss coefficients increase with relative drop inlet length. The reason the actual crest loss is low

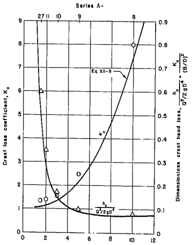

FIGURE XII–4.—The effect of relative drop inlet length on the crest loss coefficient and the dimensionless crest head loss, $t_c/D = 0.104$, $Z_p/D \approx 0.6$.

even though the coefficient is high for the long drop inlets is that the long drop inlets have a comparatively large area, low velocity, and low velocity head. When the low velocity head is multiplied by even a large crest loss coefficient, the head actually lost at the crest is low.

The dimensionless crest head loss decreases rapidly as the relative drop inlet length increases for relative drop inlet lengths B/D less than about 5. The curve decreases slowly with further increases in the relative drop inlet length. This suggests that there is an optimum inlet length that the designer may wish to determine for each two-way drop inlet.

Effect of antivortex plate height.—The relative height of the flat antivortex plate above the drop inlet crest Z_p/D has an important effect on the crest loss coefficient K_c. This effect is shown in figure XII–5. (The effect of plate overhang, also shown in figure XII–5, will be discussed in the following section.)

The crest loss coefficient is large when the plate height is low because the high velocity between the plate and the drop inlet crest causes high energy losses. The crest loss coefficients decrease with increasing plate height and approach a constant value.

The antivortex plate height selected by the designer will probably be determined by the performance criteria given previously or by other considerations rather than by the effect of plate height on the crest loss coefficients. However, figure XII–5 shows that the higher the antivortex plate is above the drop inlet crest, the lower will be the head loss at the drop inlet crest.

Effect of antivortex plate overhang.—The relative overhang of the antivortex plate beyond the outside of the drop inlet crest L_o/D was found to have a minor effect on the crest loss coefficient. This is shown in figure XII–5, where a single curve has been drawn to represent the data obtained for relative overhangs ranging from 0.3 to 4.0. While there is some spread in the data, most if not all of this spread is probably a result of experimental uncertainties and it is felt that drawing separate curves for each overhang is not warranted by the precision of the data. In any case, there is no detectable effect of plate overhang on the crest loss coefficient when the relative overhang is 0.75 or more.

The open squares, erect triangles, circles, and circled crosses and their solid counterparts plotted in figure XII–5 require explanation. The data represented by the open symbols were obtained using endwalls extending to the edge of the antivortex plate overhang. It can be seen that the open symbols deviate from the curve at the highest plate heights, especially for the shorter drop inlet lengths. The data represented by the solid symbols were obtained using endwalls extending outward 1.5D from the drop inlet wall. They show that lengthening the endwalls reduced the crest loss coefficient and caused the coefficients to agree reasonably well with the longer overhang data and the curve. It is possible that flow separation around the short endwall reduced the effective crest length and thereby caused the increase in the crest loss coefficient. This effect would be relatively more important for the short drop inlets.

The tests show that there is no effect of the antivortex plate overhang on the crest loss coefficient if long endwalls are used or if the overhang is 0.75D or greater.

Effect of drop inlet crest thickness.—The thickness of the drop inlet crest t_c had a surpris-

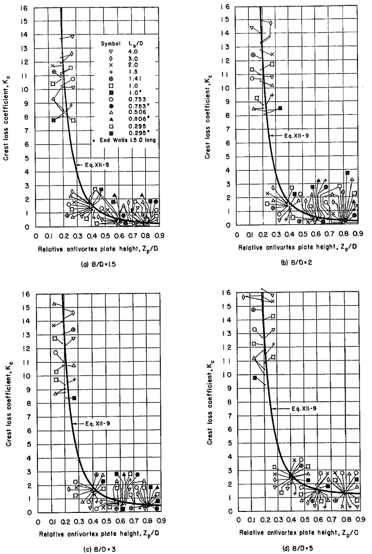

FIGURE XII-5.—The effect of antivortex plate height and overhang on the crest loss coefficient, $t_c/D = 0.50$.

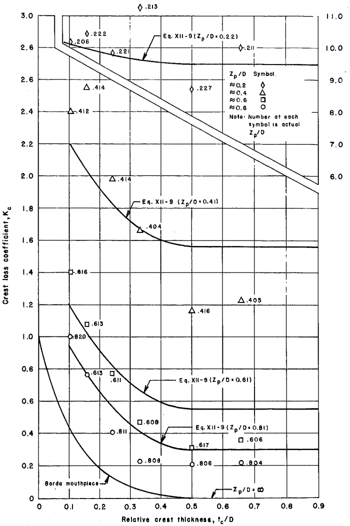

FIGURE XII-6.—The effect of crest thickness on the crest loss coefficient, $B/D = 2$.

ingly large effect on the crest loss coefficient for the thinner crests. This large crest loss coefficient for the thinner crests is possibly due to separation of the flow lines from the crest. For the thicker crests, the flow lines apparently follow the shape of the crest and the crest loss coefficients are smaller and constant. Hebaus[8] shows, however, that flow separation will occur for all crest thicknesses when $Z_p/D < \infty$.

Six thicknesses of crests ranging from 0.1D to 0.66D were tested. Each crest was rounded on its inner edge to a radius of half the crest thickness as shown in figure XII–1. The outer edge was square. Four different heights of the antivortex plate were used for each crest thickness. Typical results of the tests are shown in figure XII–6. The curves shown indicate the rapid decrease in the crest loss coefficient as the relative crest thickness increases for the smaller crest thickness, and the essentially constant value of the coefficient for greater crest thicknesses.

Equation for the crest loss coefficient.—An equation was developed to represent the crest loss coefficient as a function of the relative thickness of the drop inlet crest, the relative antivortex plate height, and the relative length of the drop inlet. This was accomplished in two steps. First, the crest thickness data shown typically in figure XII–6 were reduced to a single curve for each drop inlet length. Then an equation was developed to represent all these curves. The procedures are presented in the following subsections.

Reduction of crest thickness effect.—In analyzing the effect of crest thickness it was assumed, for thin crests, that the flow separates from the crest at the outside corners and forms a jet in the drop inlet. A transverse section through the drop inlet illustrating this assumption is shown in figure XII–7. The contracted jet is two-dimensional. Its thickness is D_j feet and its velocity is V_j feet per second.

If the head loss at the crest is due to the sudden expansion of the contracted jet to the full width of the drop inlet, then the crest head loss h_c in feet can be obtained by rearranging an equation given by Rouse [I–44, p. 413, Eq. 41][9] to express the loss in terms of the lesser drop inlet velocity V_r, the drop inlet width D, and the jet thickness D_j. The resulting equation is

$$h_c = \left(\frac{D}{D_j} - 1\right)^2 \frac{V_r^2}{2g} \qquad \text{(XII–4)}$$

If equation XII–2 is solved for h_c and equated to equation XII–4, then the crest loss coefficient equation becomes

$$K_c = \left(\frac{D}{D_j} - 1\right)^2 \qquad \text{(XII–5)}$$

Because the flow is assumed to separate from the outside corner of the crest, the effective width of the entrance is $(D + 2t_c)$. This is shown in figure XII–7. When this width is multiplied by a suitable contraction coefficient C_c, the contracted width of the jet is obtained. When $C_c\,(D + 2t_c)$ is substituted for D_j in equation XII–5,

$$K_c = \left[\frac{D}{C_c\,(D + 2t_c)} - 1\right]^2 = \left[\frac{1}{C_c\,(1 + 2t_c/D)} - 1\right]^2 \qquad \text{(XII–6)}$$

Equation XII–6 will be evaluated for several specific conditions. When the antivortex plate is high or is removed entirely, then the two-way drop inlet resembles a two-dimensional reentrant tube or Borda mouthpiece. The value of C_c given by Rouse for this entrance is 0.500 [I–44, p. 34, table 1, $\beta = 180°$, $b/B = 0.0$]. Equation XII–6 with $C_c = 0.5$ has been plotted in figure XII–6. The curve is labeled "Borda mouthpiece." Of interest is the fact that K_c is zero when t_c/D is 0.5.

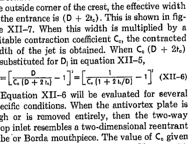

FIGURE XII–7.—Transverse section through top of drop inlet showing flow separation.

[8]See page 929, figure 4, of reference in footnote 7. For the boundary flow line to reattach to the crest, the contraction coefficient must be 0.5 or greater. But figure 4 shows that the contraction coefficient approaches 0.5 asymptotically from below as the antivortex plate height increases.

[9]See bibliography for Part I, in Preface.

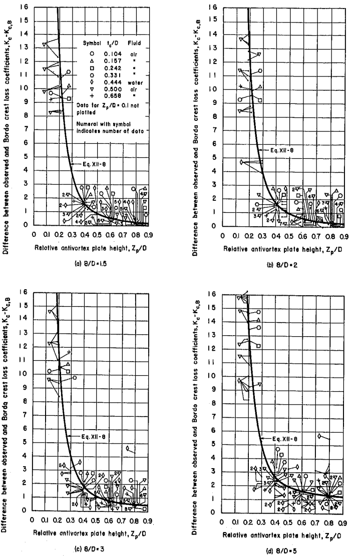

FIGURE XII-8.—Compensation for effect of crest thickness on crest loss coefficient.

This indicates that when $t_c/D > 0.5$ the flow follows the wall of the drop inlet, there is no jet expansion loss, and equation XII–6 is no longer applicable. The curve plotted in figure XII–6 also shows that K_c is 1.00 for a crest of zero thickness. This is identical to the value given by Rouse for reentrant entrances [I–44, p. 415]. These observations apply only for a Borda mouthpiece; that is, with no antivortex plate or a plate so far above the crest that it has no effect on the crest loss coefficient. The observations do, however, indicate that the trend of equation XII–6 is similar to that shown by the experimental data presented in figure XII–6 and with information presented by others [I–21, I–22, and I–24].

Strictly, the value of the crest loss coefficient for the Borda mouthpiece should be based on the velocity in a tube having a width of $(D + 2t_c)$. The relation between the Borda tube velocity $V_{r,B}$ and the drop inlet velocity V_r is

$$V_r = \frac{D + 2t_c}{D} V_{r,B}$$

If this relationship is substituted into equation XII–4, if operations similar to those used to obtain equation XII–6 are performed, and if C_c is assigned the Borda mouthpiece value of 0.5, then the Borda mouthpiece crest loss coefficient $K_{c,B}$ is

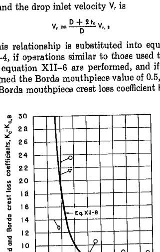

(e) B/D=10

FIGURE XII–8.—Continued.

$$K_{c,B} = \left(1 - 2\frac{t_c}{D}\right)^2 \qquad \text{(XII–7)}$$

By trial a single curve was obtained for each drop inlet length when the differences between equation XII–2 and equation XII–7 values of the crest loss coefficient were plotted against the relative antivortex plate height. The data are shown in figure XII–8. Most of the data shown are for the air tests. Data obtained during the water tests are shown only for relative drop inlet lengths of 1.5 and 2; because the piezometers were in the same relative position only for the $B/D = 2$ inlets and because the pressure measurements are greatly affected by the streamline pattern, the air and water data cannot be compared for the longer drop inlets.

The curves of figure XII–8 give the increase in the crest loss coefficient $(K_c - K_{c,B})$ that results from the decrease in drop inlet width attributable to the sidewall thickness as a function of the relative antivortex plate height. An advantage of these curves is that they reduce all the crest loss coefficients for different wall thicknesses to a common curve for each drop inlet length.

Development of the equation.—An equation representing the data in figure XII–8 was developed by:

(1) Fitting empirical curves to the plotted data for each drop inlet length.

(2) Reading points from the curves drawn to represent the data, and plotting the points on logarithmic paper.

(3) Selecting by trial a constant to subtract from each logarithmic curve to produce a single straight line on logarithmic paper.

(4) Plotting the subtractive constants against the relative drop inlet length on logarithmic paper.

(5) Drawing a straight line on this latter plot to represent the subtractive factor. The equation of the straight line plotted on logarithmic paper to represent the effect of antivortex plate height is $0.1(Z_p/D)^{-3}$. The equation of the straight line plotted on logarithmic paper which represents the subtractive factor required to account for the effect of drop inlet length is $0.02(B/D)^{5/2}$. Therefore, the equation representing the data plotted in figure XII–8 is

$$K_c - K_{c,B} = \frac{0.1}{(Z_p/D)^3} + 0.02\left(\frac{B}{D}\right)^{5/2} \qquad \text{(XII–8)}$$

The curves drawn in figure XII–8 were computed using equation XII–8. They show that equation XII–8 represents the data satisfactorily.

The equation for the crest loss coefficient can be obtained by substituting equation XII–7 in equation XII–8 and solving for K_c. Thus

$$K_c = \left\langle 1 - 2\frac{t_c}{D} \right\rangle^2 + \frac{0.1}{(Z_p/D)^3} + 0.02\left(\frac{B}{D}\right)^{5/2} \qquad \text{(XII–9)}$$

The first term in equation XII–9 represents the effect of the relative crest thickness on the crest loss coefficient. It is valid only for $t_c/D \leqq 0.5$; for values of $t_c/D \geqq 0.5$, the jet clings to the side of the drop inlet and the first term of equation XII–9 is zero—the pointed brackets indicate that the first term in equation XII–9 is zero for negative values. The second term represents the effect of the relative antivortex plate height. The third term represents the effect of the relative drop inlet length on the crest loss coefficient.

Precision of the equation.—The degree to which equation XII–9 represents the test data was determined by computing K_c for each series for which the drop inlet dimensions meet the recommended criteria; that is, for all series for which equation XII–9 is valid. Computed values of K_c and the percentage deviations from the observed values of K_c are shown in table XII–1.

The average error between the test data and equation XII–9 for the valid tests listed in table XII–1 is +22 percent. The maximum and minimum errors are +92 percent and −41 percent. The average error for the 23 valid water tests was +5 percent while the average error for the 252 valid air tests was +23 percent. However, the spread of the errors, +92 to −41 percent for the water tests and +88 to −22 percent for the air tests, was of a comparable order of magnitude.

No trend of the percentage errors with respect to antivortex plate height or overhang could be detected. There appears to be no trend of the percentage errors for relative drop inlet lengths less than 5; but, the percentage errors for $B/D = 5$ are less, although the difference may be fortuitous, than for other drop inlet lengths. However, a trend of the percentage errors with crest thickness is evident: The equation XII–9 value of the crest loss coefficient is less than the observed value for the thinner crests and becomes greater than the test value for the thicker crests; the average percentage error in the crest loss coefficient gradually changes from −13 for $t_c/D = 0.1$ to +34 at $t_c/D = 0.33$ and remains constant for thicker crests. No attempt was made to improve equation XII–9 to eliminate this trend.

The precision of equation XII–9 appears to be low. All efforts, however, to improve its precision have failed.

Barrel entrance loss coefficient

The barrel entrance energy loss coefficient describes the small energy loss that occurs between the midheight of the drop inlet and the barrel entrance plus the loss caused by the barrel entrance. The actual head lost h_l is the difference between the energy head at the drop inlet piezometer described under the paragraph heading Crest loss coefficient and the energy head measured by projecting the friction gradeline in the barrel to the barrel entrance.

The barrel entrance loss coefficient K_l is defined as

$$K_l = \frac{h_l}{V_p^2/2g} \qquad \text{(XII–10)}$$

where $V_p = Q/A_p$ is the average velocity in the barrel in feet per second and A_p is the barrel area in square feet. The following paragraphs will discuss the effect on K_l of the barrel Reynolds' number, the drop inlet length, the type of barrel entrance, and the barrel slope. As might be reasonably expected, the barrel entrance loss coefficient was independent of crest conditions such as the crest thickness or the antivortex plate height or overhang. The section will conclude with the development of equations for the barrel entrance loss coefficients and a discussion of the precision of these equations.

Effect of Reynolds' number.—The typical effect of the Reynolds' number $\mathbf{R} = V_pD/\nu$ on the barrel entrance loss coefficient is shown in figure XII–9. The curves drawn show the barrel entrance loss coefficient is constant for Reynolds' numbers exceeding 150,000. This is in reasonable agreement with the analysis of the results of tests on bends reported by Anderson[10]. This comparison is possible because the flow from the drop inlet to the barrel is akin to that in a miter bend.

The barrel entrance loss coefficients used in the subsequent analyses are the average of the experimental coefficients obtained for values of $\mathbf{R}$ ranging from a minimum of about 200,000 to the maximum obtainable with the air apparatus of

[10] Anderson, A. G. Hydraulics of conduit bends. Univ. Minn., St. Anthony Falls Hydraul. Lab., Bul. No. 1, 22 pp., illus. December 1948, p. 9.

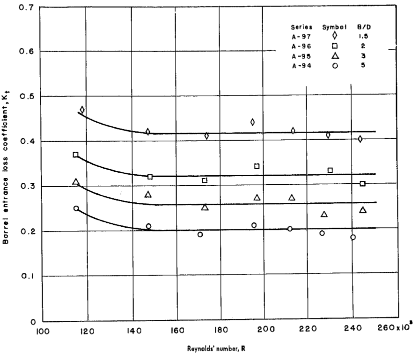

FIGURE XII-9.—The effect of Reynolds' number on the barrel entrance loss coefficient. Grooved-edged entrance, S = 0.4.

about 250,000. The maximum values of the experimental Reynolds' numbers approximate the minimum field values. Therefore, the applicability of the experimental results to field conditions assumes that the barrel entrance loss coefficient is constant for Reynolds' numbers exceeding about 200,000.

Effect of drop inlet length.—Figure XII-10 presents typical data showing that the barrel entrance loss coefficient decreases as the drop inlet length increases. This is probably a result of the better approach conditions for the flow upstream of the barrel entrance which exist as the drop inlet is lengthened.

Effect of shape of barrel entrance.—The shapes of barrel entrance tested are shown in figure XII-1 and are described in the section, Drop Inlet Description. A typical effect of the barrel entrance shape on the barrel entrance loss coefficient is shown in figure XII-10. To avoid confusion, only a sample of the data listed in table XII-1—that for $Z_p/D \approx 0.8$—has been plotted in figure XII-10.

The air data represented by open circles and squares show a small but possibly not significant increase in the square-edged barrel entrance loss coefficient if the crown of the barrel does not intersect the downstream wall of the drop inlet. Nevertheless, separate curves are shown for each entrance. The water data, represented by solid circles, generally agree well with the open circle air data.

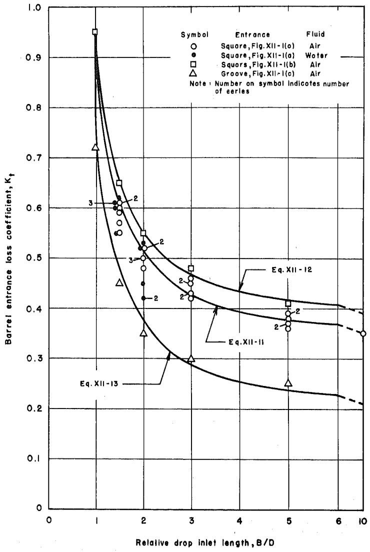

FIGURE XII-10.—The effect of drop inlet length on the barrel entrance loss coefficient, $S = 0.2$, $Z_p/D \approx 0.8$.

The groove-edged barrel entrance loss coefficient (represented by triangles) is considerably less than the square-edged coefficient. This is expected because the barrel entrance loss coefficient is a direct measure of the expansion losses in the barrel, which are sensitive to the shape of the barrel entrance edge. The larger barrel entrance resulting from the groove reduces the expansion loss as compared with the loss for the square-edged barrel entrance.

Effect of barrel slope.—The barrel entrance loss coefficient K_f decreases as the barrel slope increases. This effect is similar to that at elbows, and it is expected because the angle through which the water turns as it leaves the drop inlet and enters the barrel decreases as the barrel slope increases. Typical data are shown in figure XII–11.

As in figure XII–10, to avoid confusion only the data for $Z_p/D \approx 0.8$ are plotted in figure XII–11. For the square-edged entrance shown in figure XII–1(a), data are presented for four values of the drop inlet length. To avoid overlap, the only data plotted for the square-edged entrance shown in figure XII–1(b) are for the shortest drop inlet and the only data plotted for the groove-edged entrance shown in figure XII–1(c) are for the longest drop inlet. The effect of barrel slope on the barrel entrance loss coefficients is less for the inlet shown in figures XII–1(b) and (c) than it is for the inlet shown in figure XII–1(a).

Equation for the barrel entrance loss coefficient.—The entrance loss coefficient for each barrel entrance is a function of the barrel slope and the drop inlet length. The equation for this co-

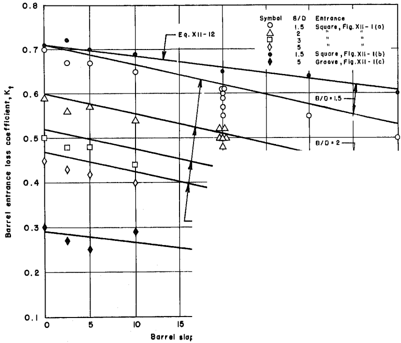

FIGURE XII–11.—The effect of barrel slope

efficient was developed from plots similar to that shown in figure XII–11, and its precision was checked against the original data. The findings are presented in the following subsections.

Development of the equation.—The data were first plotted as shown typically in figure XII–11. On these plots it was seen that the effect of barrel slope on the barrel entrance loss coefficients was the same for all drop inlet lengths, although the slope effect did vary with the form of the barrel entrance. As a result, parallel lines were drawn through the data for each barrel entrance to represent the slope effect. The intercepts of these lines at zero barrel slope were read from the plot. The intercepts are best represented by a constant that was a function of the barrel entrance shape plus 0.55 times an inverse function of the drop inlet length raised to the five-thirds power.

The equations giving the barrel entrance loss coefficients K_t for the three types of barrel entrances are:

For the square-edged barrel entrance shown in figure XII–1(a),

$$K_t = 0.43 + \frac{0.55}{(B/D)^{5/3}} - 0.45\,S \qquad \text{(XII–11)}$$

For the offset square-edged barrel entrance shown in figure XII–1(b),

$$K_t = 0.43 + \frac{0.55}{(B/D)^{5/3}} - 0.25\,S \qquad \text{(XII–12)}$$

For the groove-edged barrel entrance shown in figure XII–1(c),

$$K_t = 0.25 + \frac{0.55}{(B/D)^{5/3}} - 0.25\,S \qquad \text{(XII–13)}$$

Although equations XII–11, XII–12, and XII–13 may not give a good estimate of the barrel entrance loss coefficient in individual cases, the average estimate of K_t is good.

Entrance loss coefficient

The entrance loss coefficient represents the loss of energy between the headpool surface and the barrel entrance plus the loss in the barrel caused by the barrel entrance. An equation giving the entrance loss coefficient will be developed, and the precision with which the equation represents the data will be evaluated.

Development of the equation.—The entrance loss coefficient K_e is

$$K_e = \frac{h_e}{V_p^2/2\,g} \qquad \text{(XII–14)}$$

where V_p is the velocity in the barrel and

$$h_e = h_c + h_t \qquad \text{(XII–15)}$$

The losses h_c and h_t are defined by equations XII–2 and XII–10. When equations XII–14, XII–2, and XII–10 are solved for h_e, h_c and h_t, these values are substituted in equation XII–15, and both sides of the equation are divided by the velocity head in the barrel $V_p^2/2\,g$,

$$K_e = K_c\left(\frac{V_r}{V_p}\right)^2 + K_t \qquad \text{(XII–16)}$$

From continuity, $A_rV_r = A_pV_p$ where $A_r = BD$ is the area of the two-way drop inlet and $A_p = \pi D^2/4$ is the area of the circular barrel. When these values are substituted in equation XII–16, the expression for K_e becomes

$$K_e = K_c\left(\frac{\pi}{4\,B/D}\right)^2 + K_t \qquad \text{(XII–17)}$$

Precision of the equation.—The entrance loss coefficient K_e can be calculated from equation XII–17. Values of K_c are obtained from equation XII–9 and values of K_t from equations XII–11, XII–12, and XII–13. The computed values of K_e and the percentage deviations from the observed values of K_e are shown in table XII–1 for all series for which the drop inlet dimensions meet the recommended criteria; that is, for all series for which equation XII–17 is valid.

The average error between the test data and equation XII–17 for the 254 valid tests listed in table XII–1 is −3 percent. The maximum and minimum errors are +14 percent and −19 per-

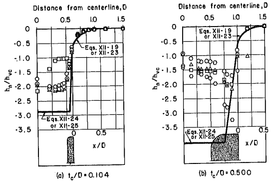

B/D	Symbol	Series number for Fig. XII-12: (a)	(b)
2	o	A-20*	A-52
3	△	A-21*	A-51
5	□	A-22*	A-50
10	o	A-23*	A-49

*See note i on Table XII-1

FIGURE XII-12.—Pressure distribution on the bottom of the antivortex plate, $Z_p/D = 0.1$.

cent. The average, maximum and minimum percentage differences for the 110 water series are −9, +13 and −19 and for the 144 air series are +1, +14 and −11. There are no readily apparent trends in the errors with respect to the drop inlet geometry. The only trend noted is that the water differences are predominantly negative and greater in absolute value whereas the air differences are predominantly positive and smaller in absolute value.

Although the prediction equations indicate maximum differences of +14 percent and −19 percent from the observed values of the entrance loss coefficients, the average difference is only −3 percent.

CAUTION regarding use of K_c and K_t to compute K_e.—Data for K_c and K_t obtained from dissimilar models cannot be used to compute K_e.

For example, the drop inlet piezometer tap in the air apparatus used to develop the equations for K_c and K_t was located on the drop inlet sidewall 1D upstream from the downstream endwall. For the water apparatus, the piezometer was located at the midlength of the drop inlet, which gives geometric similarity with the air apparatus only for the water drop inlet 2D long. The effect of this lack of similarity in the piezometer locations is that the developed equations give values of K_c for the long water drop inlets that are frequently more than 200 percent of the observed values.

Another example may be taken from the tests performed at the ARS Stillwater, Okla., Outdoor Hydraulic Laboratory. There the values of K_c are computed using six piezometers at various locations in the drop inlet; the Stillwater piezometer locations are not similar to those used at St. Anthony Falls and reported herein. As a result, the Stillwater values of K_c cannot be combined with the equations XII–11, XII–12, and XII–13 values of K_t to obtain K_e.

Valid and identical values of K_e can be obtained only if the Stillwater and St. Anthony Falls values of K_c and K_t are not combined to compute K_e. Conversely, valid and identical values of K_e can be obtained if either, but not both, the Stillwater or St. Anthony Falls values of K_c and K_t are used to compute K_e.

Spillway Pressures

To structurally design the drop inlet, the pressures on the antivortex plate, the sidewalls and the endwalls must be known. Also, to determine if cavitation may occur, the pressures on the drop inlet crest and in the barrel just inside its entrance must be known.

Pressures within the two-way drop inlet spillway were measured on the underside of the antivortex plate, on the drop inlet sidewalls (on the outside, the crest, and the inside), on the inside of the downstream drop inlet endwall and antivortex plate support walls, and in the barrel just downstream from the barrel entrance.

Pressure coefficients are presented for use by designers. These pressure coefficients—when multiplied by the velocity head between the anti-

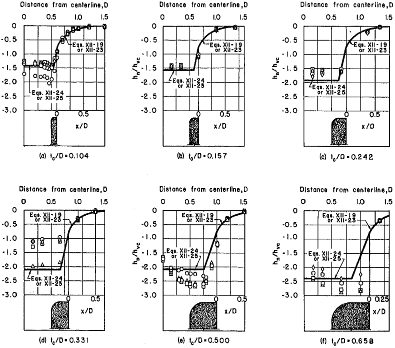

Series number for Fig. XII-13:

B/D	Symbol	(a)	(b)	(c)	(d)	(e)	(f)
1.5	◊		A-369	A-385	A-401		A-417
2	o	A-19*	A-368	A-384	A-400	A-45	A-416
3	Δ	A-18*	A-367	A-383	A-399	A-46	A-415
5	□	A-17*	A-366	A-382	A-398	A-47	A-414
10	o	A-16*				A-48	

*See note i on Table XII-1

FIGURE XII-13.—Pressure distribution on the bottom of the antivortex plate, $Z_p/D = 0.2$.

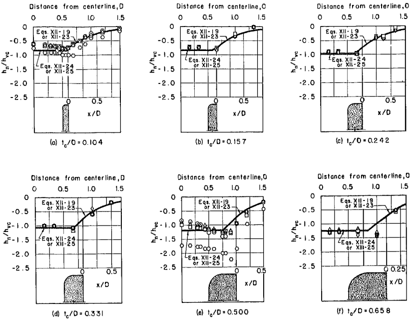

Series number for Fig. XII-14:

B/D	Symbol	(a)	(b)	(c)	(d)	(e)	(f)
1.5	◊		A-370	A-386	A-402		A-418
2	○	A-12	A-371	A-387	A-403	A-42	A-419
3	△	A-13	A-372	A-388	A-404	A-41	A-420
5	□	A-14	A-373	A-389	A-405	A-40	A-421
10	○	A-15				A-39	

FIGURE XII-14.—Pressure distribution on the bottom of the antivortex plate, $Z_p/D = 0.4$.

vortex plate and the crest, in the drop inlet, or in the barrel, whichever is applicable—give the actual pressure at the desired point.

Antivortex Plate Pressures

On the premise that the pressures on the underside of the antivortex plate are most closely related to the velocity between the antivortex plate and the drop inlet crest, these pressures were divided by the average velocity head between the antivortex plate and the drop inlet crest. This gave the pressure head coefficient for the antivortex plate h_n/h_{vc}:

$$\frac{h_n}{h_{vc}} = \frac{\Delta p_n/w}{V_c^2/2\,g} \qquad \text{(XII-18)}$$

where h_n is the difference in head in feet and Δp_n is the difference in pressure in pounds per square foot between any point n in the drop inlet and the static head or static pressure outside the drop inlet at the same elevation; $h_{vc} = V_c^2/2\,g$ is the average velocity head between the antivortex plate and the drop inlet crest in feet; V_c is the average velocity between the antivortex plate and the drop inlet crest in feet per second; w is the specific weight of water in pounds per cubic foot; and g is the gravitational acceleration in feet per second per second.

Pressure heads on the underside of the antivortex plate are always less than the static pressure head at the same elevation. As a result, the pressure head coefficients are always negative.

The pressure on the underside of the antivortex plate was measured by a row of piezometers located perpendicular to the drop inlet longitudinal centerline and one pipe diameter upstream from the downstream end of the drop inlet. Fifteen piezometers were used for the early tests made with crest thicknesses t_c/D of 0.104 and 0.500 and drop inlet lengths ranging from 1.5D to 10D. Only five piezometers were used for the tests made with crest thicknesses t_c/D of 0.157, 0.242, 0.331 and 0.658 and drop inlet lengths of 1.5D, 2D, 3D and 5D.

The pressures on the underside of the antivortex plate are shown in figures XII–12 through XII–16. The pressure coefficients are negative; they add to the load on the antivortex plate.

The antivortex plate pressures outside the drop inlet will be analyzed separately from those inside the drop inlet.

Pressure outside the drop inlet

Subfigures (a) of figures XII–12 through XII–16, which present the results of tests on the crests 0.104D thick where there were 15 piezo-

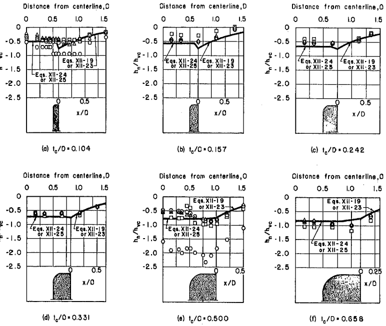

Series number for Fig. XII-15:

B/D	Symbol	(a)	(b)	(c)	(d)	(e)	(f)
1.5	◊		A-377	A-393	A-409		A-425
2	o	A-11	A-376	A-392	A-408	A-35	A-424
3	△	A-10	A-375	A-391	A-407	A-36	A-423
5	□	A-9	A-374	A-390	A-406	A-37	A-422
10	o	A-8				A-38	

FIGURE XII–15.—Pressure distribution on the bottom of the antivortex plate, $Z_p/D = 0.6$.

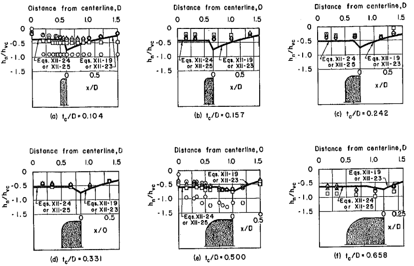

Series number for Fig. XII-16:

B/D	Symbol	(a)	(b)	(c)	(d)	(e)	(f)
1.5	◊		A-378	A-394	A-410		A-426
2	o	A-4	A-379	A-395	A-411	A-32	A-427
3	Δ	A-5	A-380	A-396	A-412	A-31	A-428
5	□	A-6	A-381	A-397	A-413	A-30	A-429
10	o	A-7				A-29	

FIGURE XII-16.—Pressure distribution on the bottom of the antivortex plate, $Z_p/D = 0.8$.

meters on the antivortex plate, were used in the preliminary analysis because these data best define the relationship between the pressure coefficients and the distance from the drop inlet. For each antivortex plate height an overlay curve was sketched and compared with the observed data. When a satisfactory fit had been obtained, an equation was developed that fit all of the overlay curves. This equation is

$$\frac{h_n}{h_{vc}} = -\log_{10}^{-1}\left[-0.125 - \frac{0.44}{Z_p/D}\frac{x}{D}\right] \quad \text{(XII-19)}$$

where x is measured outward from the outside wall of the drop inlet.

Equation XII-19 has been plotted on figures XII-12 through XII-16. The equation gives a reasonable representation of the pressure on the underside of the antivortex plate. Appreciable deviation between the equation and the observations occurs only for the 10D-long drop inlets.

Equation XII-19 can be written using V_r and h_{vr}, the average velocity and velocity head in the riser or drop inlet respectively. Since $Q = V_c\, 2B\, Z_p = V_r\, BD$,

$$V_c = \frac{V_r}{2\, Z_p/D} \quad \text{(XII-20)}$$

$$h_{vc} = \frac{V_c^2}{2g} = h_{vr}\frac{1}{(2\, Z_p/D)^2} \quad \text{(XII-21)}$$

and

$$\frac{h_n}{h_{vc}} = \frac{h_n}{h_{vr}}\left(2\frac{Z_p}{D}\right)^2 \quad \text{(XII-22)}$$

Substituting this value in equation XII-19, the pressure on the underside of the antivortex plate outside the drop inlet is, in terms of the velocity head in the drop inlet,

$$\frac{h_n}{h_{vr}} = -\frac{1}{(2\, Z_p/D)^2}\log_{10}^{-1}\left[-0.125 - \frac{0.44}{Z_p/D}\frac{x}{D}\right] \quad \text{(XII-23)}$$

Pressure inside the drop inlet

An examination of figures XII–12 through XII–16 shows that the pressures on the underside of the antivortex plate are approximately constant across the width of the drop inlet.

To make the analysis, the average minimum pressure for all values of B/D was read from each subfigure of figures XII–12 through XII–16 and was tabulated. Manipulation showed that an approximate envelope curve could be drawn on a plot of $(h_n/h_{vc})(Z_p/D)$ versus t_c/D. The envelope curve of minimum average pressure on the underside of the antivortex plate within the drop inlet has the equation

$$\frac{h_n}{h_{vc}} = -\frac{0.55 + 0.25 \log_{10}(t_c/D)}{Z_p/D} \qquad \text{(XII–24)}$$

Equation XII–24 has been plotted on figures XII–12 through XII–16. As shown in figure XII–12, for the lowest antivortex plate the equation pressures are appreciably lower than the observed pressures. And, as shown in the (e) subfigures of figures XII–14 to XII–16, the computed pressures are higher than the observed pressures for the 10D-long drop inlets. Otherwise the values of the pressures in the drop inlet computed from equation XII–24 appear to represent the data reasonably well.

Equation XII–24 can be written in terms of the drop inlet velocity head by substituting in it equation XII–22. Thus

$$\frac{h_n}{h_{vr}} = -\frac{0.55 + 0.25 \log_{10}(t_c/D)}{4\,(Z_p/D)^3} \qquad \text{(XII–25)}$$

Pressure over the crest

The pressures on the underside of the antivortex plate and over the crest can be approximated by extending the pressures given by equations XII–24 or XII–25 to over the midpoint of the crest, then varying the pressure uniformly to the pressure given by equations XII–19 and XII–23 at $x/D = 0$, the outer edge of the crest.

The suggested approximation of the pressures over the crest is shown in figures XII–12 through XII–16. The best evaluation of the approximation can be made in figure XII–12(b) and the (e) subfigure of figures XII–13 through XII–16. This is because the crest is relatively thick $(t_c/D = 0.500)$ and more piezometers are available to make the evaluation.

Although the suggested approximation is a reasonable representation of the pressures on that part of the underside of the antivortex plate which lies above the sidewall crest, it is likely that using the pressures given by equations XII–24 or XII–25 over both the inside of the drop inlet and the crests will be satisfactory for ordinary design use.

Comments

Equations XII–19, XII–23, XII–24 and XII–25 give the average maximum hydraulic loading on the antivortex plate for full conduit flow. Loadings for less than full flow will not exceed the full-flow loading.

If trash racks are used, these hydraulic loads apply only when there is a negligible head loss through the trash racks. The load resulting from partial or complete plugging of the trash racks must be added to the hydraulic loads presented herein.

Crest Pressure

To evaluate the pressure on the drop inlet crest h_{nc}, the pressure was measured at from two to four points. Pressures were always measured at the crest centerline and at 45 degrees on the curved downstream surface of the crest. Pressures were also measured at the end of the crest curve for crest thicknesses t_c/D of 0.157, 0.242, 0.331 and 0.658, and at 30 degrees from the horizontal for $t_c/D = 0.658$. All piezometers were located 1D upstream from the downstream end of the drop inlet.

The pressure coefficients h_{nc}/h_{vr} are plotted in figure XII–17. All values of h_{nc}/h_{vr} are negative. Many of the pressures for $B/D = 10$, which are shown as hexagons in figures XII–17(a) and XII–17(e), plot below the remainder of the data. The reason for this is unknown. These data were ignored in the subsequent analysis.

The extent of the vertical line through some of the data points represents the range of h_{nc}/h_{vr} observed at the several piezometer taps. In general, the smaller the symbol, the less the range of the observed pressures. Many of the pressures at the several taps on each crest agreed closely. For other crests the pressures at the several taps were significantly different. No regular pattern of the differences was discovered.

A hyperbolic equation was fitted to the data shown in figure XII–17. The equation is

$$\frac{h_{nc}}{h_{vr}} = \left\{4.5\frac{t_c}{D} - 4.25\right\} + \frac{1}{Z_p/D}\left[2 - \frac{1.6}{(Z_p/D)^{2/3}}\right] \qquad \text{(XII–26)}$$

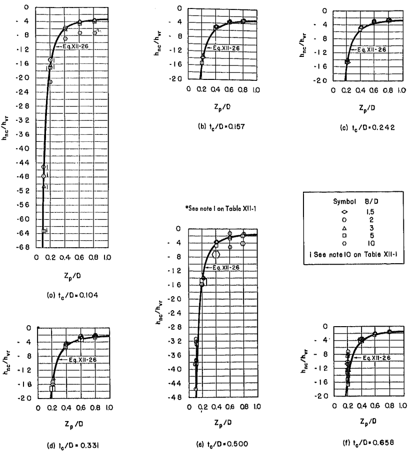

FIGURE XII-17.—Crest pressure.

where $\left\{4.5\frac{t_c}{D} - 4.25\right\} \leqq -2$; that is, for $t_c/D \geqq 0.5$ the quantity in braces is -2.

Equation XII-26 has been plotted in figure XII-17 to show that the equation well represents the data. Equation XII-26 has also been plotted in figures XII-19 through XII-23, which show the pressure distribution on the drop inlet sidewall. In figures XII-19 through XII-23, equation XII-26 has been considered to apply along the crest curve.

Sidewall Pressure

The pressure on the drop inlet sidewall was measured by a row of piezometers located one pipe diameter upstream from the downstream

end of the drop inlet. Pressures were measured on both the inside and outside of the sidewalls. The inside piezometers extended from the crest to the midheight of the 5D-high drop inlet used for these tests. They were located at distances below the drop inlet crest z/D of 0.25, 0.50, 0.75, 1.00, 1.5, 2.0 and 2.5. An exception was the uppermost piezometer when $t_c/D = 0.658$, which was located at $z/D = 0.329$—the downstream end of the crest radius. The vertical distance below the drop inlet crest z is positive below the crest elevation and negative above the crest elevation. The outside piezometers extended only to 0.75D below the crest and were installed only on the drop inlets having wall thicknesses t_c/D of 0.104 and 0.500. These piezometers were located at $z/D = 0.13$, 0.25, 0.50 and 0.75.

Pressure heads on the sidewall are always less than the static pressure head at the same elevation. As a result, the pressure head coefficients are always negative.

The pressures outside and inside the drop inlet will be analyzed separately, and then combined to determine the net load on the sidewall.

Pressure inside the drop inlet

The pressures near the top of the inside sidewall of the drop inlet were initially analyzed on the premise that the stream would separate from the sidewall, at least for the thinner sidewalls, and that the sidewall pressure in the seperation zone would be constant and equal to the pressure on the sidewall crest given by equation XII–26. On the other hand, the sidewall pressures near the midheight of the drop inlet were initially analyzed on the premise that the flow was essentially uniform, that the pressure coefficient at the midheight would be $-(K_c + 1)$ where K_c is computed from equation XII–9, and that pressures above the midheight would be a function of the pressure gradient. The problem, then, was to determine the regions where each premise was valid; to determine and evaluate the effect of antivortex plate height, sidewall thickness and drop inlet length on the sidewall pressures; and to devise methods for evaluating the pressures necessary for the structural design of the drop inlet sidewall.

An initial step in the analysis was to divide the relative pressure h_n/h_{vr} measured at each pressure tap on the drop inlet sidewall by: (1) the relative pressure on the crest h_{nc}/h_{vr} computed using equation XII–26, and (2) the quantity $-(K_c + 1)$ with K_c computed using equation XII–9.

The first ratio, $\dfrac{(h_n/h_{vr})\ \text{observed}}{(h_{nc}/h_{vr})\ \text{computed}}$, should be 1.00 if the observation point is in the separation zone. Similarly, the second ratio,

$\dfrac{(h_n/h_{vr})\ \text{observed}}{-(K_c + 1)\ \text{computed}}$, should be 1.00 at the midheight of the drop inlet and should deviate slightly from 1.00 at points above the midheight if the flow in the drop inlet is uniform. These are the principal ratios, based on the previously mentioned premises, used in the subsequent analysis.

The two ratios computed for each series were tabulated side by side to facilitate comparison. The ratio closest to 1.00 determined which denominator used to normalize the data best represented the experimental results. The number of series, expressed as a percentage, in which the ratio based on $-(K_c + 1)$ is closer to 1.00 than the ratio based on the crest pressure (equation XII–26) is listed in table XII–4 for each piezometer and crest thickness. Percentages exceeding 50 indicate that $-(K_c + 1)$ is the best normalizer; percentages less than 50 indicate that the crest pressure is the best normalizer, that is, that the piezometer is located in or is primarily affected by the separation zone. The tabulated percentages indicate that the crest pressure best normalizes the observed pressure for the pressure tap 0.25D below the drop inlet crest ($z/D = 0.25$), and for crest thicknesses less than 0.500D when $z/D = 0.50$ and crest thicknesses less than 0.331D when $z/D = 0.75$. With one exception, the pressure at the drop inlet midheight, $-(K_c + 1)$, best normalizes all other observed pressures.

Plotting the best normalized ratios averaged for all variables except antivortex plate height

TABLE XII–4.—*Percentages of inside sidewall pressure observations best normalized by* $-(K_c + 1)$

$\frac{t_c}{D}$	z/D						
	0.25	0.50	0.75	1.00	1.50	2.00	2.50
0.104	40	35	38	57	85	95	100
.157	0	0	12	24	62	82	100
.242	12	25	44	59	71	94	100
.331	25	44	62	69	88	100	100
.500	25	60	60	65	70	85	100
.658	22	53	71	75	81	94	100

against the antivortex plate height showed only random variation. As a result, no further correction for the effect of the antivortex plate height was necessary.

Plotting the best normalized ratios averaged for all variables except drop inlet length against drop inlet length showed a systematic variation for all piezometers except that piezometer located at the drop inlet midheight. Because preliminary analyses and considerations based on analysis of streamlines plotted with the aid of conductive paper indicated that the measured pressures are a function of the drop inlet length, this variation was not unexpected. However, when $z/D = 0.50$ and 0.75, a more orderly arrangement of the variations between the several piezometers was obtained when $-(K_c + 1)$ was used to normalize the pressures for all crest thicknesses instead of only those piezometers where the percentage in table XII–4 exceeds 50. As a result, the crest pressure was used to normalize the pressure only for the piezometer located at $z/D = 0.25$.

A means was sought of describing the variation of drop inlet sidewall pressure with drop inlet length. For the midheight piezometer ($z/D=2.5$), the drop inlet length effect is included in the computation for K_c and no further correction for drop inlet length is required. This is demonstrated in figure XII–18(a) where the value of

the ratio $\dfrac{(h_n/h_{vr})\ \text{observed}}{-(K_c + 1)\ \text{computed}}$ is close to 1.00

and is constant with respect to the relative drop inlet length B/D. Such constancy, however, does not exist for the piezometers located above the drop inlet midheight. This is demonstrated in figure XII–18(b), (c), and (d), where the variation of the ratio with drop inlet length increases with the distance from the midheight piezometer (decreasing z/D).

When the logarithm of the ratio $(h_n/h_{vr})\ /\ [-(K_c + 1)]$—the ratio of the observed pressure head to the velocity head in the drop inlet normalized by the pressure coefficient at the drop inlet midheight—was plotted against $(B/D)^2$—the square of the relative drop inlet length—a systematic trend was apparent. This trend can be represented by the equation

$$K_{B/D} = \frac{1.742 - \log_{10}(z/D)}{1.344}\, b^{-(B/D)^2} \qquad \text{(XII–27)}$$

for $B/D \leqq 7$ (for $B/D > 7$, use $B/D = 7$) where

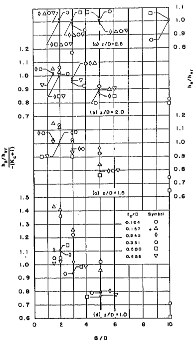

FIGURE XII–18.—Sidewall pressure divided by computed midheight pressure, $Z_p/D = 0.8$.

$K_{B/D}$ is the multiplier correction for drop inlet length to be applied to $-(K_c + 1)$, and for

$z/D = 0.5,\ 0.75,\ 1.0,\ 1.5,\ 2.0,\ 2.5,$
$b = 1.0145,\ 1.0126,\ 1.0112,\ 1.0090,\ 1.0047,\ 1.0000.$

(For $0.5 \leqq z/D \leqq 1.5$,

$$b = 0.9925 + 0.0145\left[\frac{1.742 - \log_{10}(z/D)}{1.344}\right].)$$

To test equation XII–27, the ratio $(h_n/h_{vr})\ /\ [-K_{B/D}(K_c + 1)]$ was computed for each test series. When this ratio, averaged for each crest thickness t_c/D, was plotted against t_c/D a systematic trend was apparent. This indicated a need to apply a correction for the crest thickness effect.

The multiplier correction for the effect of crest thickness $K_{t_c/D}$ is represented by the equation

$$K_{t_c/D} = \left(0.68 + 0.08\frac{z}{D}\right)\left(\frac{t_c}{D}\right)^{-\left(0.276 - 0.072\frac{z}{D}\right)} \quad \text{(XII–28)}$$

where $0.5 \leqq z/D \leqq 2.5$.

To test the product of equations XII–9, XII–27, and XII–28 against the observed data, the ratio $(h_n/h_{vr}) \;/\; [-K_{B/D} K_{t_c/D} (K_c + 1)]$ was computed for each test series. Compared with the ratios computed using the $K_{B/D}$ correction only, there was a considerable improvement in the agreement of the equations with the original data averaged for each crest thickness. The average ratios for all tests showed little change, but there was a reduction in the probable error as a result of correcting for the crest thickness effect. The average ratio and the probable error are shown in table XII–5. Excluded from these figures are the data for $B/D = 10$, which were inconsistent with the remainder of the data, and the data for $Z_p/D \approx 0.1$, which are for an antivortex plate height lower than is recommended.

A column for $z/D = 0.25$ was added to table XII–5. The values given by equation XII–26 multiplied by 0.93 were used to normalize the pressures for this piezometer.

The agreement of the equation with the observed sidewall pressures is shown in figures XII–19 through XII–23 for all available pertinent data. It can be seen that the equations do not represent the pressures when $B/D = 10$, this observation agreeing with the previous statements that the data for $B/D = 10$ are inconsistent with the remainder of the data. In addition, the equations are not representative of the data shown in figure XII–19 where $Z_p/D = 0.1$; for

TABLE XII–5.—*Average agreement of observed inside sidewall pressures with computed pressures*

Item	z/D 0.25	0.50	0.75	1.00	1.50	2.00	2.50
Ratio	1.00	.99	.99	.98	.97	.98	.99
Probable error	.08	.11	.11	.11	.09	.07	.05

$Z_p/D = 0.1$ the equation values of h_n/h_{vr} range from -91 to -181 when $t_c/D = 0.104$ whereas the data are in the range -44 to -51, and when $t_c/D = 0.500$ the values of h_n/h_{vr} range from -66 to -123 whereas the data range from -28 to -39. Furthermore, for $Z_p/D = 0.2$, figure XII–20, the equations poorly represent the data. However, because "X" in the notes of figures XII–19 and XII–20 means that the "drop inlet dimensions do not meet the recommended criteria," the lack of agreement of the equations with the observed data is of no practical significance.

The equations do well represent the observed data, except for $B/D = 10$ as noted above, when Z_p/D is 0.4 or greater. This is shown in figures XII–21, XII–22 and XII–23. In figure XII–21, where $Z_p/D = 0.4$, the data and the equations agree to within 1 h_{vr}. In figures XII–22 and XII–23, where $Z_p/D = 0.6$ and 0.8 respectively, the agreement is better—to within 0.5 h_{vr}. Thus, figures XII–19 through XII–23 show that the agreement of the equations with the data is good for all drop inlet proportions that meet the recommended design criteria.

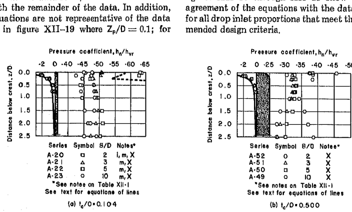

FIGURE XII–19.—Pressure distribution on the drop inlet sidewall, $Z_p/D = 0.1$.

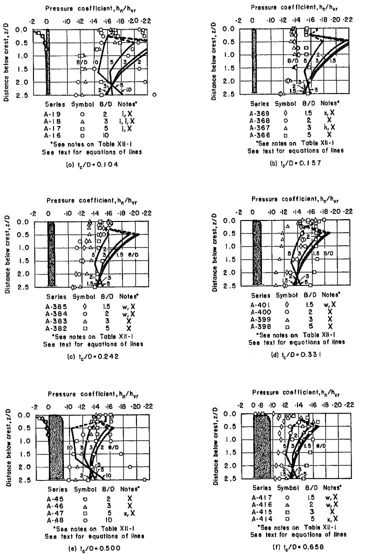

FIGURE XII–20.—Pressure distribution on the drop inlet sidewall, $Z_p/D = 0.2$.

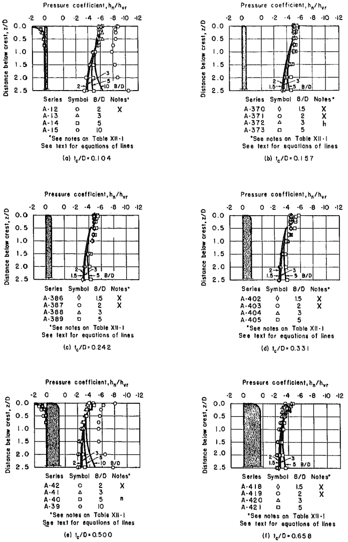

FIGURE XII-21.—Pressure distribution on the drop inlet sidewall, $Z_P/D = 0.4$.

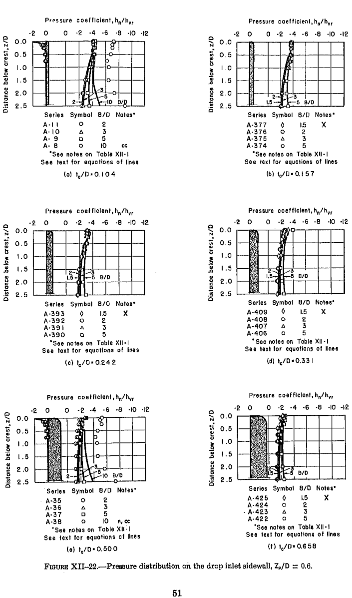

FIGURE XII-22.—Pressure distribution on the drop inlet sidewall, $Z_p/D = 0.6$.

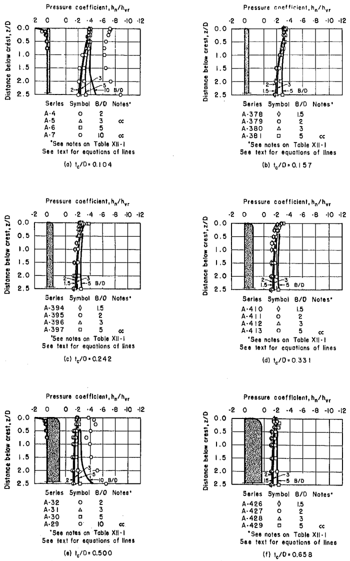

FIGURE XII-23.—Pressure distribution on the drop inlet sidewall, $Z_p/D = 0.8$.

Summary.—To compute the sidewall pressures inside the drop inlet:

when $z/D = 0.25$, multiply the value obtained from equation XII–26 by 0.93;

when $0.5 \leqq z/D \leqq 2.5$, multiply $-(K_c+1)$, with K_c computed by equation XII–9, by the drop inlet length correction given by equation XII–27 and by the crest thickness correction given by equation XII–28.

The average precision of the prediction is indicated in table XII–5. The agreement of the equations with the observations is shown in figures XII–19 through XII–23.

Pressure outside the drop inlet

Sidewall pressures outside the drop inlet were measured at distances below the creat z/D of 0.13, 0.25, 0.50, and 0.75 for drop inlet crest thicknesses t_c/D of 0.104 and 0.500 and drop inlet lengths B/D of 2, 3, 5, and 10. It was reasoned that the pressures h_n would be most closely related to the velocity between the antivortex plate and the crest h_{vc}.

An inspection of the tabulated values of h_n/h_{vc} indicated that, with respect to the distance below the drop inlet crest z/D, the relationship was hyperbolic. A tabulation of the product (h_n/h_{vc}) (z/D) showed the product to be substantially constant for each antivortex plate height Z_p/D.

When (h_n/h_{vc}) (z/D) was plotted against Z_p/D, the relationship was adequately represented by a straight line. The resulting equation for the relative pressure on the outside of the drop inlet sidewall is

$$\frac{h_n}{h_{vc}} = -\frac{Z_p/D}{8\,z/D} \qquad \text{(XII–29)}$$

which can be reduced to

$$\frac{h_n}{h_{vc}} = -\frac{1}{8}\frac{Z_p}{z} \qquad \text{(XII–30)}$$

Using equation XII–21, equation XII–29 can be expressed in terms of the velocity head in the drop inlet. Thus

$$\frac{h_n}{h_{vr}} = -\frac{1}{32\,(Z_p/D)\,(z/D)} \qquad \text{(XII–31)}$$

Equation XII–29 was tested by computing the differences between the computed and the observed relative pressures h_n/h_{vc}. The maximum average error is 0.05 and the maximum probable error is 0.03. In general, the errors increased as the antivortex plate height increased. A reason for this may be that the velocity between the antivortex plate and the crest is low for high antivortex plates. When the sidewall pressure is divided by the low velocity head, any error in the pressure measurement is magnified, so there may be a larger error for the high antivortex plates than for the low antivortex plates where the velocities are higher. However, the precision of the results is well within practical needs.

Equation XII–31 has been plotted on figures XII–19 through XII–23. It is apparent that the equations well represent the data.

Net pressure on the sidewall

The net pressure load on the sidewall is the difference between the pressures inside and outside the drop inlet.

When the drop inlet is completely full, the pressures outside the drop inlet are computed using equation XII–31. The pressures inside the drop inlet are given by equation XII–26 over the crest curve, by 0.93 times the result obtained using equation XII–26 when $z/D = 0.25$, and by $-K_{B/D}\,K_{t_c/D}\,(K_c+1)$ when $0.5 \leqq z/D \leqq 2.5$ where $K_{B/D}$ is given by equation XII–27, $K_{t_c/D}$ is given by equation XII–28 and K_c is given by equation XII–9. Because the inside pressures are always less than the outside pressures, the net load is inward.

When the drop inlet is partly full, as is the case for weir flow over the drop inlet crest, the pressures inside the drop inlet are approximately atmospheric. The pressures outside the drop inlet are the static pressures which, near the crest,

and the crest thickness; and outside the drop inlet there were from 0 to 12 piezometers. Only for crest thickness t_c/D of 0.104 and 0.500 were there sufficient piezometers outside the drop inlet to permit sketching the complete pressure contours. When $t_c/D = 0.104$, the overhang of the endwalls L_o/D was 1.86; and for $t_c/D = 0.500$, L_o/D was 1.50. For other crest thicknesses, L_o/D varied from 4.0 to 3.5 depending on the crest thickness, the same endwall being used for all crest thicknesses. Despite the large number of piezometers, there were far too few to permit accurate drawing of the pressure contours, especially in the vicinity of the crest where the endwall pressures vary rapidly with distance in any direction.

Pressure heads on the endwall are always less than the static pressure head at the same elevation. As a result, the pressure head coefficients h_n/h_{vr} are always negative.

All attempts to reduce the endwall pressures to a common denominator led to unsatisfactory presentations of the data. One of these attempts involved normalizing the pressure coefficients using the computed pressure at the drop inlet midheight $- (K_c + 1)$, K_c being computed from equation XII–9. Another attempt, equally unsuccessful, was to correct $- (K_c + 1)$ using $K_{B/D}$ and $K_{t_c/D}$ computed from equations XII–27 and XII–28.

The analytical procedure ultimately adopted was to first record the pressure coefficients for each test series on a drawing of the endwall elevation. To assist in extending the contours to the underside of the antivortex plate, the antivortex plate pressures measured 1D upstream from the downstream endwall were added to the work plots.

Pressure coefficient contours were then drawn. Inspection showed that the pressure coefficient contour patterns were approximately similar for each crest thickness, but that the magnitude of the pressure represented by each contour varied greatly with antivortex plate height and slightly with drop inlet length. Therefore, a typical pressure coefficient contour pattern was sketched on tracing paper for each crest thickness.

The contour pattern was then placed over the plotted data for each test series, and representative pressure coefficients for each contour were read and tabulated. A study of the tabulations for drop inlet lengths B/D of 1.5, 2, 3, and 5 demonstrated, within the limits of experimental precision and the variations in the sketched locations of the contours, that the variation with B/D was not significant. Therefore, a single tabulation of the pressure coefficient $-h_n/h_{vr}$ for each contour was prepared for each crest thickness t_c/D, the value of $-h_n/h_{vr}$ then being a function of the contour and the antivortex plate height Z_p/D.

The experimental results are presented in figure XII–24 in the form of lettered pressure coefficient contour lines for each crest thickness tested. The value of $-h_n/h_{vr}$ for each contour is given in an accompanying table as a function of the antivortex plate height.

A quick check on the precision of the summaries presented in figure XII–24 indicates that they represent the observed pressures to within perhaps 25 percent on the average. As noted previously, the rate of change of pressure with distance in the vicinity of the drop inlet crest is large, and there were too few piezometers to accurately define the pressure pattern there.

Barrel Entrance Pressure

Low pressures exist just inside the entrance to the barrel. If these pressures are low enough, they can induce cavitation which may, in turn, damage the conduit. Information to permit evaluating these pressures will be presented for the three types of barrel entrances shown in the subfigures of figure XII–1.

The analysis was made in terms of the pressure coefficient for the spillway barrel. The pressure coefficient for any point n along the barrel is defined as h_n/h_{vp}, where h_n is the deviation from the friction gradeline at n and h_{vp} is the velocity head in the pipe.

Point pressures were measured at both the barrel crown and invert at a distance D/2 downstream from the barrel entrance. Pressures were also measured at 17D, 33D, 49D, 65D, 81D, 97D, 113D, 129D and 137D along the barrel.

The disturbance caused by the barrel entrance is almost completely damped out at 17D, so pressures at 33D and beyond were used to compute the friction gradeline. The least squares method was used for this purpose. The measured and least squares grade line pressures beyond 17D agreed to within ±3 percent of the pipe velocity head. The least squares friction gradeline was projected back to the barrel entrance. The differ-

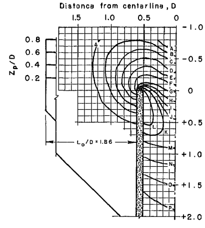

Values of $-h_n/h_{vr}$

Contour	Z_p/D			
	0.206	0.412	0.616	0.820
A	0.25	0.20	0.15	0.10
B	.5	.3	.20	.18
C	.8	.5	.3	.2
D	1.4	.7	.4	.3
E	3.0	1.2	.6	.4
F	6.0	2.0	1.0	.7
G	9.0	3.0	2.0	1.5
H	13.0	4.0	2.9	2.2
I	14.0	5.0	3.5	2.8
J	15.0	5.5	3.8	3.1
K	16.0	5.7	4.0	3.4
L	16.3	6.2	4.1	3.7
M	14.0	5.1	3.8	2.9
N	13.6	4.7	3.4	2.7
O	13.1	4.3	3.0	2.4
P	12.5	4.0	2.5	2.2

(a) $t_c/D = 0.104$

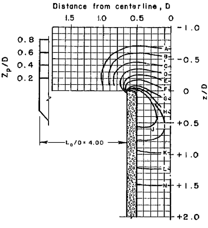

Values of $-h_n/h_{vr}$

Contour	Z_p/D			
	0.223	0.417	0.614	0.813
A	0.6	0.4	0.2	0.15
B	.8	.5	.3	.2
C	1.0	.6	.4	.3
D	3.0	1.0	.6	.4
E	5.0	1.5	.9	.7
F	8.0	2.0	1.2	1.0
G	12.0	3.3	2.0	2.0
H	13.6	4.5	3.0	2.5
I	13.9	5.0	3.4	2.8
J	14.0	5.1	3.5	3.0
K	13.7	5.0	3.1	2.5
L	13.4	4.6	2.8	2.2
M	13.1	4.4	2.5	2.0

(b) $t_c/D = 0.157$

FIGURE XII-24.—Pressure distribution on the drop inlet downstream endwall.

ence between the hydraulic gradeline and the friction gradeline is h_n. A more detailed explanation of h_n, its significance, and its use is given on page 13 of Part I[11] of this closed conduit spillway report series.

[11] See Part I reference in Preface for complete citation.

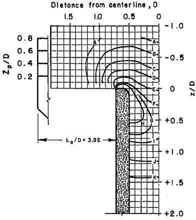

Values of $-h_n/h_{vr}$

Contour	Z_p/D			
	0.222	0.414	0.613	0.813
A	0.4	0.3	0.2	0.15
B	.8	.5	.3	.2
C	1.5	.7	.5	.3
D	3.0	1.5	.7	.5
E	10.0	2.5	1.2	1.0
F	12.5	4.0	2.3	1.5
G	13.0	4.7	2.7	1.8
H	13.6	4.8	3.0	2.0
I	13.0	4.5	2.5	1.7
J	13.0	4.2	2.2	1.6
K	12.5	3.8	2.0	1.5

(c) $t_c/D = 0.242$

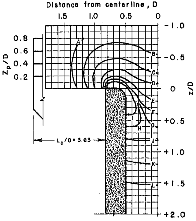

Values of $-h_n/h_{vr}$

Contour	Z_p/D			
	0.213	0.404	0.604	0.804
A	0.3	0.25	0.2	0.15
B	1.0	.6	.3	.2
C	1.7	.8	.5	.3
D	4.5	2.0	.8	.5
E	15.0	3.0	1.5	1.0
F	15.0	4.0	1.8	1.2
G	15.2	4.3	2.0	1.3
H	15.0	4.4	2.2	1.4
I	15.0	4.5	2.3	1.5
J	15.0	4.0	1.8	1.3
K	14.0	3.5	1.7	1.3
L	13.0	3.2	1.6	1.3

(d) $t_c/D = 0.331$

FIGURE XII-24.—Continued.

For the square-edged entrance a data were obtained for drop inlet lengths B/D of 1.5, 2, 3 and 5; for crest thicknesses t_c/D of 0.104, 0.157, 0.242, 0.331, 0.500 and 0.658; for antivortex plate heights Z_p/D of 0.1, 0.2, 0.4, 0.6, and 0.8; and for barrel slopes S of 0.00, 0.025, 0.05, 0.10, 0.20, 0.30, and 0.40. For the square-edged entrance b similar ranges of Z_p/D and S were tested, but an additional drop inlet length—$B/D = 1$—and only one crest thickness—$t_c/D = 0.500$—were used. For the groove-edged entrance c the ranges of B/D and t_c/D were the same as for the square-edged

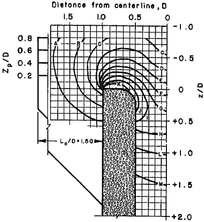

Values of $-h_n/h_{vr}$

Contour	Z_p/D 0.220	0.416	0.610	0.808
A	0.30	0.19	0.13	0.10
B	.60	.30	.20	.18
C	2.0	.70	.40	.25
D	6.0	1.0	.5	.3
E	8.0	1.5	.7	.4
F	11.0	2.0	.8	.5
G	12.0	2.5	1.3	.7
H	13.0	2.9	1.4	1.3
I	13.2	3.0	1.5	1.3
J	13.4	3.5	2.0	1.5
K	13.4	3.8	2.6	1.5
L	12.4	2.6	1.4	1.3
M	11.5	2.5	1.4	1.3

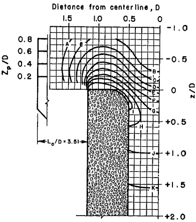

Values of $-h_n/h_{vr}$

Contour	Z_p/D 0.212	0.405	0.605	0.803
A	----	---	---	0.2
B	----	---	.4	.3
C	1.5	.9	.6	.4
D	2.0	1.5	.7	.5

(e) $t_c/D = 0.500$

FIGURE XII-2

entrance b, but only one antivortex plate height —$Z_p/D = 0.8$—was used.

Pressure coefficients are presented in figures XII-25, XII-26, and XII-27 for the three barrel

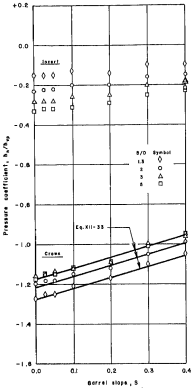

FIGURE XII-25.—Pressure coefficients at D/2 inside square-edged barrel entrance a. $t_c/D = 0.500$, $Z_p/D = 0.80$.

it is possible to compare the three entrances. From these figures it can be seen that most of the invert barrel entrance pressure coefficients are a little below the friction gradeline (h_n/h_{vp} is negative) while the crown pressure coefficients are about one barrel velocity head below the friction gradeline. It is also apparent that the pressures increase as the drop inlet length B/D and the barrel slope S increase. The explanations for these increased pressures are similar to the explanations presented previously during the discussion of the Barrel entrance loss coefficient.

Because it is the lower crown pressures which are most likely to produce cavitation, no analysis of the invert pressures was attempted. The crown pressures, however, were analyzed to evaluate the effect on them of crest thickness, drop inlet length, and barrel slope. These analyses were made for each entrance.

Effect of crest thickness

Only for the square-edged entrance a were data available to determine the effect of crest thickness on the barrel entrance crown pressure.

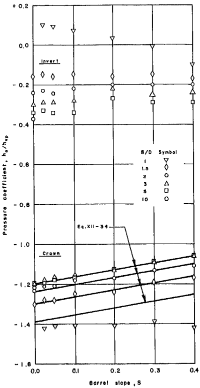

FIGURE XII-26.—Pressure coefficients at D/2 inside square-edged barrel entrance b. $t_c/D = 0.500$, $Z_p/D \approx 0.81$.

The analysis was made for one barrel slope—$S = 0.2$—the only slope for which complete data were available. Because there was no apparent systematic variation of the crown pressure coefficient with the crest thickness, the working plot is not presented here. There is, in fact, little reason to suspect that the crest thickness would affect the pressures in the barrel; the available data confirm this reasoning.

Effects of barrel slope and drop inlet length

The effects of barrel slope S on the pressure coefficients are shown by the slopes of the lines in figures XII–25, XII–26 and XII–27 for the three types of barrel entrances tested. The effect of relative drop inlet length B/D is indicated by the location of the lines. The straight lines shown in the figures can be defined by an equation having the general form

$$\frac{h_n}{h_{vp}} = a + b S \qquad \text{(XII–32)}$$

where a, the intercept at $S = 0$—different for each line—varies with the drop inlet length and b determines the magnitude of the barrel slope effect. The problem, then, is to evaluate a and b for each barrel entrance.

Equation for square-edged barrel entrance $\underline{a}$. —The lines drawn in figure XII–25 are parallel so the coefficient b is constant for all drop inlet lengths. It has a value of 0.55.

The intercept a of the line for each B/D was read from figure XII–25 and an equation developed for a. It was found that the equation best representing a is $a = -1.365 + 0.5 \log_{10} (B/D)$ for values of B/D between 1.5 and 2.4. The drop inlet length had no effect on the barrel entrance crown pressure coefficient for values of B/D exceeding 2.4; for drop inlet lengths longer than $2.4D$, $B/D = 2.4$ should be used in the equation for a.

The equation representing the pressure coefficient at the crown of square-edged barrel entrance $\underline{a}$ at a distance $D/2$ inside the barrel entrance is

$$\frac{h_n}{h_{vp}} = -1.365 + 0.5 \log_{10} \frac{B}{D} + 0.55 S \qquad \text{(XII–33)}$$

for $1.5 \leq B/D \leq 2.4$. (For $B/D > 2.4$, use $B/D = 2.4$.)

The agreement of equation XII–33 with the data is shown in figure XII–25. In addition, equation XII–33 was tested by computing values of h_n/h_{vp} and comparing them with the observed values. The computed values of h_n/h_{vp} were lower than the observed values. The maximum deviation was $0.15\ h_{vp}$ but only 16 of the 79 computed values deviated from the observed values by more than 0.05 barrel velocity heads. There was no detectable variation of the deviations with respect to crest thickness or barrel slope, but the difference did increase somewhat with respect to antivortex plate height, the computed values for the lower antivortex plate heights being lower than the observed values. Because the magnitude

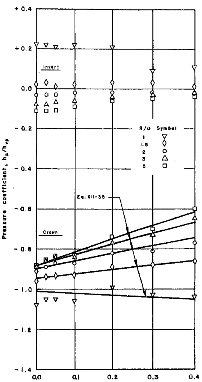

FIGURE XII–27.—Pressure coefficients at $D/2$ inside groove-edged barrel entrance $\underline{c}$. $t_c/D = 0.500$, $Z_p/D = 0.812$.

of the variation was small (about 0.04 h_{vp}), no attempt was made to correct for the apparent slight effect of antivortex plate height.

Equation for square-edged barrel entrance b. —As in figure XII–25, parallel lines have been drawn in figure XII–26 to represent the crown pressure coefficient D/2 inside the square-edged barrel entrance b. The slope of these lines—coefficient b in equation XII–32—is 1/3, and constant a is $-1.385 + 0.5 \log_{10} (B/D)$ for values of B/D between 1.5 and 2.4.

The equation representing the pressure coefficient at the crown of the square-edged barrel entrance b at a distance D/2 inside the barrel entrance is

$$\frac{h_n}{h_{vp}} = -1.385 + 0.5 \log_{10} \frac{B}{D} + \frac{S}{3} \qquad \text{(XII–34)}$$

for $1.5 \leq B/D \leq 2.4$. (For $B/D > 2.4$, use $B/D = 2.4$.)

The agreement of equation XII–34 with the data is shown in figure XII–26. The agreement is excellent except for $B/D = 1$, a drop inlet length which does not meet the limiting design criteria. In addition, equation XII–34 was tested by comparing the computed and observed values of h_n/h_{vp}. The agreement of the computed and observed values is excellent, averaging better than about 0.01 barrel velocity heads. Deleted from the average were the values obtained for drop inlets which do not meet the recommended criteria. The computed pressures were lower than the observed pressures, but the maximum difference of 35 observations was only 0.06 barrel velocity heads. There was no observable trend of the differences with either antivortex plate height or barrel slope.

Equation for groove-edged barrel entrance c. —The lines drawn in figure XII–27 to represent the crown pressure coefficient D/2 inside groove-edged barrel entrance c diverge. This indicates that the drop inlet length affects the relationship between the pressure coefficient and the barrel slope. The slope of these lines—coefficient b in equation XII–32—is $b = 0.85 - 0.95/(B/D)$ and constant a is $-1.01 + 0.38 \log_{10} (B/D)$ for values of B/D between 1 and 2.2.

The equation representing the pressure coefficient at the crown of the groove-edged barrel entrance c at a distance D/2 inside the barrel entrance is

$$\frac{h_n}{h_{vp}} = -1.01 + 0.38 \log_{10} \frac{B}{D} + \left(0.85 - \frac{0.95}{B/D}\right) S \qquad \text{(XII–35)}$$

for $1 \leq B/D \leq 2.2$ in the second (log) term. (For $B/D > 2.2$, use $B/D = 2.2$.) In the third (S) term $1 \leq B/D \leq 5$.

The agreement of equation XII–35 with the data is shown in figure XII–27. Even for $B/D = 1$, a drop inlet length shorter than recommended, the equation well represents the data. In addition, equation XII–35 was tested by comparing the computed and observed values of h_n/h_{vp}. The agreement of the computed and observed values is again excellent, averaging about 0.01 pipe velocity heads. Deleted from the average were the values obtained for drop inlets which do not meet the recommended criteria. The computed pressures were both greater and less than the observed pressures, the maximum difference of 28 observations being only +0.03 and −0.02 barrel velocity heads. Again, there was no observable trend of the differences with barrel slope. Because only one antivortex plate height was used for these tests, the effect of antivortex plate height, if any, could not be determined.

Recommendation Summary

The only information included in this summary of the results of the two-way drop inlet spillway tests are the recommendations for proportioning the drop inlet, for determining the spillway capacity, and for evaluating the pressures. The bases for these recommendations can be found in the text.

For convenience of use, the recommendations are presented in:

Figure XII–28 for proportioning the drop inlet,

Figure XII–29 for determining the spillway capacity, and

Figure XII–30 for evaluating the pressures in the spillway.

With the single exception of the minimum antivortex plate height, all of the results in figures XII–28, XII–29 and XII–30 are expressed in dimensionless units or in a dimensionally correct form. Therefore, any consistent system of units—for example, English or metric—can be used. In dimensionless units, the criteria for minimum antivortex plate height are, for $B/D = 1.5$, $Q/\sqrt{g}\,D^{5/2} \approx 1.30$ and, for $B/D \geqq 2$, $Q/\sqrt{g}\,D^{5/2} \approx 0.90$. To make equations I–1 and I–2 dimensionally correct, add the terms $\sqrt{2g}$ to the right side, the values of the dimensionless discharge coefficient $C/\sqrt{2g}$ then being 0.39 for $C = 3.1$ and 0.50 for $C = 4.0$.

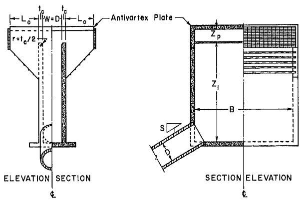

DROP INLET HEIGHT, Z_I

$Z_I \geq 3D$

DROP INLET LENGTH, B

$B \geq 1.5D$

MINIMUM ANTIVORTEX PLATE OVERHANG, L_o

Table XII-3. Minimum Antivortex Plate Overhang

B/D	$(L_o/D)_{minimum}$
1.5	1.0
2	0.6
3	0.5
5	0.4
10	0.1
*	0.75

* To eliminate effect of antivortex plate overhang on crest loss coefficient K_c

SLOPE, S

0.2 only slope tested

MAXIMUM ANTIVORTEX PLATE HEIGHT, Z_p

The headpool surface elevation at which the weir flow and pipe flow discharges are equal – the intersection of the weir and pipe flow head-discharge curves in, for example, Fig. XII-29.

MINIMUM ANTIVORTEX PLATE HEIGHT, Z_p

is the weir flow head for:

$Q \gtrapprox 7.4D^{5/2}$ when $B = 1.5D$

$Q \gtrapprox 5.1D^{5/2}$ when $B \geq 2D$

or

Table XII-2. Minimum Antivortex Plate Height

B/D	$(Z_p/D)_{minimum}$ C=3.1	C=4.0
1.5	0.85	0.72
2	0.55	0.47
3	0.42	0.36
5	0.30	0.25
10	0.19	0.16

C is the weir flow coefficient in the equation

$$Q = CLH^{3/2} \qquad (I-1)$$

or

$$\frac{Q}{D^{5/2}} = C\frac{L}{D}\left(\frac{H}{D}\right)^{3/2} \qquad (I-2)$$

FIGURE XII-28.—Recommended proportions of the two-way drop inlet.

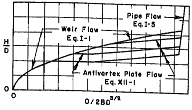

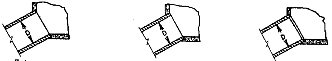

Entrance a　　Entrance b　　Entrance c

WEIR FLOW

Use published equations or $Q = CLH^{3/2}$ (Eq.I-1) where $L = 2B$ and C is evaluated from published information.

ANTIVORTEX PLATE FLOW *

$$\frac{H}{D} = \frac{Z_p}{D} - \left\langle \frac{0.2}{B/D} - 0.1 \log_{10} \frac{L_c}{D} \right\rangle + \left\langle 0.1 - 0.05 \frac{L_c}{D} \right\rangle \frac{Q}{2BD^{3/2}} \geq \frac{Z_p}{D} \qquad \text{(XII-1)}$$

PIPE FLOW

$$Q = \frac{\pi D^2}{4} \sqrt{\frac{2gH_t}{K_e + K_c + \cdots + f\frac{\ell}{D} + f_r \frac{\ell_r}{4R_r}\left(\frac{A_p}{A_r}\right)^2}} \qquad \text{(I-5)}$$

Crest Loss Coefficient*

$$K_c = \left\langle 1 - 2\frac{t_c}{D} \right\rangle^2 + \frac{0.1}{(Z_p/D)^3} + 0.02\left(\frac{B}{D}\right)^{5/2} \qquad \text{(XII-9)}$$

Barrel Entrance Loss Coefficient

Square-edged barrel entrance a

$$K_t = 0.43 + \frac{0.55}{(B/D)^{5/6}} - 0.45S \qquad \text{(XII-11)}$$

Offset square-edged barrel entrance b

$$K_t = 0.43 + \frac{0.55}{(B/D)^{5/6}} - 0.25S \qquad \text{(XII-12)}$$

Groove-edged barrel entrance c

$$K_t = 0.25 + \frac{0.55}{(B/D)^{5/6}} - 0.25S \qquad \text{(XII-13)}$$

Entrance Loss Coefficient

$$K_e = K_c\left(\frac{\pi}{4B/D}\right)^2 + K_t \qquad \text{(XII-17)}$$

* The quantity in pointed brackets, $\langle\ \rangle$, is zero for negative values.

FIGURE XII-29.—Capacity of the two-way drop inlet.

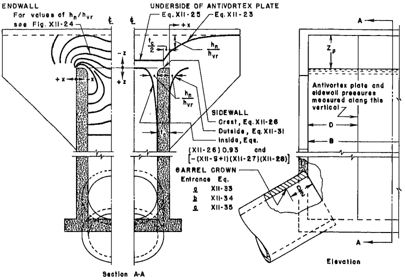

EQUATIONS

ENDWALL, Interpolate from Fig. XII-24

BARREL CROWN, D/2 inside the barrel for:

Entrance a

$$\frac{h_n}{h_{vp}} = -1.365 + 0.5 \log_{10}\frac{B}{D} + 0.65\,S \qquad \text{(XII-33)}$$

where for $B/D > 2.4$, use $B/D = 2.4$

Entrance b

$$\frac{h_n}{h_{vp}} = -1.385 + 0.5 \log_{10}\frac{B}{D} + \frac{S}{3} \qquad \text{(XII-34)}$$

where for $B/D > 2.4$, use $B/D = 2.4$

Entrance c

$$\frac{h_n}{h_{vp}} = -1.01 + 0.38 \log_{10}\frac{B}{D} + \left(0.85 - \frac{0.95}{B/D}\right) S \qquad \text{(XII-35)}$$

where, in the log term, for $B/D > 2.2$, use $B/D = 2.2$;
and, in the S term, $1 \leq B/D \leq 5$

FIGURE XII-30.—Pressures in the two-way drop inlet.

UNDERSIDE OF ANTIVORTEX PLATE

Inside Drop Inlet

$$\frac{h_n}{h_{vr}} = -\frac{0.55 + 0.25 \log_{10}(t_c/D)}{4(Z_p/D)^2} \qquad \text{(XII-25)}$$

Outside Drop Inlet

$$\frac{h_n}{h_{vr}} = -\frac{1}{(2Z_p/D)^2}\log_{10}^{-1}\left[-0.125 - \frac{0.44}{Z_p/D}\frac{x}{D}\right] \qquad \text{(XII-23)}$$

SIDEWALL

Crest

$$\frac{h_n}{h_{vr}} = \left\{4.5\frac{t_c}{D} - 4.25\right\} + \frac{1}{Z_p/D}\left[2 - \frac{1.6}{(Z_p/D)^{2/3}}\right] \qquad \text{(XII-26)}$$

where $\left\{4.5\frac{t_c}{D} - 4.25\right\} \leq -2$

Inside Drop Inlet

For $z/D = 0.25$, use 0.93 times the pressure on the crest given by Eq. XII-26

For $0.5 \leq z/D \leq 2.5$

$$\frac{h_n}{h_{vr}} = -(K_c + 1)K_{B/D}K_{t_c/D}$$

where the:

Crest loss coefficient, K_c

$$K_c = \left\langle 1 - 2\frac{t_c}{D}\right\rangle^2 + \frac{0.1}{(Z_p/D)^3} + 0.02\left(\frac{B}{D}\right)^{2/3} \qquad \text{(XII-9)}$$

where $\left\langle 1 - 2\frac{t_c}{D}\right\rangle = 0$ for negative values

Correction for drop inlet length, $K_{B/D}$

$$K_{B/D} = \frac{1.742 - \log_{10}(z/D)}{1.344}\, b^{-(B/D)^2} \qquad \text{(XII-27)}$$

where for $B/D > 7$, use $B/D = 7$; and for

z/D = 0.5 , 0.75 , 1.0 , 1.5 , 2.0 , 2.5

b = 1.0145, 1.0126, 1.0112, 1.0090, 1.0047, 1.0000

Correction for crest thickness, $K_{t_c/D}$

$$K_{t_c/D} = \left(0.68 + 0.08\frac{z}{D}\right)\left(\frac{t_c}{D}\right)^{-\left(0.276 - 0.072\frac{z}{D}\right)} \qquad \text{(XII-28)}$$

where $0.5 \leq z/D \leq 2.5$

Outside Drop Inlet

$$\frac{h_n}{h_{vr}} = -\frac{1}{32(Z_p/D)(z/D)} \qquad \text{(XII-31)}$$

FIGURE XII-30.—Continued.

Nomenclature

a a constant, dimensionless
A_p area of barrel, in square feet
A_r area of drop inlet or riser, in square feet
b a constant, dimensionless
B drop inlet length, in feet
C discharge coefficient in equation I–1, in English units
C_c contraction coefficient for the jet in the drop inlet, dimensionless
D barrel diameter and drop inlet width, in feet
D_j width of the jet in the drop inlet, in feet
f Darcy-Weisbach friction factor in the barrel, dimensionless
f_r Darcy-Weisbach friction factor in the drop inlet or riser, dimensionless
g gravitational acceleration, in feet per second per second
h_c head loss at the drop inlet crest, in feet
h_e total head loss for the drop inlet, in feet
h_n in the barrel, the local pressure head deviation from the friction gradeline, in feet; in the drop inlet, the local pressure head relative to the pressure at the same elevation outside the drop inlet, in feet
h_{nc} the pressure head on the drop inlet crest relative to the pressure in the reservoir at crest elevation, in feet
h_t head loss caused by the barrel entrance or transition, in feet
h_{vc} velocity head between the antivortex plate and the drop inlet crest $= V_c^2 / 2\,g$, in feet
h_{vp} velocity head in the barrel $= V_p^2 / 2g$, in feet
h_{vr} velocity head in the drop inlet $= V_r^2 / 2\,g$, in feet
H head on crest, in feet
H_t total head from water surface to point at which the hydraulic gradeline pierces the plane of the outlet $=$

$$H + Z + \left\langle \frac{D}{2} - \beta\, D \right\rangle \cos^{-1} (\sin S),$$

or to the tailwater surface, in feet
$K_{B/D}$ multiplier correction for drop inlet length, dimensionless
K_c crest loss coefficient, dimensionless
$K_{c,\,B}$ Borda mouthpiece crest loss coefficient, fictitious crest loss coefficient for an infinite plate height based on the outside width of the drop inlet, dimensionless
K_e entrance loss coefficient, dimensionless
K_o outlet loss coefficient, dimensionless
K_t barrel entrance loss coefficient, dimensionless
$K_{t_c/D}$ multiplier correction for crest thickness, dimensionless
ℓ length of conduit, in feet
ℓ_r length of drop inlet or riser, in feet
L crest length, in feet
L_o antivortex plate overhang, in feet
n a specific point in the spillway
Q discharge, in cubic feet per second
r radius of inside corner of crest, in feet
R_r hydraulic radius of drop inlet or riser, in feet
R Reynolds' number, dimensionless
S conduit slope, sine
t_c crest thickness, in feet
V_c velocity between the antivortex plate and the drop inlet crest, in feet per second
V_j velocity of the jet in the drop inlet, in feet per second
V_p velocity in the barrel, in feet per second
V_r average velocity in the riser or drop inlet, in feet per second
$V_{r,\,B}$ fictitious average velocity in drop inlet based on the outside drop inlet width, in feet per second
w unit weight of water, in pounds per cubic foot
W drop inlet width, in feet
x distance from outside wall of drop inlet, in feet
z vertical distance below drop inlet crest, in feet. z is positive below and negative above the crest elevation.
Z difference in elevation between inlet crest or conduit invert at inlet and centerline of outlet, in feet
Z_i height of drop inlet, crest to invert of barrel at entrance, in feet
Z_p height of antivortex plate above the drop inlet crest, in feet
Δp_n difference between the pressure at any point in the drop inlet and the static pressure outside the drop inlet at the same elevation, in pounds per square foot
β ratio of the distance above the invert at which the projected hydraulic gradeline pierces the plane of the conduit exit to the conduit diameter, dimensionless
ν kinematic viscosity, in square feet per second
σ surface tension, in dynes per centimeter
$\langle\,\rangle$ the quantity in the pointed brackets is zero for negative numbers